HYDRAULIC MODELING ON THE MIDDLE RIO GRANDE, NEW MEXICO

RIO PUERCO REACH

MIDDLE RIO GRANDE,

NEW MEXICO

DRAFT DECEMBER 2005

FINAL JULY 2006

PREPARED FOR:

US BUREAU OF RECLAMATION

ALBUQUERQUE, NEW MEXICO

UPDATED BY

SEEMA SHAH

PREPARED BY

CHAD VENSEL

GIGI RICHARD

CLAUDIA LEÓN

DR. PIERRE JULIEN

COLORADO STATE UNIVERSITY

ENGINEERING RESEARCH CENTER

DEPARTMENT OF CIVIL ENGINEERING

FORT COLLINS, COLORADO 80523

ABSTRACT

The 10-mile long Rio Puerco reach of the Middle Rio Grande, located from the mouth of the Rio Puerco to the San Acacia Diversion dam, is included in the habitat designation for two federally-listed endangered species, the Rio Grande silvery minnow and the southwestern willow flycatcher. To facilitate restoration efforts for these species, it is necessary to determine the historic, current and potential future geomorphic configuration of the channel. Analyses of historic data, including water discharge, suspended sediment discharge, aerial photos, cross-section surveys and bed material size, revealed changes in the processes acting on the channel and the resulting impacts on the channel configuration.

Results of the geomorphic analyses showed a recent trend (from 1992 to 2002) toward a slightly narrower and slightly shallower channel with relatively constant width-depth ratio and sinuosity and decreased velocity and slope. This is confirmed by the analysis of the suspended sediment record, which showed aggradation and an overall decrease in sediment supply to the reach during the same time period. In addition, the data from the mean bed elevation supports that aggradation has occurred. The narrowing trend is consistent with Schumm's (1969) model of channel metamorphosis for decreased sediment supply, as well as with the narrower stable channel width predicted by SAM and some hydraulic geometry equations. It is anticipated that a continued decrease in sediment supply could result in continuation of the trend toward a narrower, deeper and single-thread channel that is considerably different from the historic conditions found in the Rio Puerco reach prior to 1972. However, response of the reach to changes in sediment supply has indicated that stabilization of several parameters has been evident and the channel has reversed its previous trend of degradation to aggradation. The response of the reach to discharge changes after 2002 have not been analyzed, therefore it is difficult to extrapolate the observed trends beyond 2002.

The sediment transport, hydraulic geometry and SAM analyses showed that subreach 2 is closest to an equilibrium configuration. Prediction of an equilibrium slope by balancing the incoming sand-sized bed material load with the bed material sediment transport capacity of the reach produced varying results. Application of Yang's (1973) sediment transport equation, to estimate the transport capacity of the channel, suggested small variations in slope for subreaches 1 and 2 and a large slope decrease for subreach 3.

TABLE OF CONTENTS

LIST OF FIGURES

LIST OF TABLES

1 INTRODUCTION

In July 1999, the US Fish and Wildlife Service (USFWS) designated the Middle Rio Grande, New Mexico, from just downstream of Cochiti Dam to the railroad bridge at San Marcial, as critical habitat for the Rio Grande silvery minnow (*Hybognathus amarus)*, a federally listed endangered species. Alterations in the hydrologic regime and the hydraulic and sediment character of the channel during the last century, through construction of diversion dams and channelization, have reduced the quality and quantity of habitat for the minnow. The silvery minnow prefers shallow water with a sandy and silty substrate. Recent changes in the channel have resulted in a narrower, deeper and armored configuration (USFWS 1999).

Deterioration of native plant and animal communities, associated with the riparian bosque habitat, has also occurred. In February 1995, the USFWS listed the southwestern willow flycatcher (*Empidonax traillii extimus*) as an endangered species. This species is a small, grayish-green migratory songbird found only in riparian habitats characterized by dense growths of willows, arrowweed and other species that provide foraging and nesting habitat. The loss of southwestern cottonwood-willow riparian habitat has been cited as the main reason for the decline of the population of the southwestern willow flycatcher (USFWS 2000).

The Rio Grande from the mouth of the Rio Puerco to San Acacia Diversion Dam defines the Rio Puerco study reach (Figure 1-1) and is included in both critical habitat designations. This reach has potential to provide suitable habitat for the minnow and the flycatcher through restoration efforts. Development of a successful habitat restoration plan requires a thorough understanding of the past and present hydraulic, geomorphic and sediment conditions in the reach. In addition, prediction of future equilibrium conditions of the Rio Puerco reach will allow better planning for management of the reach and to identify sites that are more conducive to restoration efforts.

This report characterizes the recent historic and current geomorphic conditions of the reach, and evaluates potential future equilibrium conditions. The objective is to identify temporal and spatial trends in channel geometry and pattern on a reach-averaged basis and to identify the potential future equilibrium configuration of the reach. The results of this report will be helpful to the US Bureau of Reclamation (Reclamation) in determining the suitability of the Rio Puerco reach for silvery minnow and southwestern willow flycatcher (SWWF) habitat. Additionally, it can be used for analysis of restoration alternatives to identify additional field geomorphic analysis.

Extensive data are available for the Rio Puerco reach, including aerial photos, cross section surveys, water and sediment discharge data, and bed and suspended sediment particle size data. The objectives of the study are met through the following analyses:

- Analysis of cross-section survey data to characterize spatial and temporal trends in channel geometry and longitudinal profile.
- Planform classification via analysis of aerial photos and channel geometry data.
- Analysis of temporal trends in water and sediment discharge, sediment concentration, and sediment continuity using USGS gaging station data.
- Assessment of the equilibrium state of the river via use of hydraulic geometry and minimum stream power methods, as well as determination of the equilibrium slope based on estimated incoming sediment load and channel sediment transport capacity.

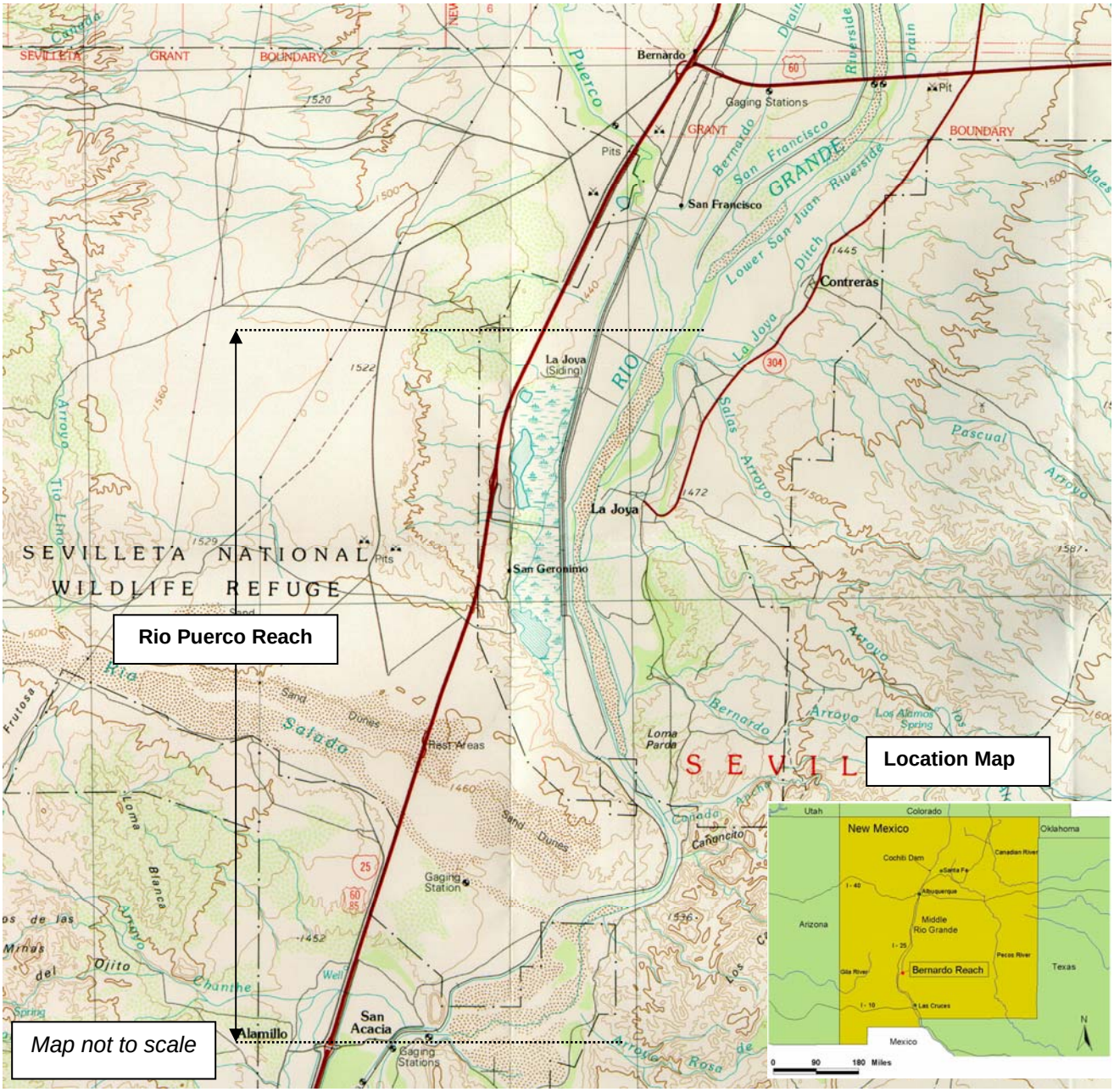

Figure 1-1 Rio Puerco reach Location Map

2 SITE DESCRIPTION AND BACKGROUND

The Rio Puerco study reach of the middle Rio Grande spans 10 miles from just downstream of the mouth of the Rio Puerco (agg/deg 1101) to the San Acacia Diversion dam (agg/deg line 1206) (Figure 1-1). The reach is generally straight with a sinuosity close to one and a valley slope of 0.0008. The reach is characterized primarily by a sand-bed channel with median bed material size less than 1 mm (Bauer 1999). Historically, the Rio Puerco reach has been aggrading, and as a result, Reclamation constructed levees and performed channelization to mitigate potential flooding (Scurlock 1998, Woodson and Martin 1962, Graf 1994).

In November of 1973, Cochiti Dam was constructed to mitigate water and sediment. The construction of the dam helped reduced the quantity of sediment being deposited in Elephant Butte Reservoir. Additionally, other municipal and agricultural diversions decrease the flow in the Rio Grande between Cochiti Dam and the Rio Puerco reach. Figure 2-1 shows the impact of Cochiti Dam and other diversions and losses on a typical spring runoff hydrograph. The Otowi gaging station is located upstream of Cochiti Dam. Reduction of the spring runoff peak and attenuation of the hydrograph is evident between Otowi and the gages located downstream of the dam. Flow discharge data from 1974 to 1988 at Rio Grande at Otowi Bridge and Rio Grande below Cochiti Dam stations indicate that peak outflows from Cochiti can historically occur as much as 62 days after, or as much as 225 days prior to the peak inflows to the reservoir (Bullard and Lane 1993).

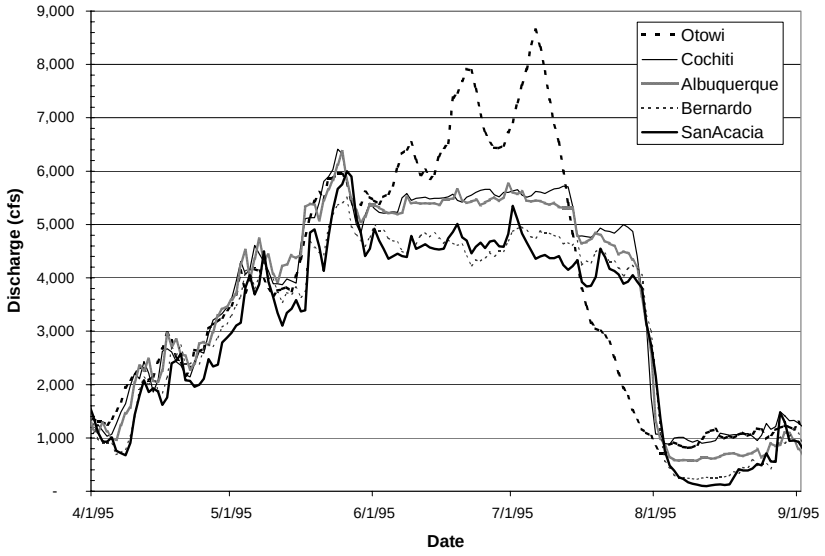

Figure 2-1 1995 Rio Grande Hydrograph

Cochiti dam also traps virtually all of the sediment entering the reservoir from upstream. As a result, downstream of Cochiti dam, tributary input and erosion of the channel bed and banks are the primary sources of sediment to the Middle Rio Grande (Richard 2001). Figure 2-2 shows the change in annual suspended sediment yield from upstream of Cochiti dam to downstream.

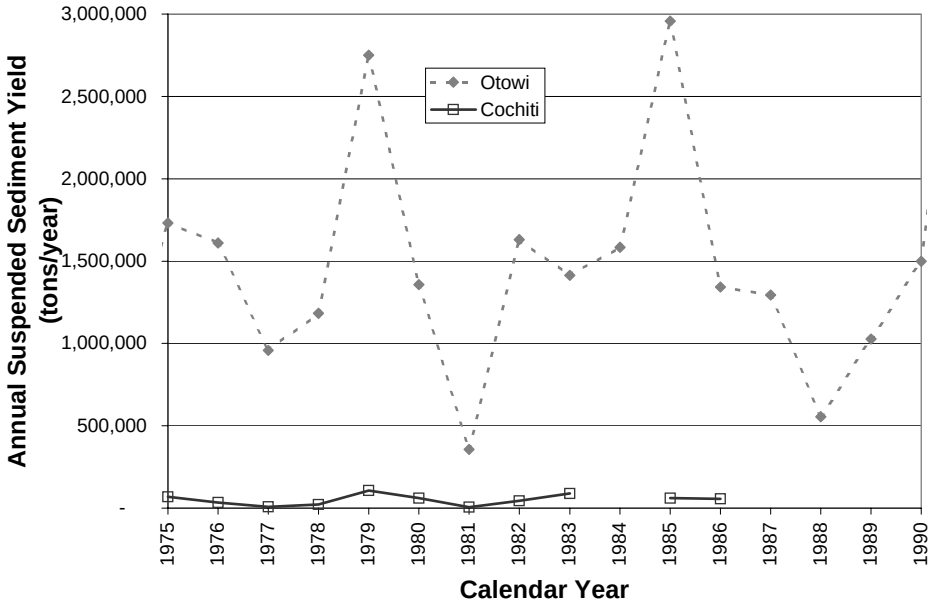

Figure 2-2 Annual Suspended Sediment Yield in the Rio Grande at Otowi Gage (upstream of Cochiti Dam) and Cochiti Gage (downstream of Cochiti dam)

Two major ephemeral tributaries, Rio Puerco and Rio Salado enter the main stem from the west and form significant deltas in the river, altering the course of the main channel. Both tributaries drain several square miles of sparsely vegetated Colorado Plateau territory, which consists of easily erodible sandstones and shales. As a result, high sediment loads have been noted in both tributaries. Historically the Rio Puerco contributed 83% of the total load and 5.6 % of the total runoff to the Rio Grande from 1948 to 1973 (Gellis, 1992). It has been estimated in the past that close to 71% of the total sediment load in the Rio Puerco was comprised of bedload (Graf 1994). Presently most of the Rio Puerco sediments are silt and clay. The Rio Puerco contributes about fifty percent of the sediment and about two percent of the water in the Rio Grande below its confluence (Baird, Personal communication, 2000). The reduction in sediment is attributed to arroyo evolution, where the channel begans to deepen and then widen (Gellis, 1992). As the channel widens, flows are less erosive, vegetation within the floodplain thicken and the channel begins to aggrade. This results in an overall decrease in sediment loads to the river.

Four other major arroyos enter the Rio Grande from the east in this study reach. These arroyos are all ephemeral and likely also contribute significant amounts of sediment to the river, particularly during summer months as a result of thunderstorms and rapid runoff. Additionally, there are noticeable deltas at the mouths of each of these arroyos. The locations of these arroyos may be viewed in the aerial photos in Figure 2-3 and 2-4. Four minor arroyos also enter the Rio Grande from the east between agg/deg lines 1165 and 1178. Significant deltas, in the main channel, from these arroyos are not evident within the aerial photos (Bauer 1999).

2.1 SUBREACH DEFINITION

To aid in the geomorphic characterization, the Rio Puerco reach was subdivided into three subreaches that exhibit similar channel characteristics, such as width and planform. The subreach definition is outlined in Table 2-1 and in Figure 2-5. Subreach 1 is 4.8 miles long and spans from just below the mouth of the Rio Puerco to the mouth of the Bernardo Arroyo. Subreach 2 is 2.7 miles long and spans from the mouth of the Bernardo Arroyo to just downstream from the mouth of the Rio Salado. Subreach 3 is 2.5 miles long and spans from just downstream of the mouth of the Rio Salado to the San Acacia Diversion Dam.

Table 2-1 - Rio Puerco reach Subreach Definition

	Agg/Deg Line		
	From	To	Approximate Average Active Channel Width (feet)
Subreach 1	1101	1110	199
	1111	1123	572
	1124	1128	378
	1129	1134	527
	1135	1136	477
	1137	1149	731
	1150	1151	295
Subreach 2	1152	1179	167
	1180	1181	282
Subreach 3	1182	1184	300
	1185	1186	733
	1187	1192	596
	1193	1199	616
	1200	1205	718

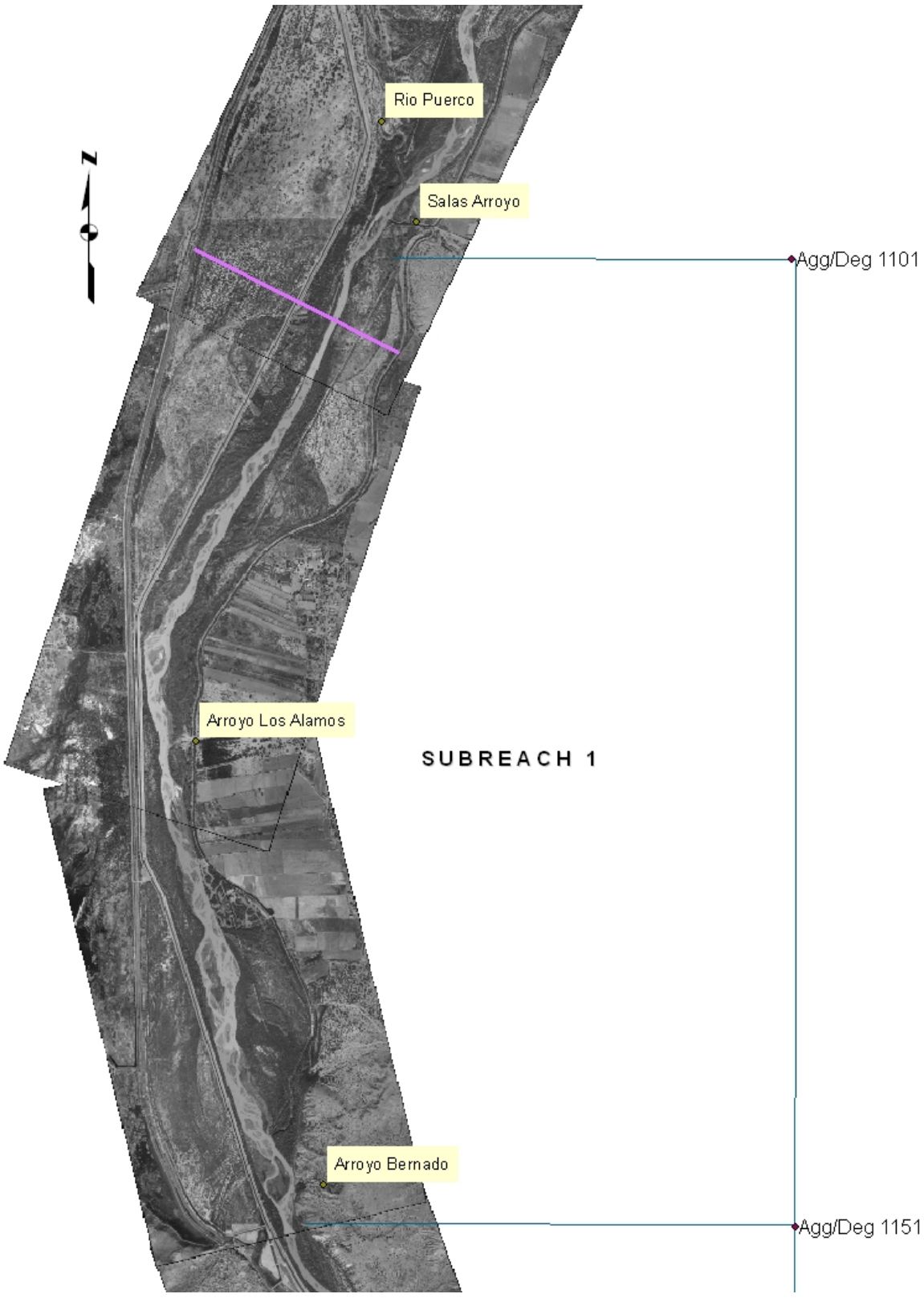

Figure 2-3 Aerial Photo of Subreach 1

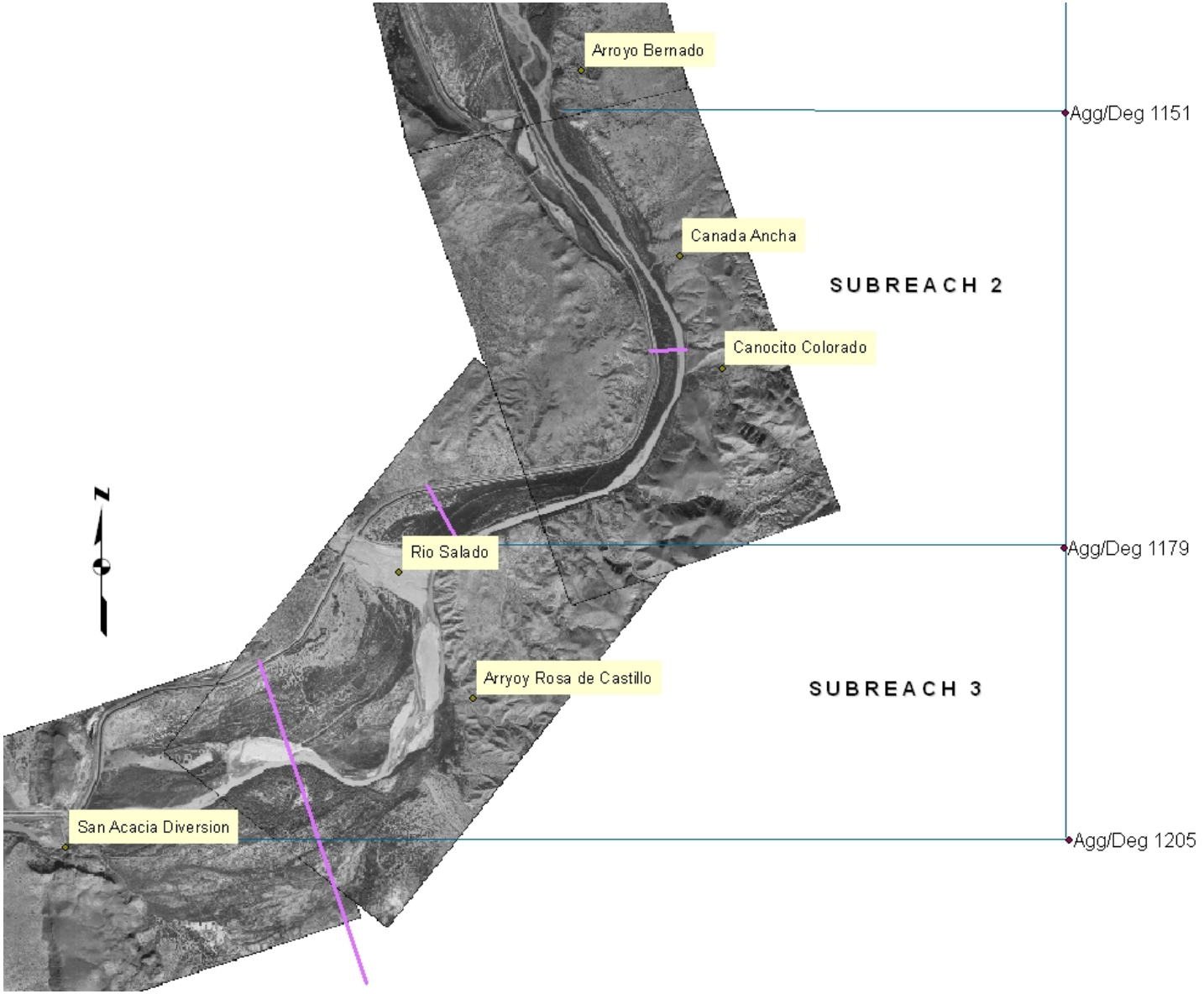

Figure 2-4 Aerial Photo of Subreaches 2 and 3

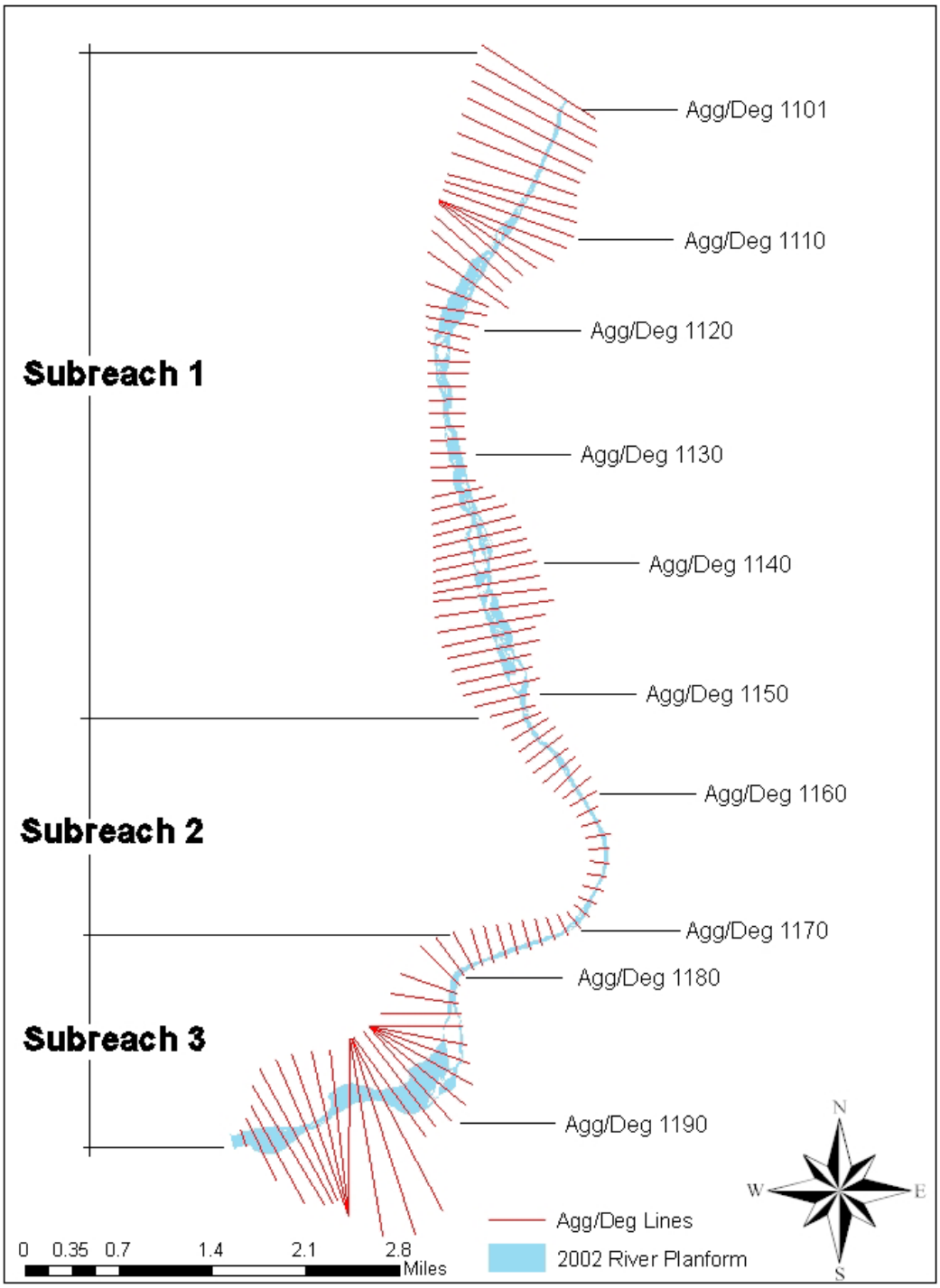

Figure 2-5 Rio Puerco reach Subreach Definitions

2.2 AVAILABLE DATA

The data utilized in this study were compiled into an electronic database by Colorado State University (CSU) for Reclamation in 1999 (Bauer et al. 1999). The data were collected by the U.S. Geological Survey (USGS), Reclamation, Soil Conservation Service (presently Natural Resources Conservation Service, NRCS) and the U.S. Army Corps of Engineers (the Corps). More detailed descriptions of the data used in this study are provided in this section.

USGS gaging stations are located just upstream of the start of the reach (Rio Grande near Bernardo) and at the conclusion of the reach (Rio Grande near San Acacia) (Figure 1-1). In addition, gaging stations are located on the Rio Puerco and the Rio Salado just upstream of their confluences with the Rio Grande. Other ephemeral arroyos, such as Salas, Los Alamos, Bernardo, and Rosa de Castillo are not gagged. Data specific to the sediment and water discharges that contribute to the main stem have been and are presently unavailable. The gaging station records for both the Bernardo and San Acacia gages include data from the Low Flow Conveyance Channel (LFCC) and the floodway, as well as combined data. The combined gage data were used when available, and for years where combined data were unavailable, the LFCC and floodway data were summed. Table 2-2 summarizes the available discharge and sediment data from the USGS gages.

Table 2-2 Periods of record for discharge and continuous suspended sediment data collection by the USGS

Station	Gage ID	Mean Daily Discharge	Suspended Sediment Discharge	Bed Material
		Period of Record	Period of Record*	Period of Record*
Rio Grande Convayance Channel Near Bernardo	USGS 08331990	1952-2004	1964 to 1974	
Rio Grande near Bernardo	USGS 08332000	1937 to 1958	1955 to 1964	
Rio Grande Floodway Near Bernardo	USGS 08332010	1957 to current	1964 to 1994	1976 to 1996
Rio Puerco near Bernardo	USGS 08353000	1939 to 2005	1955 to 1994	1961 to 1996
Rio Salado near San Acacia	USGS 08354000	1947 to 1984		
Rio Grande at San Acacia	USGS 08355000	1936 to 1964	1946 to 1956	
Rio Grande Floodway at San Acacia	USGS 08354900	1958 to current	1959 to 1994	1976 to 1996
Rio Grande Conveyance Channel at San Acacia	USGS 08354800	1958 to 2004	1959 to 1989	1989

* Not Continuous

Bed material data were collected at the USGS gaging stations at Bernardo and San Acacia approximately once per month. Particle size distributions are available from these bed material samples. Additionally, bed material samples were collected at the CO-lines during the 1990's.

Four sets of aggradation/degradation (agg/deg) surveys are available, 1962, 1972, 1992 and 2002. These surveys are estimated from aerial photos and therefore do not provide

detailed bathymetry. The agg/deg lines are spaced approximately 500 feet apart and provide mean bed elevation, water surface elevation and topography of the floodplain. The mean daily discharges in the channel on the exact dates of the aerial photos are listed in Appendix A. The 1962 and 1972 photos were taken on days when the mean daily discharge was less than 10 cfs, therefore significant portions of the channel bed were exposed. The mean daily discharge during the 1992 survey date was 753 cfs and the mean monthly discharge for the March 2002 survey was approximately 311 cfs.

The Cochiti (CO) range lines were field surveyed in this reach in the 1990's for Reclamation. However, there are only four lines located in this study reach (Figure 2-6). CO-1104 is located 0.3 miles downstream from agg/deg line 1101 in subreach 1. CO-1164 is located in subreach 2 just above the mouth of Cañoncita Colorado. CO-1179 is the last line in subreach 2, where the channel begins to transition from a single-thread, just upstream of the mouth of the Rio Salado. CO-1194 is located in subreach 3 about a mile upstream of the San Acacia diversion dam. CO-1104 and C0-1164 were surveyed in 1992, 1995, 1996 and 1998. CO-1179 and CO-1194 were surveyed in 1992, 1995 and 1998. Table 2-3 summarizes the survey dates for the CO-Lines.

Table 2-3 Surveyed Dates for the Cochiti Range Lines

Cross Section	***Surveyed Dates***
CO-1104	Aug 6, 1992 Jul 31, 1995 May 24, 1996 Sep 3, 1998
CO-1164	Aug 6, 1992 Jul 31, 1995 May 24, 1996 Sep 3, 1998
CO-1179	Aug 6, 1992 Jul 31,1995 Sep 3, 1998
CO-1194	Aug 6, 1992 Jul 31, 1995 Sep 3, 1998

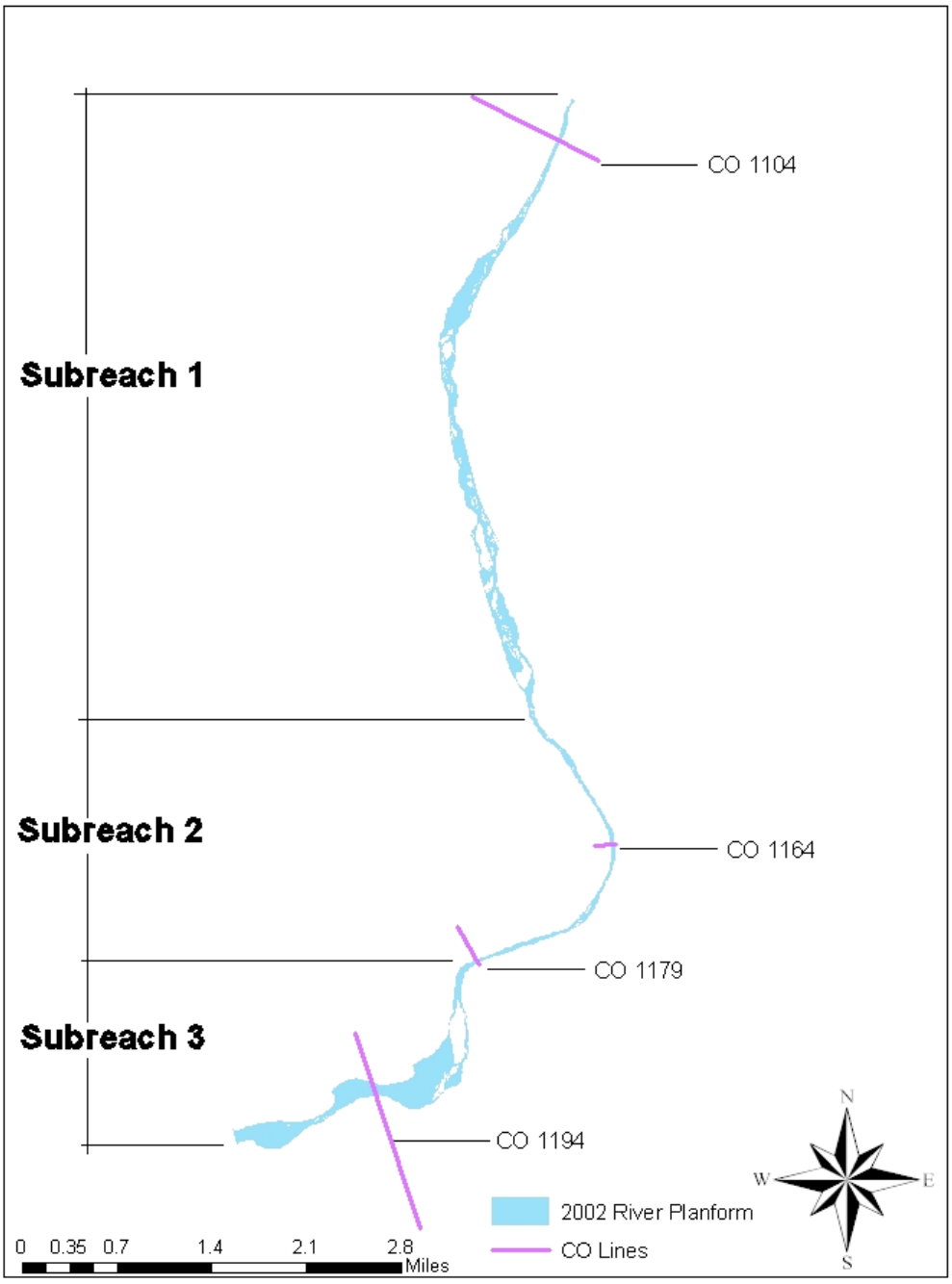

Figure 2-6 2002 River planform of the Rio Puerco reach indicating locations of the subreaches.

Reclamation's GIS and Remote Sensing group in Denver, CO digitized the non-vegetated active channel and other important channel features from aerial photos and topographic surveys. These GIS coverages are available for 1918, 1935, 1949, 1962, 1972, 1992 and 2002.

2.3 CHANNEL FORMING DISCHARGE

Reclamation's Albuquerque office performed an analysis to determine the "channel forming" discharge at the San Acacia gage. They determined that the "channel forming" flow in the Rio Grande is actually a range of flows that constantly transports large amounts of sediment. As a result, it was decided to use flow rates of 3,000 cfs, 5,000 cfs and 7,000 cfs in analyses in this study. Based on Reclamation's "effective discharge" analysis for the San Acacia gage for the 1986 to 1997 time period, it was determined that the flows, which transport the majority of the sediment, are within the range of 2,000 to 4,000 cfs (Reclamation 2003). Hence, the selection of a 3,000 cfs flow. Additionally, they developed a flow duration curve for post-Cochiti dam discharge data at San Acacia. The two-year discharge corresponds to about 5,000 cfs. In August 1999, a thunderstorm in the Rio Puerco drainage basin, resulted in a discharge of 7,000 cfs on the Rio Grande. Reclamation estimates that this was just above bankfull. Based on these analyses, 3,000 and 7,000 cfs were selected as the lower and upper bounds, respectively, for estimating the channel forming discharge, and 5,000 cfs is used as a mid-range estimate.

Figure 2-7 shows the annual maximum daily mean discharges, recorded by the USGS, at the Bernardo, Rio Puerco and San Acacia gaging stations. Since the 1940's there have been no flows recorded at San Acacia exceeding 10,000 cfs (Figure 2-7). At the Bernardo gage, the last flow exceeding 10,000 cfs was in 1958. Since 1972, peak flows on the Rio Puerco have not exceeded 2,000 cfs. Generally, the trend for the last 30 years has been fewer extreme events exceeding 8,000 cfs and fewer extremely low flow years.

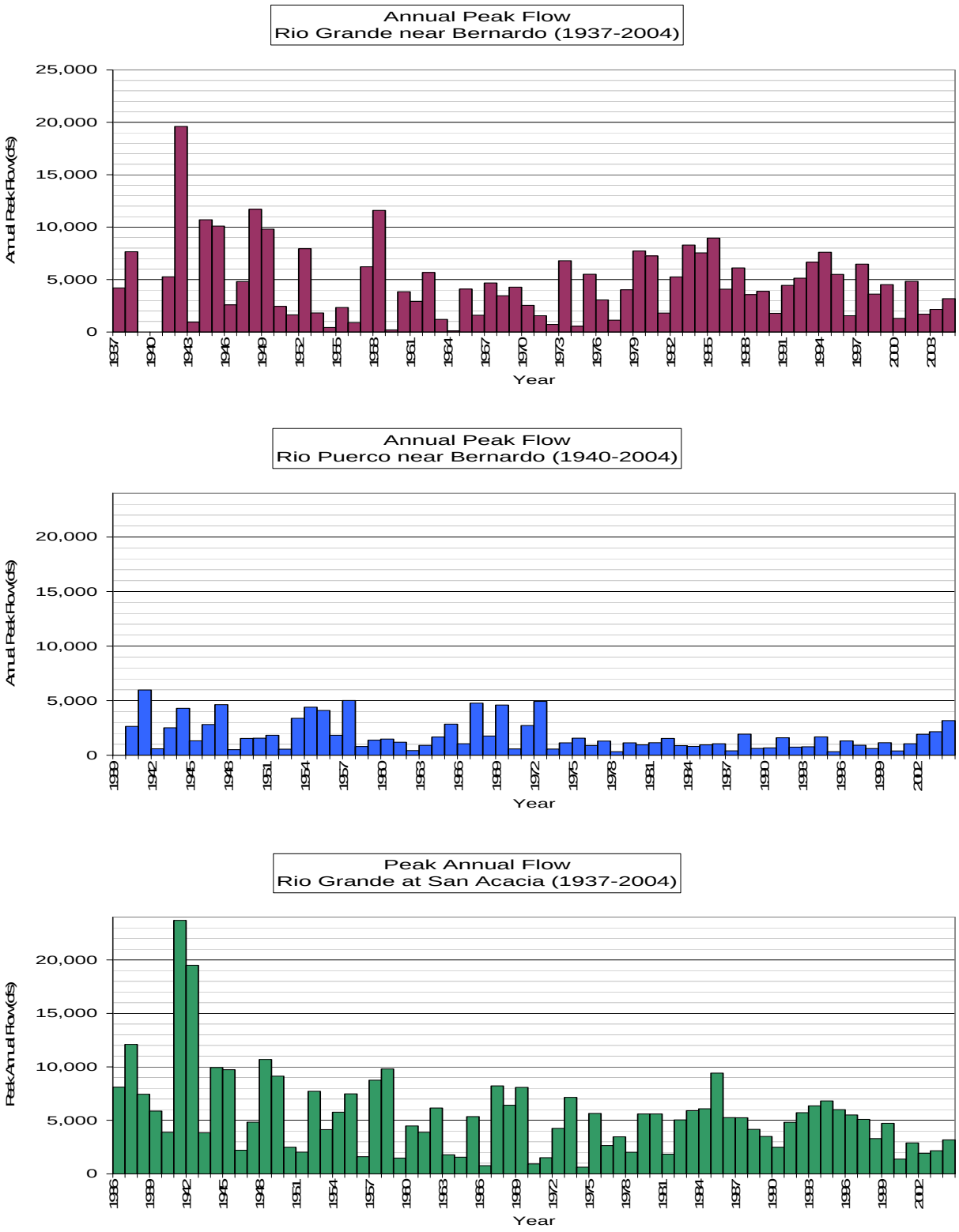

Figure 2-7 Annual Peak Daily-Mean Discharges - Rio Puerco and Rio Grande 1937-1997

3 GEOMORPHIC CHARACTERIZATION

3.1 METHODS

Channel Classification

Qualitative observations were made, regarding the current channel pattern, based on examination of the 2002 aerial photos with reference to Bauer's (1999) study of the Rio Grande from Bernalillo to San Acacia. Additionally, the GIS coverages of the historic active channel were used to produce qualitative descriptions of the changes in the channel planform from 1918 to 2002.

Several methods of channel classification have been applied to the Rio Puerco reach to determine spatial and temporal trends in the pattern of the reach. Methods that incorporate slope-discharge relationships were applied, including Leopold and Wolman (1957), Lane (1957, from Bauer 1999, pp. 69), Henderson (1963, from Henderson 1966), Ackers and Charlton (1970, from Ferguson 1987), and Schumm and Khan (1972). Rosgen's (1996) method of stream classification, based on channel morphology, was also applied. Additionally, several methods that utilize the concept of unit stream power were computed for the Rio Puerco reach, including Chang (1979), van den Berg (1995), Knighton and Nanson (1993), and Nanson and Croke (1992). Parker's (1976) method, which employs slope/Froude number and flow depth/flow width, was also applied to the subreaches as well as the entire Rio Puerco reach.

Leopold and Wolman (1957) were among the first to classify channel planform as meandering, braided and straight and to assign a slope-discharge relationship to distinguish between these planform classes. Braided channels are separated from meandering by a line described by the equation:

$$S_o = 0.06\ Q^{-0.44}$$

Q = Bankfull discharge, cfs

S_o = Channel slope

They also define meandering as a function of sinuosity (thalweg length to valley length) when it is >1.5. Braiding refers to channels with relatively stable alluvial islands.

Lane (1957, from Bauer 1999) also proposed a slope-discharge relationship to distinguish meandering from braided channel patterns. The relationship between annual discharge in cfs, slope in foot/foot and sand bed river pattern is $SQ^{0.25} = K$. If K is less than or equal to 0.0017, the river trend is towards a meandering pattern. When K is greater than or equal to 0.010, the planform is braided. If K is between these two values, the classification is an intermediate sand bed stream.

Henderson (1963, from Henderson 1966) added bed material to the slope-discharge relationship to describe channel pattern. Plotting the ratio of $S/0.06Q^{-0.44}$ against median bed size *d* (in feet), a line can be drawn having the equation,

$$S = 0.64d^{1.14}Q^{0.44}$$

such that most of the channels with straight or meandering pattern fall close to the line. All braided channels had values of *S* that were substantially greater than indicated by the equation. He notes that this discriminates between braided and single-thread channels, which include both straight and meandering channels.

Ackers and Charlton (1979, from Ferguson 1987) also proposed slope discharge relationships to describe channel pattern. Their focus was on the transition from straight to meandering where:

- Straight channels:

$$S < 0.001Q^{-0.12}$$

- Straight channels with alternating bars:

$$0.001Q^{-0.12} < S < 0.0014Q^{-0.12}$$

- Meanders develop if:

$$S > 0.0014Q^{-0.12}$$

Later, Ackers (1982, from Ferguson 1987) noted that sand-bed river and canal data are compatible with

$$S = 0.0008\ Q^{-0.21}$$

as a threshold from straight to meandering.

Schumm and Khan (1972) proposed to define channel pattern based on valley slope thresholds derived from flume experiments where:

- Straight $S < 0.0026$
- Meandering thalweg $0.0026 < S < 0.016$
- Braided $S > 0.016$

Rosgen's (1996) channel classification system is based on channel morphology and sediment. Classification is determined from slope, entrenchment, sinuosity, and bed material.

Parker's (1976) analysis provides a determination of braided vs. meandering that is independent of sediment transport. He notes that braided rivers can be in quasi-equilibrium, and that aggradation can push the transition from meandering to braided. If the slope and the width-depth ratio are high then braided planform is favored and if the slope and the width-depth ratio are low then meandering planform is favored.

His classification is based on the relative magnitudes of the depth-width ratio and the ratio of the channel slope to the flow Froude number according to the following trends:

$S/F << d_o/B$ = Meandering

$S/F >> d_o/B$ = Braided

$S/F \sim d_o/B$ = Transition

Van den Berg (1995) proposed a discriminator between braided and single-thread channels that is based on unit stream power and bed material size. The following equation defines this discriminator:

$$\omega_{v,t} = 900 \cdot D_{50}^{0.42}$$

ω_v = potential unit stream power, for sand-bed:

$$\omega_v = 2.1 \cdot S_v \sqrt{Q_{bf}} \quad (\text{kW/m}^2)$$

D_{50} = median grain size (mm)

S_v = Valley slope

Knighton and Nanson (1993) defined channel pattern in terms of the following three variables:

- Flow strength
- Bank erodibility
- Relative sediment supply

Their general classification is based on the continuum from straight to meandering to braided corresponding to increases in the three variables listed above. The flow strength can be measured by either stream power or shear stress. They suggest that bank erodibility could be measured by the silt-clay content of the bank material and that the relative sediment supply is represented by the bed and suspended sediment load.

Knighton and Nanson (1993) don't quantify thresholds for these variables. However, it is possible to look at changes in these variables in the Rio Puerco reach in relative terms.

Nanson and Croke (1992) developed a classification of floodplains based on specific stream power and sediment characteristics. For non-cohesive floodplains, the following groupings apply:

- Confined coarse-textured floodplain - ω = >1,000 W/m^2
- Confined vertical-accretion sandy floodplain - ω = 300-1,000 W/m^2
- Cut and fill floodplain - ω = ~300 W/m^2
- Braided river floodplain - ω = 50-300 W/m^2
- Lateral migration (actively meandering) - ω = 10-60 W/m^2

Cohesive floodplains fall into the low-energy anastomosing category:

- Anastomosing and straight - ω = <10 W/m^2

They define gross stream power to be $\Omega = \gamma QS$ and specific stream power to be $\omega = \Omega/W$ and is calculated for bankfull flow conditions.

Chang (1979) analyzed changing channel pattern based on stream power and presents a classification using slope and discharge.

Sinuosity

The sinuosity of the Rio Puerco reach and the subreaches was estimated by dividing the channel length by the valley length. Reclamation's GIS and Remote Sensing Group, Denver, CO measured both of these lengths from digitized active channel from aerial photos and topographic maps. The channel length was measured by estimating the location of the thalweg within the active channel.

Variability in the water level in the channel at the different survey dates as well as the quality of the photos and surveys contributed to variability in identification of the channel length. The 1918 GIS coverage was created by digitizing a hand-drafted topographic survey. As a result, only active channel and vegetated island were delineated. The corresponding meta-data file states "The center line of the active channel was determined by comparing the open water area to the center line of the active channel for 1935. Where the 1935 data was of no assistance, the best guess was made after comparing the 1918 elevations, which are suspect, and the 1935 photographs of the channel." Other notes in the meta-data file describe difficulty in defining the thalweg of the active channel for 1962 and 1972.

Longitudinal Profile

Thalweg Elevation

The thalweg elevation was measured as the lowest elevation in the channel cross section. The mean channel bed elevations of the agg/deg lines were estimated by Reclamation based on the water surface elevation, slope, channel roughness and discharge at the time of the survey. As a result, the only available thalweg elevation data for the Rio Puerco reach are for the CO-lines for 1992, 1995 and 1998. There are only four CO-lines in this reach, and as such, they do not provide an accurate picture of the profile of the reach. Changes in the thalweg elevation with time for each cross section were plotted to identify temporal trends in the thalweg elevation at these four locations.

Mean Bed Elevation

The channel bed elevations for the agg/deg lines are average bed elevations. Mean bed elevations at the CO-lines were computed by Bauer (1999). Longitudinal profiles were plotted for each of the subreaches as well as the entire Rio Puerco reach from the agg/deg lines. The reach-averaged mean bed elevation was computed for each of the subreaches from the agg/deg line data.

Energy grade

The energy grade line slope was estimated at each cross section from HEC-RAS runs of the channel-forming discharges of 3,000, 5,000 and 7,000 cfs. The slopes were then averaged over the reach and each subreach by using the sum of one-half of the distance to each adjacent cross section as the weighting factor.

Channel Geometry

The channel geometry of the Rio Puerco reach was estimated by modeling the reach with HEC-RAS, utilizing all of the available agg/deg line data for 1962, 1972, 1992 and 2002. The resulting model included 105 cross-sections spaced approximately 500 feet apart. Channel-forming flows of 3,000 cfs, 5,000 cfs and 7,000 cfs were routed through the reach. A Manning's n value of 0.019 was used for the channel and 0.1 for the floodplain. Levee and main channel stations were defined by comparing the aerial photos with the cross-section survey data and determining appropriate delineations of the main channel.

The HEC-RAS results were also divided into main channel flow and overbank flow. For most of the analyses, the main channel results were utilized due to the fact that the majority of sediment transport occurs within the main channel. Additionally, in 1992 and 2002, at a flow rate of 5,000 cfs, most of the flow was contained within the main channel of the reach, with very little overbank flow. More overbank flow occurred in 1962 and 1972 than in 1992 and 2002. The weighting factor used in the reach averaging was one-half the distance to each of the adjacent upstream and downstream cross-sections.

The reach-averaged width of the channel was estimated using the digitized aerial photos and from HEC-RAS modeling results. The non-vegetated active channel width for each subreach was measured from GIS coverages, which were digitized from aerial photos for the

following years: 1918, 1935, 1949, 1962, 1972, 1985, 1992 and 2002. Reclamation's GIS and Remote Sensing Group, Denver, CO digitized the photos. The exact dates of the photos and quality of the data are listed in Appendix A. The width was measured as the total active channel area divided by the centerline length of the channel. The main channel widths, resulting from the HEC-RAS runs, were also averaged for each subreach and the entire reach.

The following channel geometry parameters were also computed, by reach and subreach, averaging the main channel HEC-RAS results from each agg/deg line:

Wetted Perimeter = P

Wetted Cross Section Area = A

Mean Flow Velocity = $V = Q/A$

where, Q = Flow discharge

Mean Depth = $h = A/W$

where, W = Top Width

Width-Depth ratio = W/h

Sediment

Bed Material

Particle size distributions were plotted from data collected at the USGS gaging stations and at the CO-lines. Spatial and temporal variability of the particle sizes and the distributions were noted. The median grain size (d50) was computed for relevant bed material samples and apparent temporal and spatial trends were noted.

3.2 RESULTS

Channel Classification

Historic and Current Channel Pattern Description

The current channel pattern description is based on study of the 2002 aerial photos, taken during the month of March, where the mean monthly discharge was approximately 311 cfs. At flows below bankfull (< 5,000 to 7,000 cfs), the Rio Grande exhibits a generally braided pattern in the region near the mouth of the Rio Puerco (Figure 2-3). Immediately below the mouth of the Puerco, the Rio Grande narrows to a single-thread for about 3,000 feet, where it again

widens and transitions toward a braided, multi-channel planform. Approximately 5 miles downstream from the Rio Puerco, about 3,000 feet below the mouth of the Bernardo Arroyo, the Rio Grande enters a constriction and travels through a large bend. In this 2.7-mile segment (designated as subreach 2) (Figure 2-4), the channel narrows and becomes single-thread. Upon emerging from the constriction, the channel widens into a braided, multi-thread pattern for the next 2.5 miles until it reaches San Acacia Diversion Dam, the conclusion of the study reach (Figure 2-4). At flows closer to bankfull (>5,000 to 7,000 cfs), the entire Rio Puerco reach is single thread.

Figure 3-1 was produced from Reclamation's GIS coverages of the Rio Puerco reach and illustrates the change in river planform that occurred in the non-vegetated active channel between 1918 and 2002. The planform maps in Figure 3-1 illustrate the fact that the channel has narrowed and straightened, significantly, over the past century. Based on qualitative observation of the GIS coverages, the narrowing trend continued progressively from 1918 to 2002, with the greatest decrease in width occurring between 1949 and 1962. In 1918 and 1935 the channel was very wide and straight. The 1949 and 1962 coverages reveal a narrower and somewhat more sinuous active channel. In 1972, 1985, 1992 and 2002, the width decreased further and the active channel straightened once again.

Scurlock's (1998, p. 282) description of the channel pattern of the Middle Rio Grande illustrates the variety in planform found in the Rio Puerco reach. He noted that the channel has been described as low sinuosity meandering, straight and braided meandering. Additionally, he pointed out that downstream of the Rio Puerco and the Rio Salado, a braided meandering pattern was found. The tendency toward a braided planform is seen in subreaches 1 and 3 contrasted with the narrower pattern of subreach 2 (Figure 3-1).

The values of the input parameters for the different channel classification methods applied to the 1962, 1972, 1992 and 2002 surveys of the Rio Puerco reach are presented in Table 3-1. These methods produced descriptions of the channel that range from straight to meandering and braided (Table 3-2).

Table 3-1 Input Parameters for Channel Classification Methods

1962	Q (cfs)	Channel Slope	Valley Slope	d50 (ft)	Width (ft)	Depth (ft)	Velocity (ft/s)	Fr	EG Slope
Subreach 1	5,000	0.00069	0.00083	4.92E-04	685.74	2.45	3.75	0.421	0.00087
Subreach 2	5,000	0.00067	0.00072	6.56E-04	501.32	2.86	3.92	0.408	0.00074
Subreach 3	5,000	0.00077	0.00096	6.56E-04	839.96	2.29	3.50	0.407	0.00095
Bernardo Reach	5,000	0.00071	0.00083	6.56E-04	674.62	2.52	3.73	0.414	0.00085
1972									
Subreach 1	5,000	0.00080	0.00088	6.56E-04	727.17	2.93	3.32	0.342	0.00069
Subreach 2	5,000	0.00063	0.00066	6.56E-04	341.50	4.01	5.08	0.447	0.00091
Subreach 3	5,000	0.00069	0.00087	6.56E-04	969.66	2.25	3.40	0.399	0.00085
Bernardo Reach	5,000	0.00073	0.00082	6.56E-04	684.36	3.05	3.81	0.385	0.00079
1992									
Subreach 1	5,000	0.00066	0.00070	9.84E-04	498.60	3.05	3.90	0.393	0.00076
Subreach 2	5,000	0.00047	0.00049	9.84E-04	192.63	5.39	5.09	0.386	0.00056
Subreach 3	5,000	0.00126	0.00153	9.84E-04	405.80	2.83	5.25	0.550	0.00162
Bernardo Reach	5,000	0.00076	0.00082	9.84E-04	392.98	3.63	4.56	0.422	0.00092
2002									
Subreach 1	5,000	0.00063	0.00066	7.87E-04	491.61	3.00	4.01	0.408	0.00071
Subreach 2	5,000	0.00055	0.00054	7.87E-04	214.99	5.01	4.95	0.390	0.00052
Subreach 3	5,000	0.00111	0.00121	7.22E-04	476.46	2.89	4.42	0.458	0.00111
Bernardo Reach	5,000	0.00073	0.00075	7.65E-04	413.31	3.52	4.36	0.410	0.00076

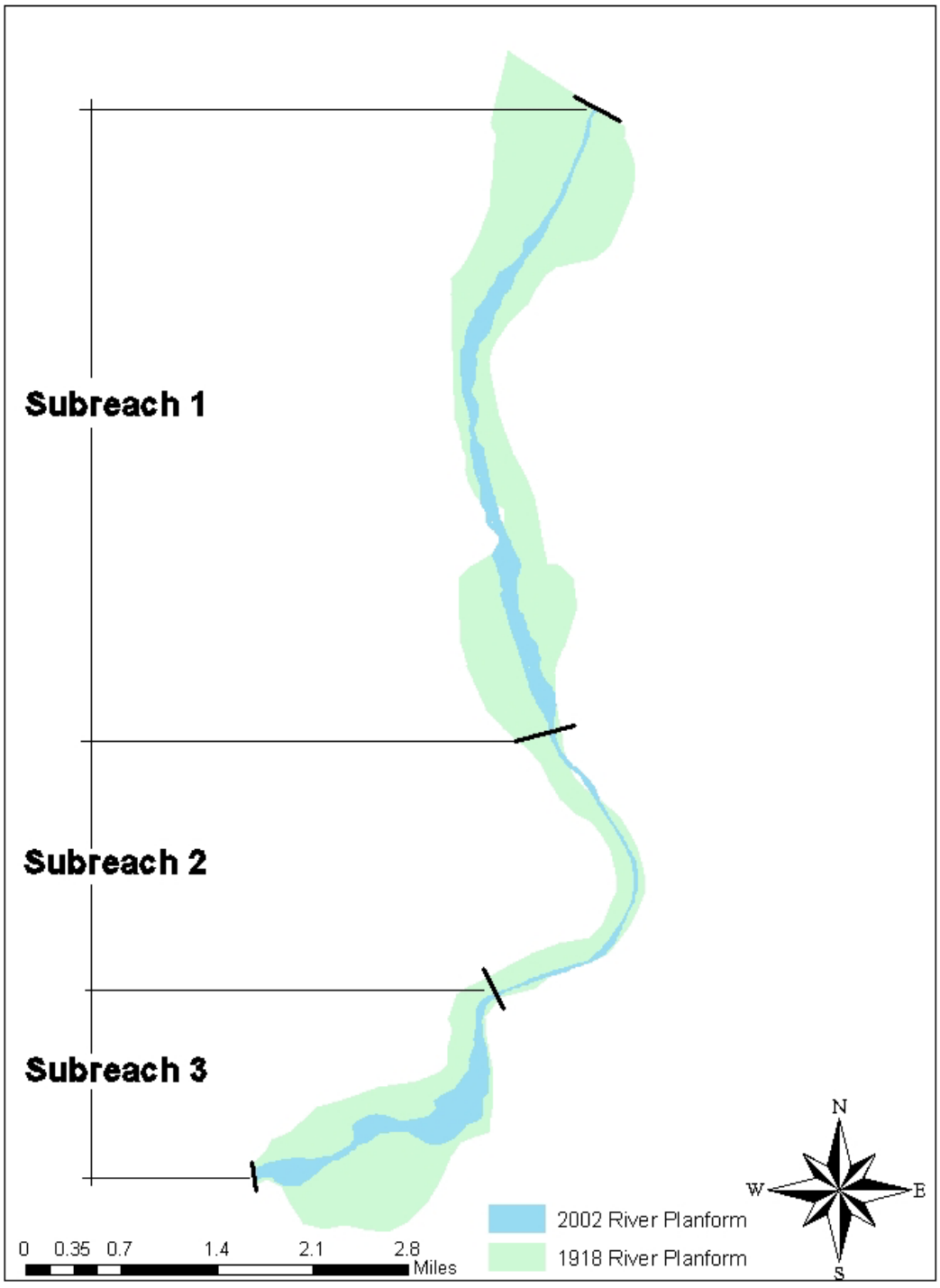

Figure 3-1 Non-vegetated Active Channel of the Rio Puerco reach. 1918 Planform from Topographic Survey. 2002 Planform from Aerial Photo.

The methods that employed a relationship between slope and discharge (Leopold and Wolman 1957, Lane 1957 - from Bauer 1999, pp. 69, Henderson 1963 - from Henderson 1966, Ackers and Charlton 1970 - from Ferguson 1987, Schumm and Khan 1972) produced a variety of results. Henderson (1963) was the only method that predicted a braided planform for the entire reach for all years. In 1992, the steep slope of subreach 3 pushed the Lane (1957) classification into the braided regime, however, in 2002 the classification returned to an intermediate regime as it had been prior to 1992.

Rosgen's (1996) and Parker's (1976) classification systems are based on channel morphology parameters. The Rio Puerco reach did not wholly fit into any one of Rosgen's particular categories, but instead bridged between two classifications. The best fit in his system was a D5c, which is a multiple-channel with very high width-depth ratio, low sinuosity, mild slope and sand bed. Typically D5c streams are characterized by a braided pattern, a channel slope that approximates the valley slope and high bank erosion rates. Portions of the Rio Puerco reach, particularly subreach 2, do not exhibit a multiple channel pattern. However, Rosgen's system does not include a single-thread channel pattern with the high width-depth ratio, low sinuosity and mild slope as found in subreach 2. Using Parker's (1976) method, the entire reach was classified as meandering/tranistional in 2002, except for subreach 2, which was classified as meandering due to decreased width-depth ratios, which was also the case in 1992.

The stream power methods of Nanson and Croke (1992) and Chang (1979) generally classified the reach as either straight or meandering. However, in 1992 and 2002, the Chang method classified subreach 2 as transitional and subreach 3 as steep braided due to increased bed slopes. The van den Berg stream power method classified the entire reach as a single thread channel for each year of analysis. As previously stated, the width of the reach has been progressively and steadily decreasing. This decrease in width has changed the van den Berg classification from a high energy single thread wide channel, in 1962 and 1972, to a low energy single thread narrow channel, in 1992 and 2002.

Knighton and Nanson (1993) did not quantify thresholds values for flow strength, bank erodibility and sediment supply. However, it is possible to look at changes in these variables in the Rio Puerco reach in relative terms. Since construction of Cochiti dam, the flow

strength (water discharge) has decreased and the relative sediment supply has decreased. The bank erodibility was moderate to high. The combination of these factors indicates a likely shift from braiding to meandering planform. Subreach 2 however, was not braided in 1962 and 1972. This could be a result of confinement (lower bank erodibility) or lower slope (due to control point at downstream end at mouth of the Rio Salado) and lower flow strength.

Note: Several discrepancies, in channel classification, were present between the 2001 and 2005 versions of this report. In particular, the d50's, as listed in Table 3-1 of both reports, were erroneously converted from millimeters to feet in the 2001 version. The magnitude of this error was approximately of one order, which can obviously be quite significant with respect to mean particle diameter. Most classification methods were in general agreement between the two versions of the report, however, the method of Schumm and Khan showed significant differences in classification.

Table 3-2 Channel Pattern Classification

Year	Subreach	D_{50} type	Slope-discharge						Channel Morphology		Stream Power		
			Leopold and Wolman	Lane	Henderson	Ackers & Charlton		Schumm & Khan	Rosgen	Parker	van den Berg	Nanson & Croke	Chang
						using S_o	*using* S_v						
1962	1	Fine Sand	Straight	Intermediate	Braided	Straight with alternating bars	Meandering	Straight	C5c/D5c	Meandering/ Transitional	High energy single thread wide channel	Straight	Meandering
	2	Fine Sand	Straight	Intermediate	Braided	Straight with alternating bars	Straight with alternating bars	Straight	C5c/D5c	Meandering/ Transitional	High energy single thread wide channel	Straight	Meandering
	3	Fine Sand	Straight	Intermediate	Braided	Meandering	Meandering	Straight	C5c/D5c	Meandering/ Transitional	High energy single thread wide channel	Straight	Meandering
	Total	Fine Sand	Straight	Intermediate	Braided	Straight with alternating bars	Meandering	Straight	C5c/D5c	Meandering/ Transitional	High energy single thread wide channel	Straight	Meandering
1972	1	Fine Sand	Straight	Intermediate	Braided	Straight	Straight	Straight	C5c/D5c	Meandering/ Transitional	High energy single thread wide channel	Straight	Meandering
	2	Fine Sand	Straight	Intermediate	Braided	Meandering	Meandering	Straight	C5c/D5c	Meandering/ Transitional	High energy single thread wide channel	Straight	Meandering
	3	Fine Sand	Straight	Intermediate	Braided	Straight with alternating bars	Straight with alternating bars	Straight	C5c/D5c	Meandering/ Transitional	High energy single thread wide channel	Straight	Meandering
	Total	Fine Sand	Straight	Intermediate	Braided	Straight with alternating bars	Meandering	Straight	C5c/D5c	Meandering/ Transitional	High energy single thread wide channel	Straight	Meandering
1992	1	Medium Sand	Straight	Intermediate	Braided	Straight with alternating bars	Meandering	Straight	C5c/D5c	Meandering/ Transitional	Low energy single thread narrow channel	Straight	Meandering
	2	Medium Sand	Straight	Intermediate	Braided	Straight	Straight	Straight	C5c/D5c	Meandering	Low energy single thread narrow channel	Meandering	Transition
	3	Medium Sand	Straight	Braided	Braided	Straight with alternating bars	Straight with alternating bars	Straight	C5/D5	Meandering/ Transitional	Low energy single thread narrow channel	Meandering	Steep Braided
	Total	Medium Sand	Straight	Intermediate	Braided	Straight	Straight	Straight	C5c/D5c	Meandering/ Transitional	Low energy single thread narrow channel	Straight	Meandering
2002	1	Fine Sand	Straight	Intermediate	Braided	Meandering	Meandering	Straight	C5c/D5c	Meandering/ Transitional	Low energy single thread narrow channel	Straight	Meandering
	2	Fine Sand	Straight	Intermediate	Braided	Straight with alternating bars	Meandering	Straight	C5c/D5c	Meandering	Low energy single thread narrow channel	Meandering	Transition
	3	Fine Sand	Straight	Intermediate	Braided	Straight	Straight	Straight	C5/D5	Meandering/ Transitional	Low energy single thread narrow channel	Meandering	Steep Braided
	Total	Fine Sand	Straight	Intermediate	Braided	Straight with alternating bars	Straight with alternating bars	Straight	C5c/D5c	Meandering/ Transitional	Low energy single thread narrow channel	Straight	Meandering

Sinuosity

The sinuosity of the Rio Puerco reach has remained below 1.2 since 1918 (Figure 3-2). This is typical of the Middle Rio Grande, which is very straight with a low sinuosity (Leon 1998, Bauer 1999, Richard 2001). The lower value of sinuosity, for all subreaches, may be attributable to the quality of the 1918 topographic survey and the difficulty in determining the region of greatest flow. In addition, the degree of braiding was higher in 1918, which resulted in a straighter planform. In 1935, the higher sinuosity was due to a meandering thalweg within the braided channel.

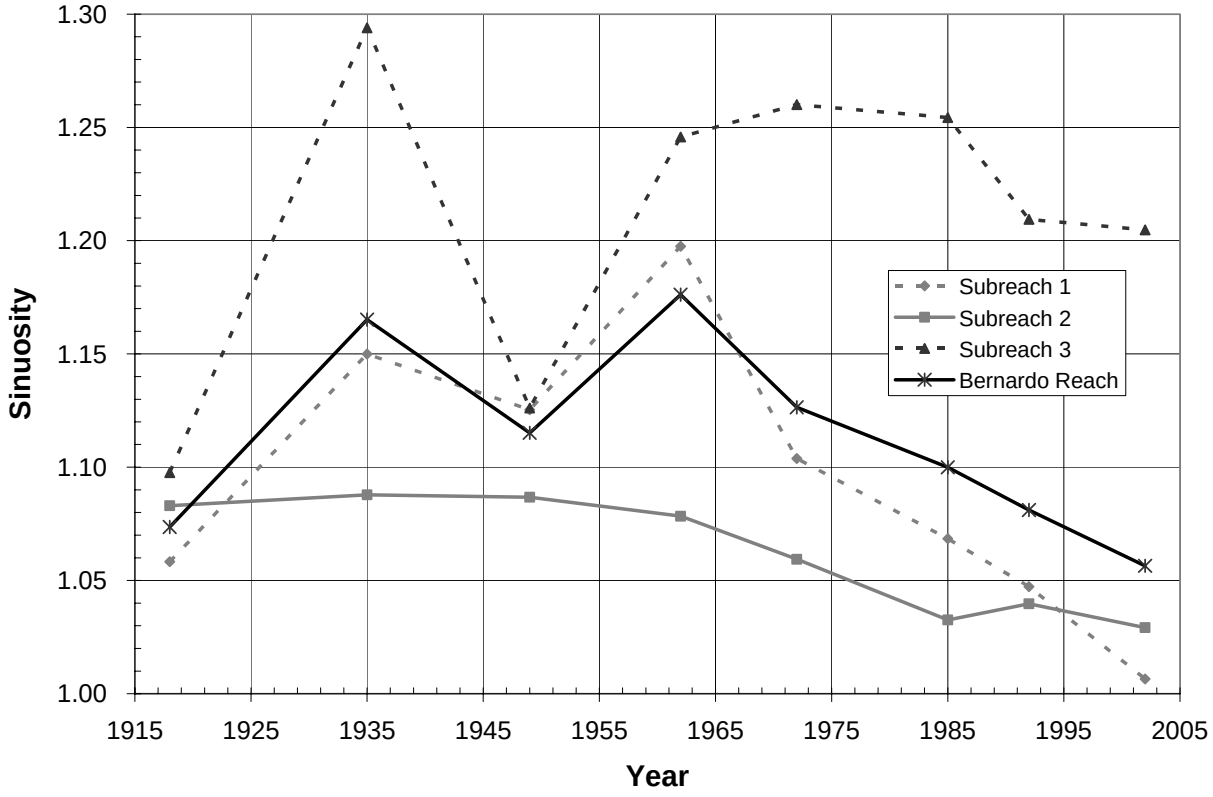

Figure 3-2 Time series of sinuosity of the Rio Puerco reach as measured from the digitized aerial photos by dividing the thalweg length by the valley length.

From 1930 to 1935, the Middle Rio Grande Conservancy District constructed a floodway along the Middle Rio Grande in order to provide flood control along the Middle Valley. As a result, from the 1930's through the 1960's it is difficult to distinguish the impacts of channelization and other channel engineering works on the reach from natural processes. Levees were constructed only on the west side of the river from below the Rio Puerco to the

village of San Antonio, spanning a distance of about 50 river miles. The design capacity of the floodway in this reach was 50,000 cfs (Woodson and Martin 1962).

Additionally, major channelization works occurred in the Middle Rio Grande between 1950 and 1962 and channel engineering works were completed in the Rio Puerco reach by July 1964 (Graf 1994). According to Scurlock (1998), who references the New Mexico State Engineer Office, channelization of the Middle Rio Grande was initiated in 1953 by Reclamation and completed between 1956 and 1959. Channelization was performed to clear the channel of all obstructions to maintain "channel capacity for carrying high flows and moving sediment through the valley" (Scurlock 1998, p. 282).

Longitudinal Profile

Thalweg elevation

Plots showing changes in the thalweg elevation with time at each of the four CO-lines are presented in Figure 3-3. The CO-lines in the Rio Puerco reach have only been surveyed four times between 1992 and 1998, and have not been surveyed since 1998. These surveys were completed at different times of the year and therefore at different points in the annual flow regime. The August 1992 and September 1998 surveys were both taken after the spring runoff, during the summer thunderstorm period. The July 1995 survey was taken during the receding limb of the spring runoff hydrograph at ~3,000 cfs. The May 1996 survey was taken following the small spring runoff peak during a discharge of about 170-cfs.

Mean bed elevation

The changes in average bed elevation measured at the agg/deg lines between 1962 and 1972, 1972 and 1992, and 1992 and 2002 are plotted in Figures 3-4, 3-5, and 3-6, respectively. Based on the mean bed elevation taken from agg/deg surveys, between 1962 and 1972, the reach was generally subject to aggradation, (Figure 3-4) except between agg/deg 1129 (just downstream of the Arroyo los Alamos) and 1157, which degraded. All but four of the agg/deg lines degraded between 1972 and 1992 (Figure 3-5). However, aggradation trends between 1992 and 2002 (Figure 3-6) were dominant throughout the reach, which has indicated a positive progression toward dynamic equilibrium within the reach. Minor degradation also occurred, between agg/deg lines 1126 and 1131, during this time period.

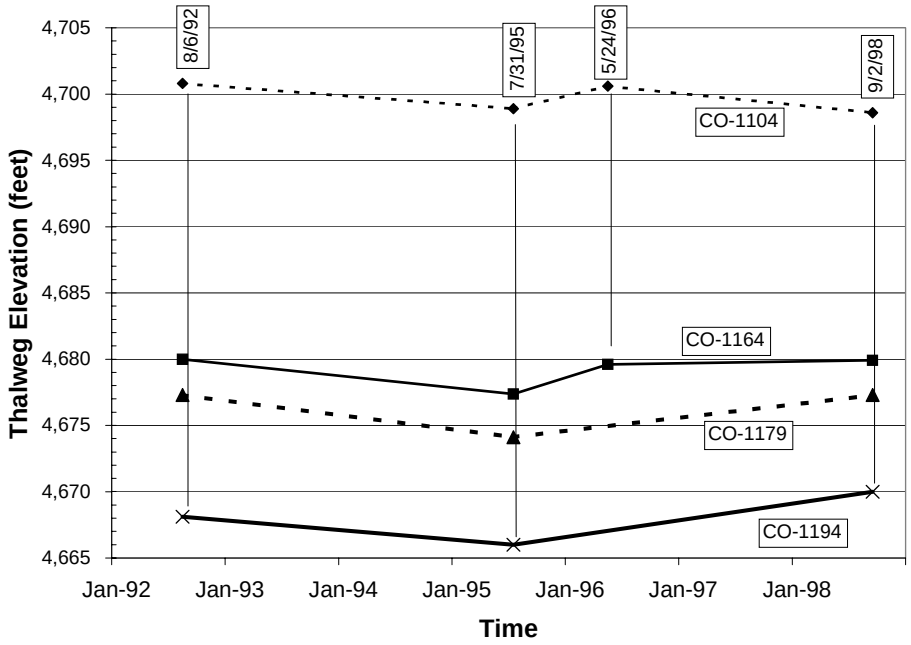

Figure 3-3 Change in thalweg elevation with time at the CO-lines.

The changes in bed elevation in Figures 3-4 and 3-5 are supported by the analysis performed by Bauer (1999). From combined agg/deg and CO-line survey data, Bauer (1999) computed six feet of degradation at CO-1104 between 1972 and 1992. Bauer suggested that the degradation was a result of channel incision through the deltaic deposits at the mouth of the Rio Puerco. Additionally, he determined through sediment budgets for 1971 and 1992 that in 1971 more sediment entered the reach than exited it, and in 1992, more exited it than entered it. This suggested aggradation in 1971 and degradation in 1992. Figure 3-6 shows that the bed elevation from 1992 to 2002 had a tendency to aggrade. Based on sediment continuity analysis (Section 4.5) the sediment input to the reach exceeded the sediment output to the reach resulting in the tendency for this reach to aggrade.

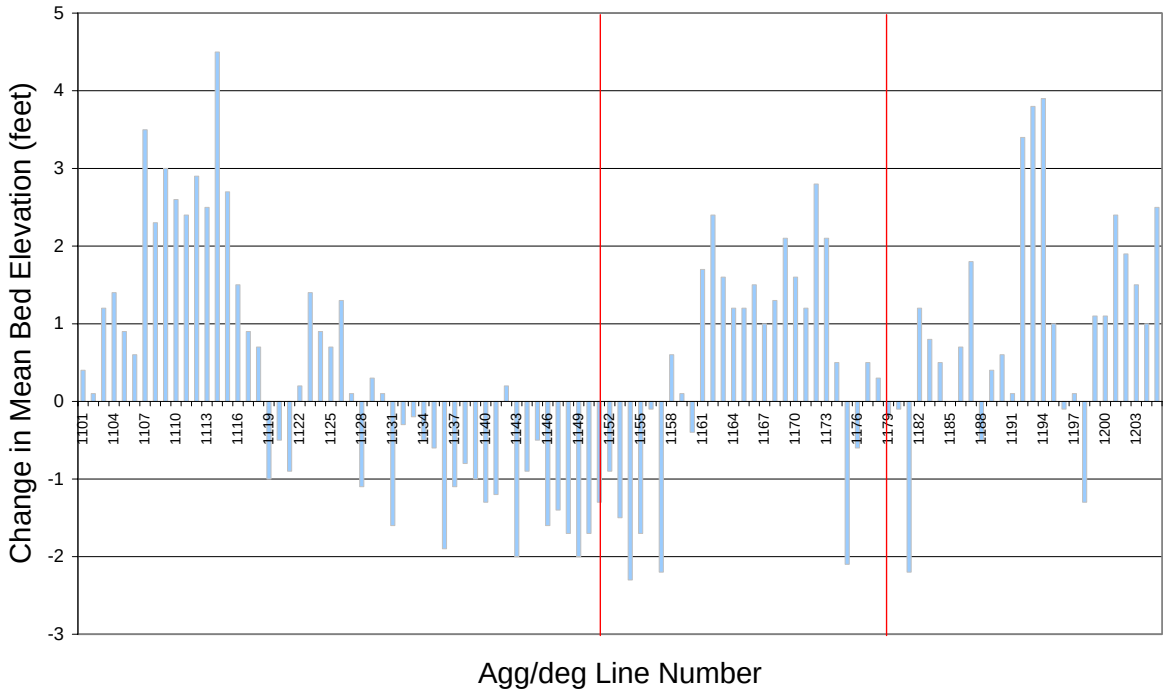

Figure 3-4 Change in mean bed elevation at agg/deg lines between 1962 and 1972.

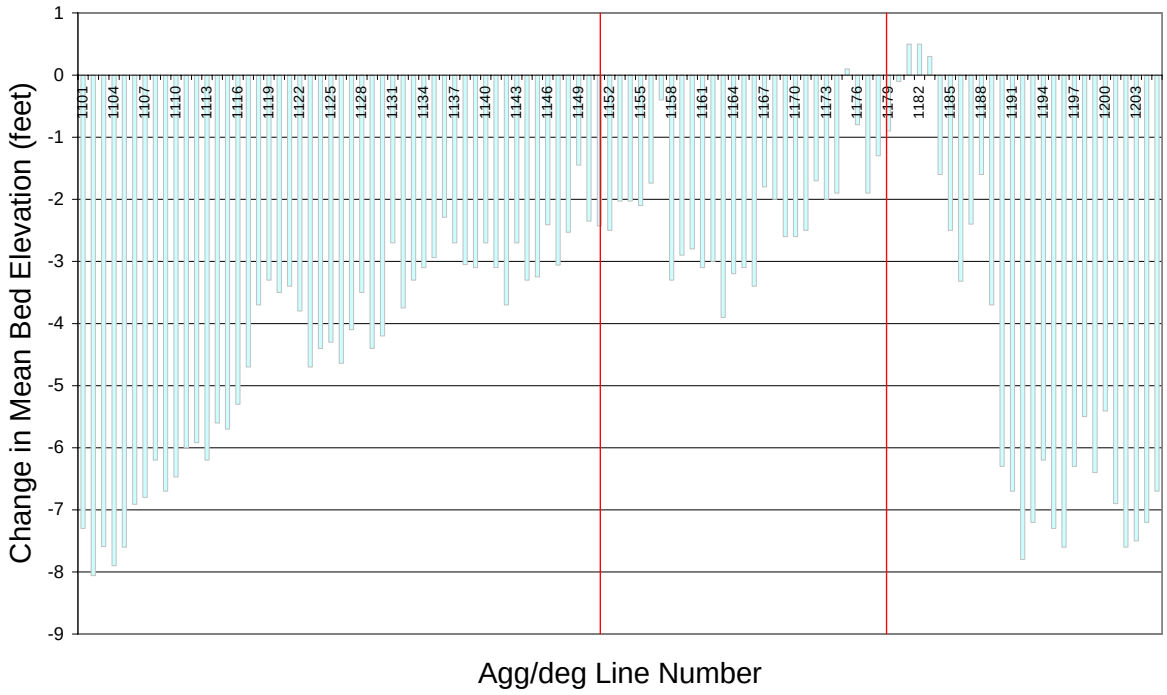

Figure 3-5 Change in mean bed elevation at agg/deg lines between 1972 and 1992.

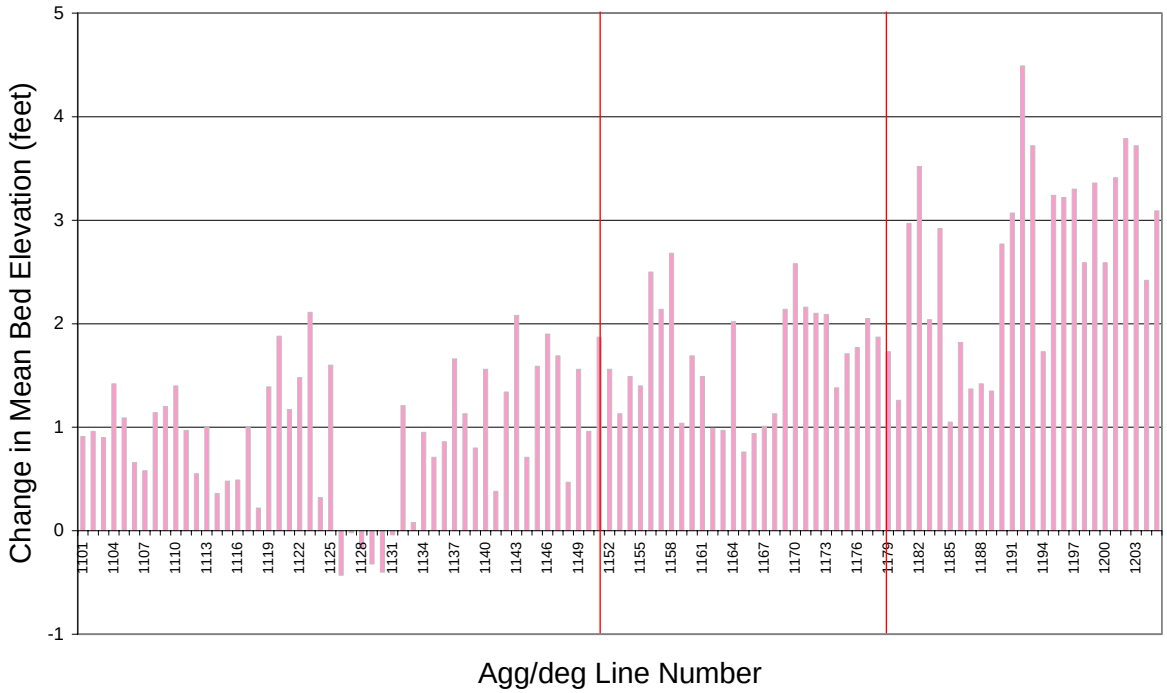

Figure 3-6 Change in mean bed elevation at agg/deg lines between 1992 and 2002.

Reach averaged bed elevations were also computed. Table 3-3 summarizes the reach-averaged mean bed elevation changes between 1962 and 1972, 1972 and 1992, and 1992 and 2002. Figure 3-7 shows the time series of reach-averaged mean bed elevations for 1962, 1972, 1992 and 2002. Degradation occurred in all three of the subreaches between 1972 and 1992, while aggradation occurred in all three subreaches between 1962 and 1972 and 1992 and 2002.

Table 3-3 Reach averaged change in mean bed elevation.

Reach #	1962-72 Agg/Deg	1972-92 Agg/Deg	1992-02 Agg/Deg
1	0.21	-4.37	0.92
2	0.46	-2.21	1.66
3	1.01	-4.76	2.69
Total	0.48	-3.88	1.56

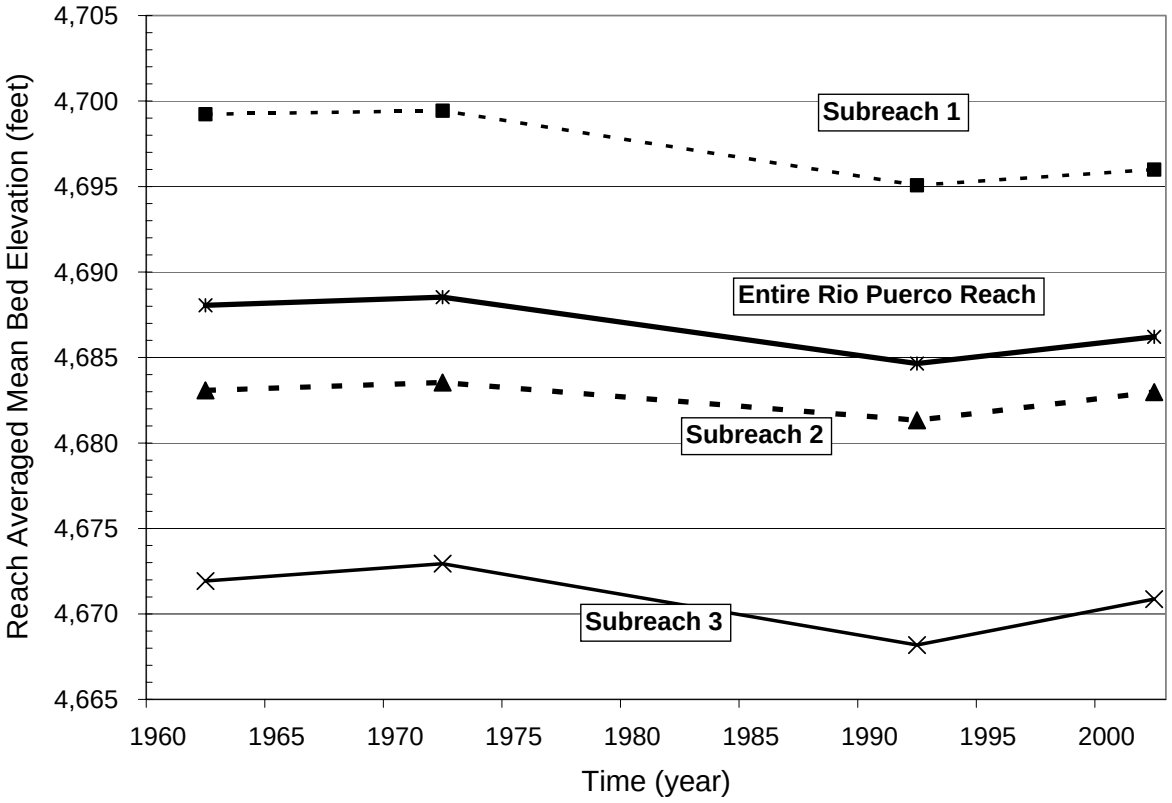

Figure 3-7 Time series of reach-averaged mean bed elevations.

Longitudinal profiles of the mean bed elevation are presented in Figures 3-8 and 3-9. Between 1972 and 1992 subreach 1 exhibited consistent degradation, which was largest at the upstream end just below the mouth of the Rio Puerco (Figure 3-8). Subreach 2 degraded less than subreach 1, with no degradation found at the mouth of the Rio Salado. The smaller ephemeral arroyos in subreach 2 did not appear to have an impact on the profile. In subreach 3, degradation increased with distance downstream from the Rio Salado, with a maximum just upstream from the diversion dam. Between 1992 and 2002 subreach 1 exhibited consistent aggradation, which was largest near the Bernardo Arroyo (Figure 3-8). Subreach 2 aggraded more than subreach 1, particularly near the mouth of the Rio Salado, where aggradation was significant and extended several thousand feet upstream (approximately 6,000 to 7,000 feet). In subreach 3, aggradation persisted, increasing slightly in the downstream direction to the diversion dam.

The CO-line data are also shown on the subreach plots (Figure 3-9). At CO-1194, the bed elevation increased between the February 1992 agg/deg survey and the August 1992 CO-line survey. At subsequent CO-line surveys in 1995 and 1998, the bed elevation remained at this higher level, which is closer to the 1962 and 1972 bed elevations. This change could be due to dredging or a result of operation of San Acacia diversion dam. For instance, the bed just upstream of the dam might degrade in winter when water is not being diverted and then aggrade in late summer when agricultural diversions are occurring.

Energy grade

A time series plot of the energy grade is shown in Figure 3-10(e). In 1992 and 2002, subreach 3 exhibited the steepest energy grade line slope, but decreased from 0.0016 to 0.0011 between 1992 and 2002. For subreaches 1 and 3 and the entire reach, the slope decreased from 1962 to 1972, increased from 1972 to 1992, and again decreased from 1992 to 2002. The increase in slope between 1972 and 1992 for subreach 3 is a result of the degradation just upstream of San Acacia Diversion Dam and the decrease in slope between 1992 and 2002 is a result of the aggradation just upstream of the dam, as previously discussed.

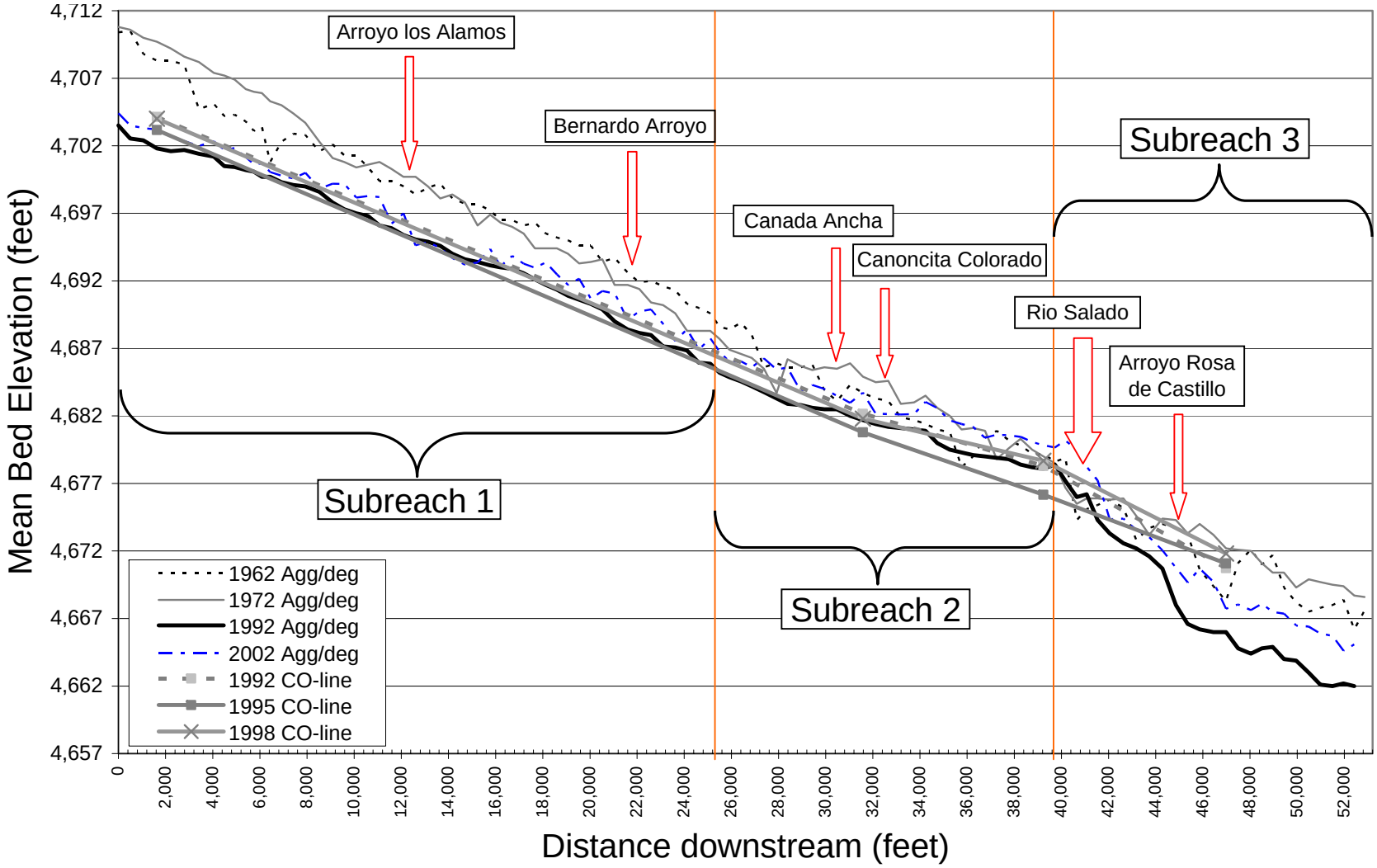

Figure 3-8 Mean Bed Elevation Profile of entire Rio Puerco reach. Distance downstream is measured from agg/deg 1101.

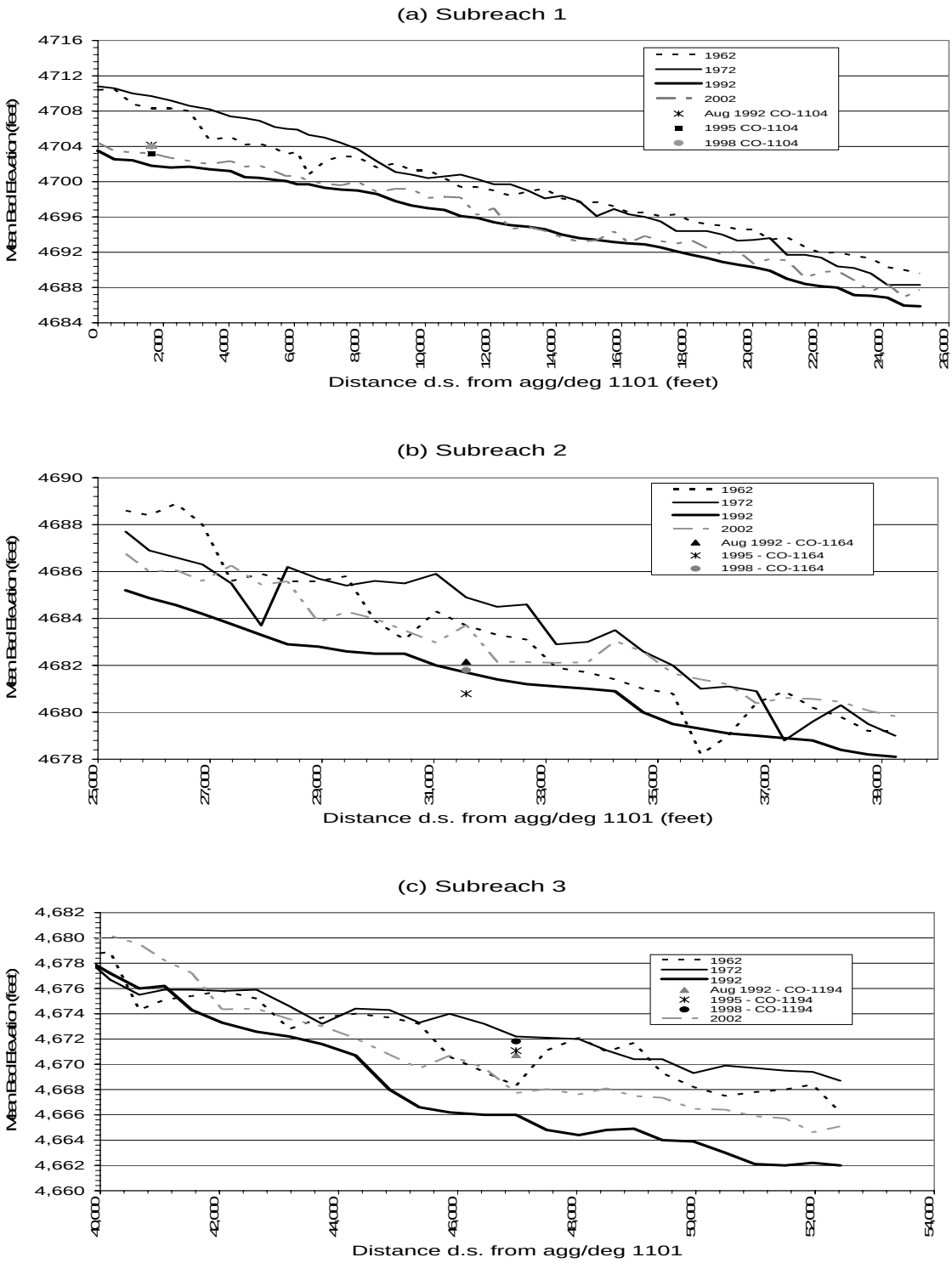

Figure 3-9 Mean bed elevation profiles of the subreaches from the agg/deg surveys. Mean bed elevations at CO-lines are shown as points.

Channel Geometry

The temporal changes in reach-averaged channel geometry are summarized in Figure 3-10. The changes in channel geometry generally showed opposite trends for subreaches 2 versus subreaches 1 and 3.

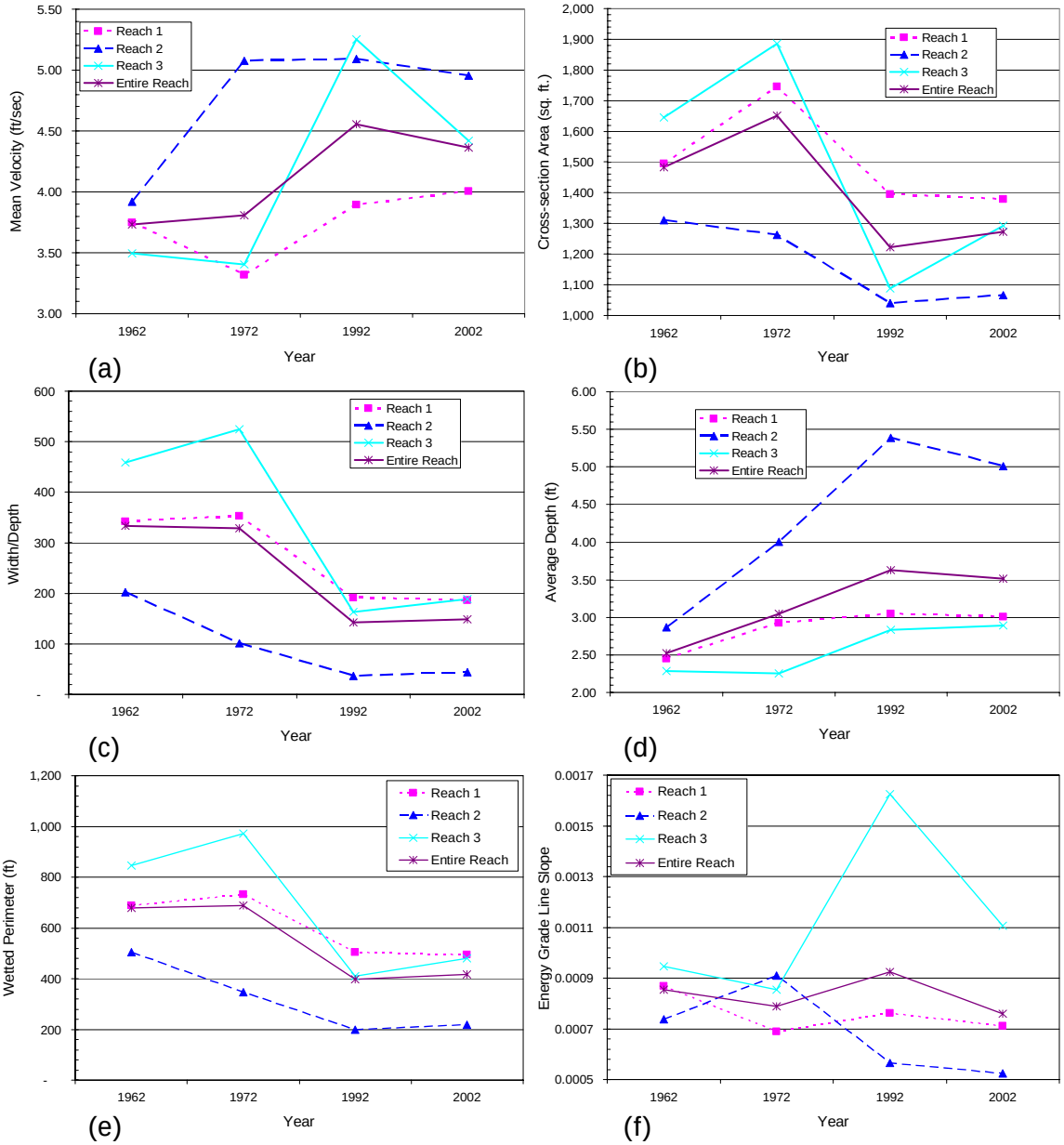

Figure 3-10 Reach-averaged main channel geometry from HEC-RAS results for Q = 5,000 cfs

Width

From the active channel width measured from the GIS coverages, all of the reaches exhibited declining width with time from 1918 to 1992 (Figure 3-11). Between 1992 and 2002, the general trend of decreased width was minimal or negligible. The width of subreach 2, which is confined and single-thread, has been relatively constant since 1985. The main-channel widths predicted by HEC-RAS modeling runs of 5,000 cfs, for 2002, exhibited slight variability in width changes (Figure 3-12). Slight increases in width were present in subreaches 2 and 3 as well as the full reach. However, slight decreases in width were present in subreach 1. Generally, the recent trend toward relatively constant widths, from the GIS coverage analysis, was confirmed by the HEC-RAS modeling results.

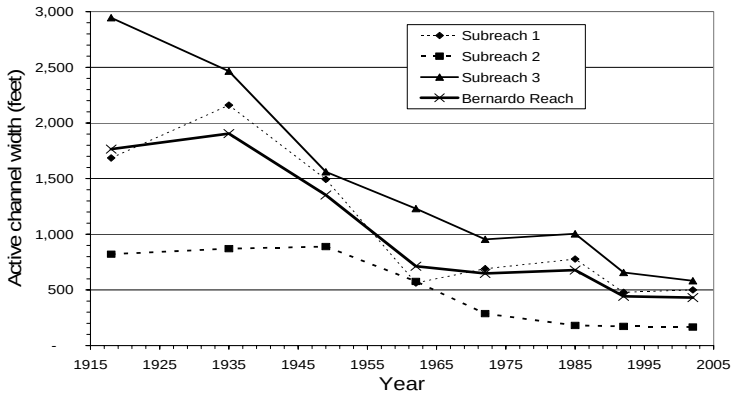

Figure 3-11 Active Channel Width measured as the total active channel area divided by the centerline length of the channel.

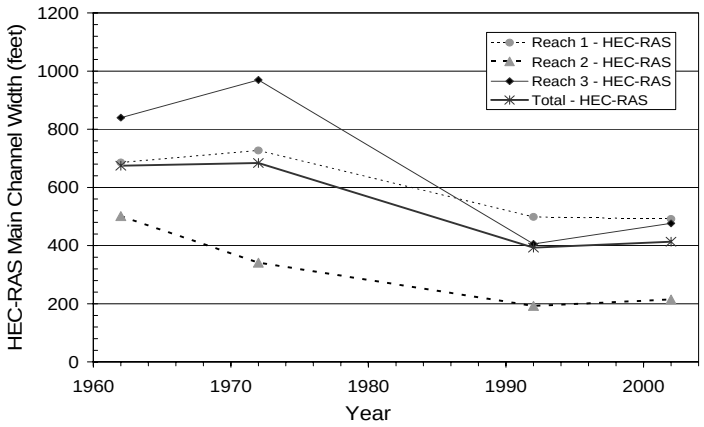

Figure 3-12 Reach Averaged Main Channel Width from HEC-RAS at Q = 5,000 cfs

Sediment - Bed Material

The median grain sizes from the bed material samples at Bernardo were comprised of very fine sand and fine sand until 1989 when the median grain size increased to medium sand for some samples. From USGS bed material samples at San Acacia gage (1966 – 2002) the d_{50} was classified as very fine, fine and medium sand, with a majority of the samples falling in the fine sand and medium sand classes. Few samples contained gravel prior to 1983. Changes in the classification of the median bed material size at San Acacia are shown in Table 3-4. In general, the bed material grain size has coarsened with distance downstream from the mouth of the Rio Puerco, probably due to tributary inputs and coarsened with time, likely due to sediment detention by Cochiti dam. Bauer (1999) found a similar trend and noted an increase in median grain size at CO2-1104, the first CO-line downstream of the mouth of the Rio Puerco. In 2002, classification the bed material grain size was found to be of fine sand, indicating a recent fining trend within the reach.

Table 3-4 - Classification of bed material at San Acacia gage

Time Period	Classification of bed material at San Acacia gage
1966-1978	Fine sand
1979-1989	Very fine sand and fine sand
1989-1996	Medium sand
1997-2002	Fine sand

For the 1992 sediment transport and equilibrium analyses, bed material samples from the CO-lines were used to determine the grain size distributions for each subreach. Bed material data from CO-1104 were used for subreach 1, CO-1164 for subreach 2 and CO-1194 for subreach 3. Average values for each cross section were computed using all of the samples at each section. A weighted averaged was performed using the distance across the cross section (location at which each sample was taken) as the weighting factor. A plot of the average distributions for these samples is shown in Figure 3-13. The 1995 CO-line samples show increased coarsening with two samples containing coarse sand and gravel with d_{50}'s greater

than 0.5 mm. Since no new surveys at the CO-lines had been completed since 1998, the bed material analysis for the most recent years was completed utilizing the gaging station data from the Rio Grande at Bernardo gage and the Rio Grande at San Acacia gage.

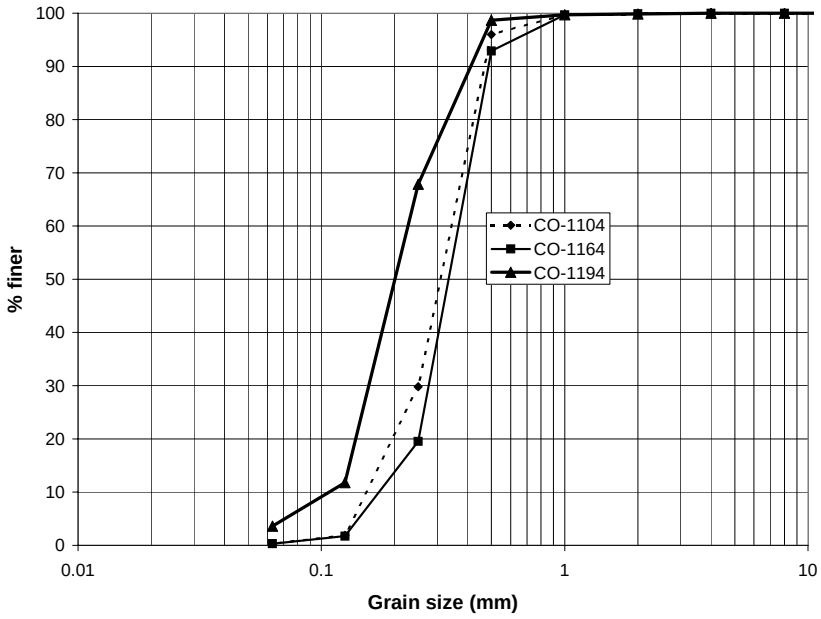

Figure 3-13 1992 Bed-material samples taken by FLO engineering at the CO range lines.

4 SEDIMENT CONTINUITY ANALYSIS

4.1 METHODS

Trends in water and sediment flow in the Rio Puerco reach were analyzed via the development of single-mass curves, double-mass curves, and difference-mass curves. The details of each of these analyses are described as follows.

For the Bernardo and San Acacia gages, for the entire period of record, the following curves were developed:

- Mass curve of water discharge (acre-feet/year)
- Mass curve of sediment discharge (tons/year)
- Double mass curve with water and sediment discharge for trends in sediment concentration (mg/L)

The slopes of each curve and the time periods of breaks in the curves were also estimated.

The sediment continuity of the reach was analyzed by creating a cumulative difference curve of sediment inflow minus sediment outflow. The Rio Grande at Bernardo (LFCC and floodway combined) and Rio Puerco gage data were used as input to the reach and the Rio Grande at San Acacia (LFCC and floodway combined) gage data as the outflow. The difference in the annual suspended sediment load (tons/year) was computed as follows:

(Bernardo + Rio Puerco) – San Acacia = Change in sediment volume in reach

The differences were summed over the time period and plotted against time. A negative change in volume indicates that more sediment left the reach that year and therefore, the reach potentially degraded (negative slope). A positive value indicates storage of sediment in the reach or aggradation (positive slope). Sediment inputs from all of the arroyos are not accounted for, so the resulting differences may be slightly less than the actual values.

The LFCC data was included at Bernardo because the USGS topographic maps of the reach show that the flow in the conveyance channel at Bernardo is returned to the Rio Grande upstream from San Acacia. Suspended sediment was measured in the conveyance channel at Bernardo from 1967 to 1974. An attempt was made to estimate the sediment in the LFCC from 1975 to 1995 using a regression equation based on measured water discharge. However, the water discharge in the conveyance channel decreased so much after 1974 that the post-1974 water discharges were beyond the range of accuracy of the regression equation. As a result, no sediment inputs were added to the analysis for the conveyance channel from 1975 to 1995. The combined LFCC and floodway data at San Acacia were used to most accurately represent the true outflow of the reach because the diversion into the conveyance channel at San Acacia occurs beyond the extent of this study reach.

4.2 RESULTS

Single-mass Curves

Discharge Mass Curves

The discharge mass curves for San Acacia and Bernardo floodway and conveyance channel have similar trends, indicating that there is not a significant water input from the ephemeral tributaries along the reach. However, recent trends indicate that these tributaries may be becoming more significant as the separation of the San Acacia and Bernardo trend lines continues to grow. A break in the slope occurs in 1978, with an increase in annual discharge rate from 1978 to 1999 (Figure 4-1). Another break in slope occurs in 1999, with a recent decrease in annual discharge rate. The recent slope (1999-2003) is close to that of the slope that was present prior to 1978.

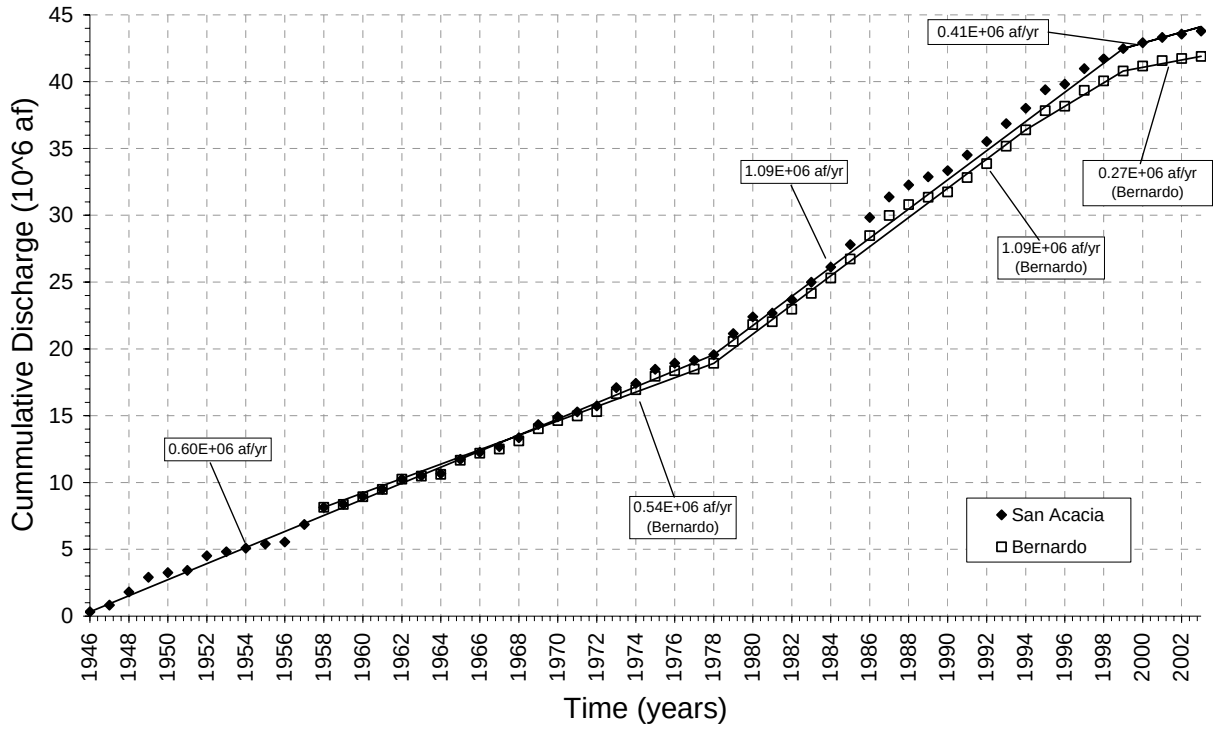

Figure 4-1 Discharge mass curve (floodway and conveyance channel) at Bernardo and San Acacia

Suspended Sediment Mass Curve

The suspended sediment mass curve for San Acacia (floodway + conveyance channel) shows two breaks in slope in 1973, 1986 and 1999. Changes in suspended sediment rate were appreciable among the three periods 1946 to 1973, 1973 to 1986, 1986 to 1999 and 1999 to 2003 (Figure 4-2). The 1973 break matches with the closure of Cochiti Dam. The suspended sediment mass curve at Bernardo has a slope break in 1991, where the suspended sediment load increased (Figure 4-2). From 1973 to 1986, the annual sediment load at San Acacia was greater than at Bernardo. This may be a result of degradation/bank erosion in the reach or from tributary inputs that were not accounted for. From 1991 to 1995, the annual sediment load at Bernardo was greater than that at San Acacia. This indicates potential storage of sediment within the reach. From 1995 to 2003, the annual sediment load was significantly smaller than it had been in all previous years at both gaging stations. This can likely be attributed to the decrease in discharge in the reach and the aggradation also present within the reach during this time period.

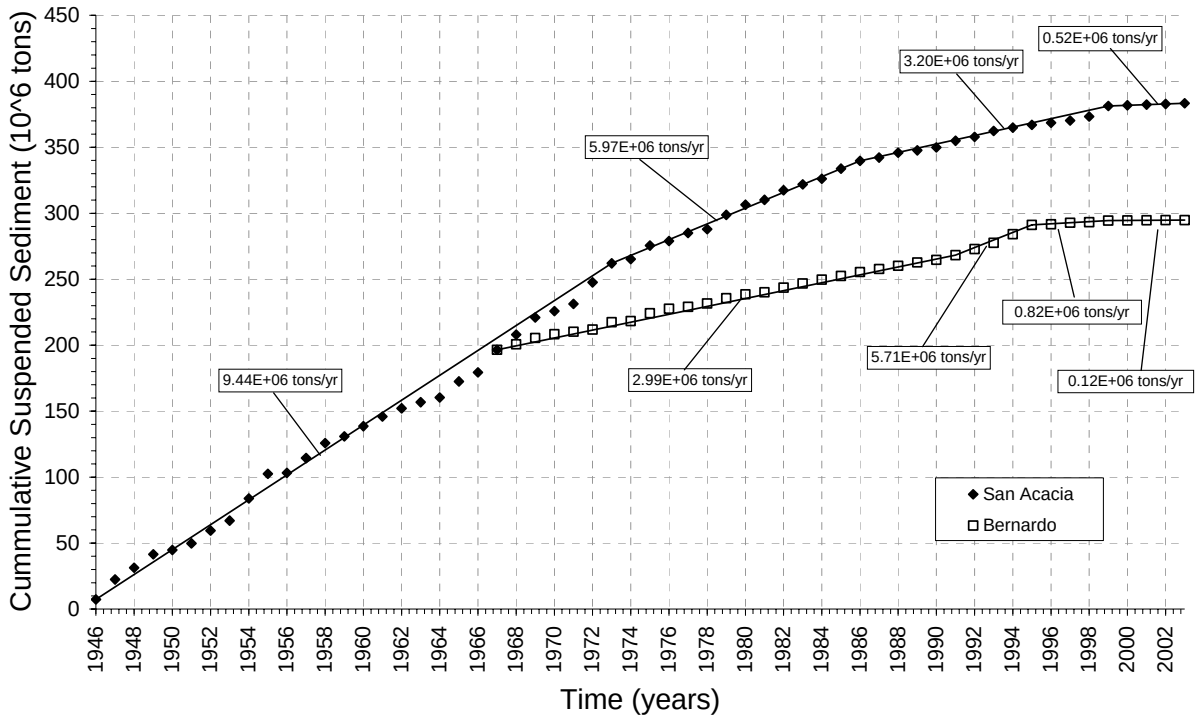

Figure 4-2 Suspended sediment mass curve (floodway + conveyance channel) at San Acacia and Bernardo

Double mass curves

The double mass curves of cumulative water discharge versus cumulative sediment discharge provide insights into how the suspended sediment concentration changed with time. The curves, using the floodway only, show how the sediment concentration in the floodway changes. Combining the low flow conveyance channel and the floodway in this analysis shows what the average concentration of sediment was between the floodway and the conveyance channel. The plot using the floodway only at San Acacia shows a relatively high concentration of suspended sediment from 1946 to 1977 with average concentration varying from 7,250 mg/l to 31,145 mg/l (Figure 4-3). After 1977, the concentration did not exceed 5,000 mg/l until 1997. The slope of the combined double mass curve of Rio Grande near Bernardo and Rio Puerco near Bernardo (floodway only) shows high suspended sediment concentration from 1963 to 1978, decreasing after 1978 to a constant value of 2,290 mg/l. The suspended sediment concentrations at San Acacia from 1982 to 1997 and at Bernardo and Rio Puerco after 1978 were almost equal.

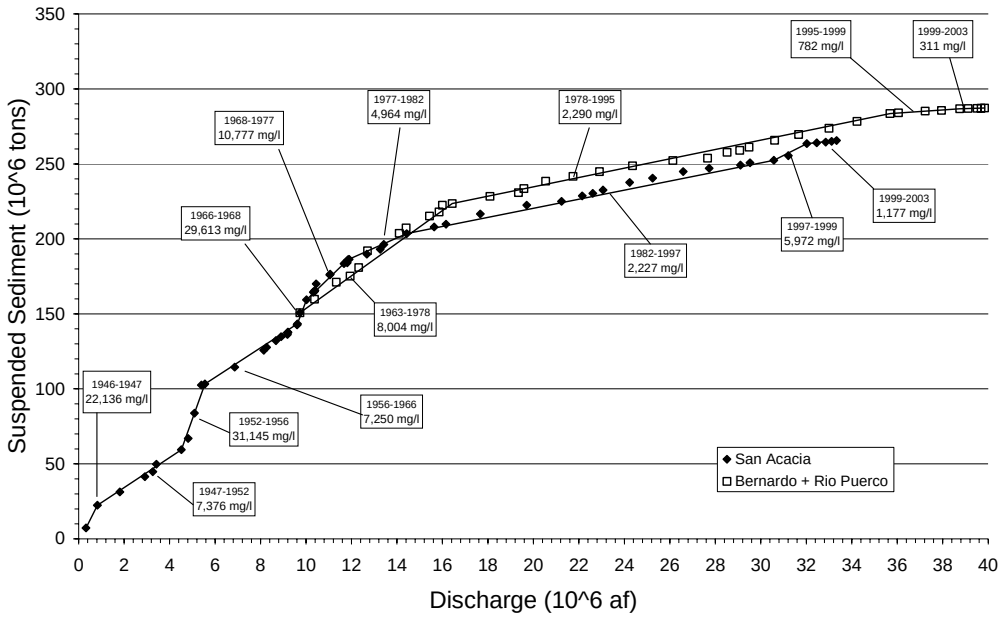

Figure 4-3 Cumulative discharge vs. cumulative suspended sediment load at Rio Grande near Bernardo, Rio Puerco near Bernardo and San Acacia Floodway (1946 - 2003)

The combined floodway and conveyance channel double mass curve at San Acacia (figure 4-4) shows different break points from the floodway only plot (Figure 4-3). Rather than an abrupt change after 1977, the concentrations changed smoothly from 1966 to 1982. In general, concentration values were lower in the combined floodway and conveyance channel curve at San Acacia, indicating that more water and less sediment was flowing in the conveyance channel.

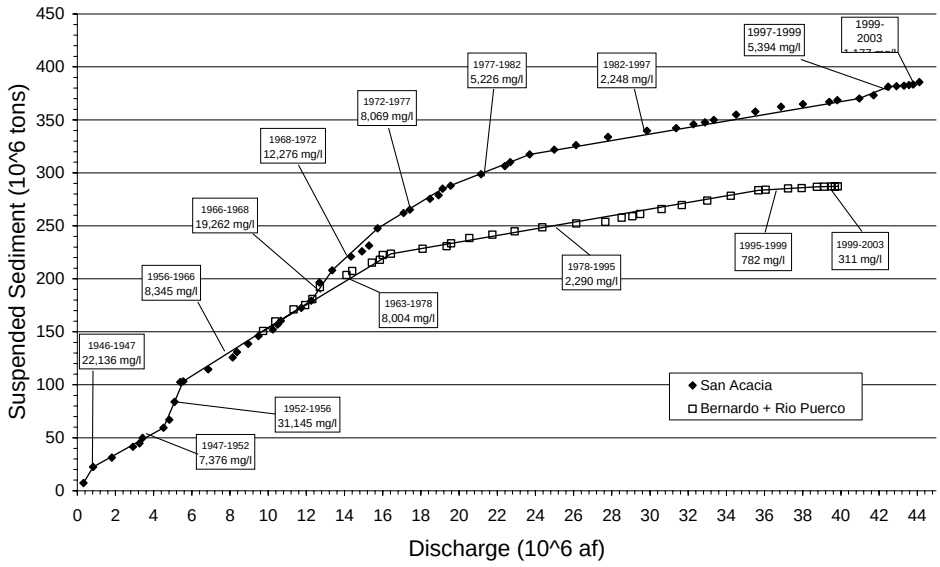

Figure 4-4 Cumulative water discharge vs. cumulative suspended sediment discharge Rio Grande at Bernardo and San Acacia Floodway and Conveyance Channel (1946 - 2003)

Difference Mass Curves

The combined floodway and conveyance channel data more accurately represented the responses of the Rio Puerco reach (see discussion of conveyance channel flow in Section 4-1 Methods). The suspended sediment difference mass curve for the conveyance channel and floodway together shows degradation, with the outflow of sediment at San Acacia being greater than the inflow (Bernardo and Rio Puerco) from 1967 to 1986 (Figure 4-5). In 1985, the slope of the mass curve flattened out indicating no significant aggradation or degradation from the late 1980's to 1993. After 1993, the slope of the mass curve increased rapidly, indicating significant aggradation within the reach. The recent cumulative suspended sediment values exceeded the original 1967 just after 2001 and has since continued to increase with time.

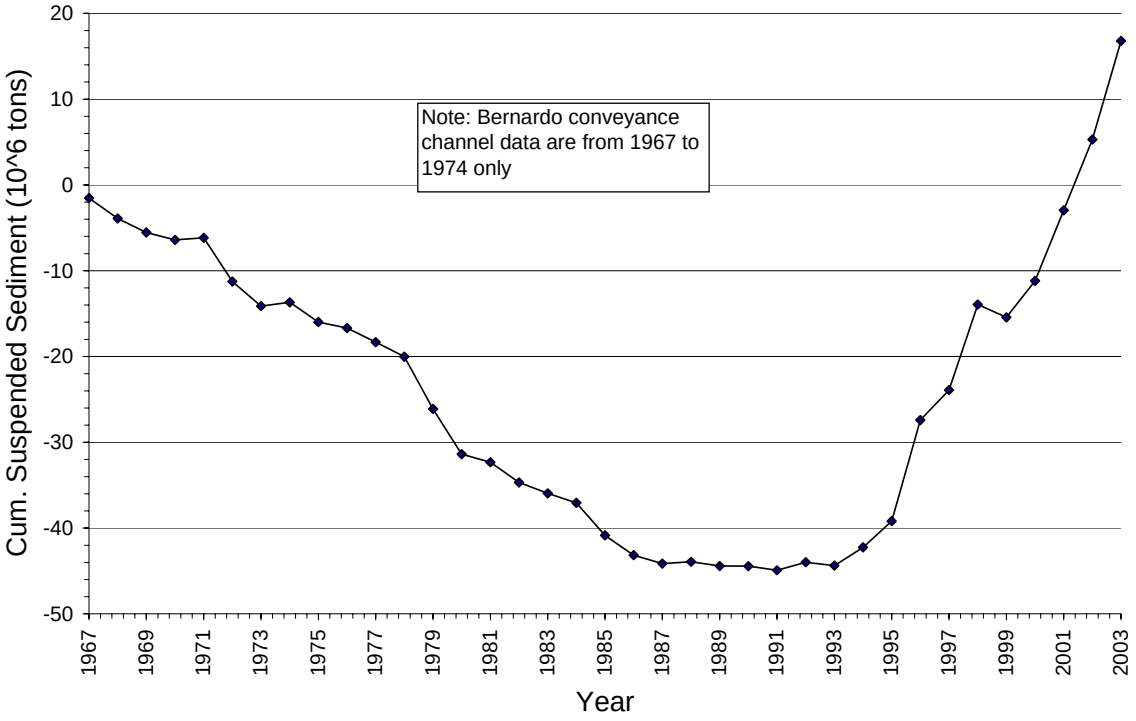

Figure 4-5 Difference (Inflow – Outflow) suspended sediment mass curve of floodway and conveyance channel from Bernardo to San Acacia.

5 EQUILIBRIUM STATE PREDICTORS

5.1 EQUILIBRIUM SLOPE BASED ON SEDIMENT TRANSPORT ANALYSIS

Methods

One definition of an equilibrium channel is one in which the slope is adjusted so that the inflow of sediment to the reach equals the outflow of sediment (Knighton 1998). Using this definition, the equilibrium slope of the channel was estimated by balancing the capacity of the channel to transport sand with the incoming bed material sand-sized load. The following section describes the methods by which the incoming bed material sand-sized load and the bed material sediment transport capacity of the study reach were estimated. The channel slope was then varied in the bed material sediment transport equations until the resulting transport capacity approximately equaled the incoming bed material sand load.

The total sand-sized sediment input to the reach was estimated using the Bureau of Reclamation Automated Modified Einstein Procedure (BORAMEP). The input data, detailed cross section geometry measurements, suspended sediment samples, and bed material samples were taken at the Bernardo gage by the USGS from 1960 to 2002 and are presented in Appendix C. These data were collected specifically for the purpose of estimating the total sediment load using the BORAMEP.

The data were subdivided by separating snowmelt, summer thunderstorms, and winter flow. The snowmelt period was defined as April to June based on study of the mean-daily discharge record for the Bernardo gaging station from 1990 to 2002. Using the snowmelt data for the period of 1990 to 2002, the BORAMEP was utilized to compute the total sediment load.

The resulting sand-sized sediment load estimate from the BORAMEP, using the Bernardo gage data, was plotted against the measured water discharge to create a sand-load rating curve. A power-law function was fit to the data. The Bernardo rating curve was used to the estimate the incoming sand-sized bed material load for subreaches 1 and 2, based on the observation that the Rio Puerco currently contributes mostly silt and clay to the Rio Grande (Baird, pers. comm. 2000). Therefore, the sediment flow at the Bernardo gage (located upstream of the study reach) adequately estimated the incoming load to the reach.

Reclamation created a similar rating curve for the San Acacia gage (Reclamation 2003). The San Acacia rating curve was used to estimate the sand input to subreach 3. This subreach is located downstream from the mouth of the Rio Salado. The sediment flow at the San Acacia gage therefore represents the sediment load in this reach more accurately than the Bernardo gage estimates.

The proportions of the incoming sand-load that equals the bed material load and the washload of the reach were estimated based on the bed and suspended sediment particle size distribution data at the Bernardo gage. The washload comprises the range of fine particles not found in large quantities in the bed ($ds < d_{10}$). The incoming sand-load to the reach was estimated from the BORAMEP sand-load rating curve at a water discharge of 5,000 cfs. Then, the incoming sand-sized bed material load was computed by multiplying the incoming sand-load at 5,000 cfs by the percentage of suspended sediment material finer than the d_{10} of the bed material. The d10 of the bed material was determined from analysis of gaging station data.

The bed-material transport capacities of the subreaches were estimated using several sediment transport equations, including Engelund and Hansen, Ackers and White (d50), Yang – Sand (d50), Einstein, Laursen and Toffaleti (Stevens and Yang 1989). The channel geometry predicted by HEC-RAS for Q = 5,000 cfs, was used as input to the sediment transport capacity equations to compute the bed-material transport capacity of the channel. The product of the reach-averaged values of width, depth and velocity determined from HEC-RAS resulted in a discharge greater than 5,000 cfs. In order to satisfy continuity, the average velocity was re-calculated by dividing the discharge (5,000 cfs) by the average cross-section area. The new velocity values are shown in Table 5-1 and are closer in magnitude to the cross-section averaged velocities measured in the Rio Puerco reach in the 1990's by the USGS. Further modeling of flow in the main channel should be performed to determine if this correction is reasonable.

In order to select which sediment transport method best represented the current sediment transport capacity of the reach; the estimated bed material capacity using the existing slope was compared to the incoming bed material sand-load estimate. Sediment transport capacities were calculated for the existing channel slope values and for a discharge equal to 5,000 cfs using the same six sediment transport equations. Bed material sediment transport capacities for subreaches 1 and 2 were compared to the incoming sand-sized bed material load estimated

from the MEP rating curve at Bernardo. Results at subreach 3 were compared to the incoming sand-sized bed material load estimated from the MEP rating curve at San Acacia. The method that produced the minimum sum-squared difference or sum of the squared error (SSE) between the estimated capacity and incoming sand-sized bed material load was considered most appropriate for use in that subreach.

The ability of the transport formulae to duplicate individual values from the BORAMEP was also evaluated through the discrepancy ratio (i_b observed / i_b calculated), where i_b is the transport load (Gomez and Church 1989). A perfect prediction produces a discrepancy ratio equal to one.

The channel slope was then adjusted to produce a transport capacity that approximated the incoming sand-sized bed material load estimate. The slope adjustment was performed for each sediment transport equation separately. The slope computed from the method with the lowest discrepancy ratio and minimum SSE was selected as the equilibrium slope. This method of selecting the sediment transport capacity equations inherently results in an equilibrium slope that is closest to the existing slope. However, based on the assumption that the channel is capacity limited, (sediment supply exceeds transport capacity) this method of selection is appropriate given the available data.

Results

The sand-load rating curve for the incoming sand-sized sediment load at the Bernardo gage predicted by the BORAMEP is presented in Figure 5-1. Using a channel forming discharge of 5,000 cfs, the estimated sand-load at the Bernardo gaging station is 17,800 tons/day.

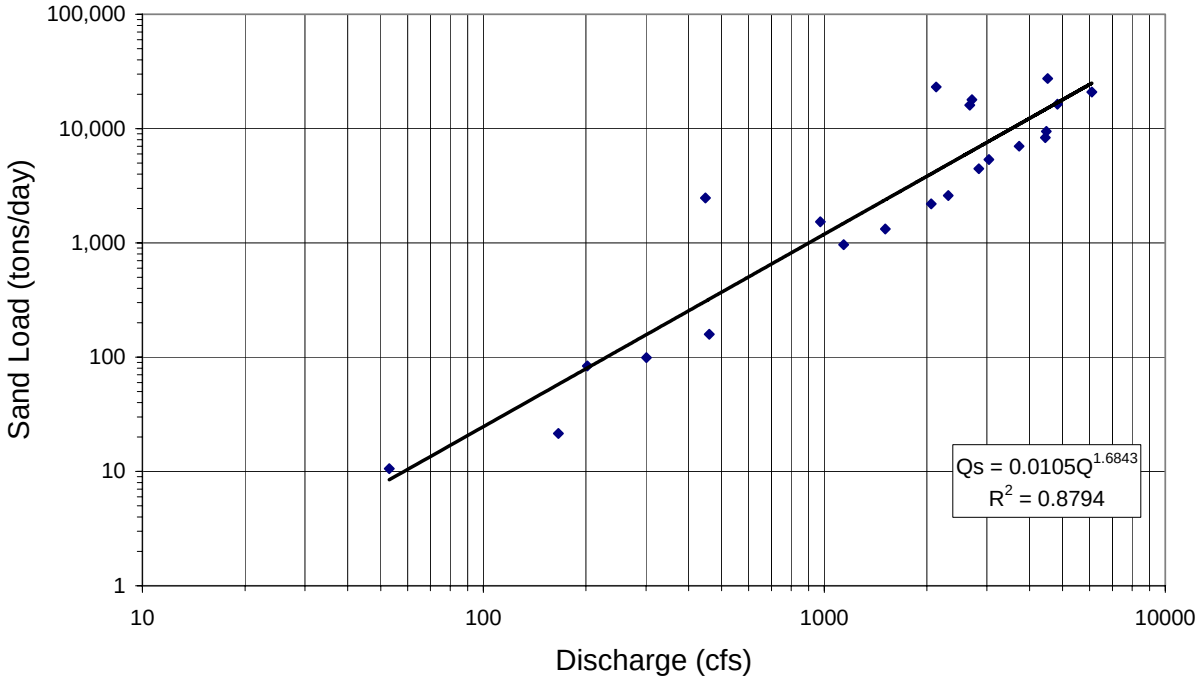

Figure 5-1 Bernardo Snowmelt BORAMEP Sand Load Rating Curve

From the bed material particle size distributions from the Bernardo gaging station, the d_{10} is between 0.105 and 0.16 mm or very fine to fine sand and the average d_{10} is 0.125 mm. On average, 45% of the suspended material is finer than 0.125 mm. Therefore, 55% of the total sand load corresponds to the sand-sized bed material load. The resulting sand load being transported at the bed is 9,790 tons/day. Based on this analysis, 9,800 tons/day was used as the bed-material load input to the subreaches for the following analysis.

The results of the sediment transport equations using the existing conditions are given in Appendix C. The slope of the channel was adjusted to make the capacity equal the incoming sand-sized bed-material load (9,800 tons/day). The adjusted slopes and resulting capacity estimates are presented in Table 5-1. The average and median of the adjusted slopes and the average of the adjusted slopes less than the existing slopes are also included in Table 5-1.

Table 5-1 Results of equilibrium slope predictions from sediment transport capacity equations.

	Subreach 1		Subreach 2		Subreach 3	
Estimated Sand Load input (t/day) =	9800		9800		9800	
Existing Channel Slope =	0.00063		0.00055		0.00111	
Mean Velocity (ft/s) = Q/A = (Q = 5,000 cfs)	3.63		4.69		3.87	
Sediment Transport Equations	Sed. Tranport Capacity (t/day)	Slope	Sed. Tranport Capacity (t/day)	Slope	Sed. Tranport Capacity (t/day)	Slope
Engelund & Hansen	9881	0.00045	9739	0.00033	9646	0.00043
Ackers & White (d50)	9861	0.00038	9662	0.00024	9712	0.00031
Yang - Sand (d50)	9766	0.00067	9790	0.00053	9791	0.00063
Einstein	9774	0.00082	9970	0.00031	9835	0.00057
Laursen	9729	0.00054	9911	0.00043	9785	0.00045
Toffaleti	9808	0.00029	-	-	9905	0.00018
Average Slope		0.00053		0.00037		0.00043
Median Slope		0.00050		0.00033		0.00043
Average (Slopes < Existing Slopes)		0.00042		0.00037		0.00043

The sediment transport capacity estimates varied widely for each subreach as seen in Table 5-1. Yang's equation produces the closest slope to the existing channel slope of the three subreaches and suggests milder equilibrium slopes. Computation of the SSE and the discrepancy ratio proved useful in selecting an appropriate sediment transport equation. The results of the SSE and discrepancy ratios are provided in Appendix C. The Engelund and Hansen, Akers and White and Colby equations most closely estimated the incoming sand-sized bed material load in subreaches 1 and 2 based on the discrepancy ratios. The Colby, Einstein and Yang equations produced the lower SSE values for the three subreaches. However, Yang and Einstein's equations predicted steeper slopes than the 2002 channel slope for subreach 1, which will reverse the aggradational trend of the river bed. Based on these criteria, Yang's equation is deemed to be the more appropriate equation for application to the three subreaches.

The average and median of the adjusted slope values yield milder channel slopes for all 3 subreaches. However, the average and median slopes for subreach 1 are relatively close to the 2002 channel slope. The degradational trend observed between 1972 and 1992 was reversed by decreasing the channel slope between 1992 and 2002, resulting in aggradation. The average of the predicted slope values that are less than the 2002 slopes suggest a 34%, 34% and 61% decrease from the measured 2002 slopes for subreaches 1, 2 and 3 respectively.

5.2 HYDRAULIC GEOMETRY

Methods

Hydraulic geometry equations are a means of estimating stable channel geometry based on a channel-forming discharge. Some methods also require bed material size, channel slope, and/or sediment concentration. Most hydraulic geometry methods are developed from and applied to either man-made canals or single-thread natural channels. The input data used in the computation described in this section are presented in Table 5-2. The 50-year return period discharges are from Bullard and Lane (1993) report. The averaged suspended sediment concentration values are estimated from the double mass curve (Figure 4-3) developed from the Rio Grande at Bernardo (includes Rio Puerco) and San Acacia floodway data. The Rio Grande data at Bernardo plus Rio Puerco was used for subreaches 1 and 2, while the San Acacia floodway data is used for subreach 3.

Table 5-2 - Hydraulic geometry equation input data

1962	Q (cfs)	Q50/Q	d50 (m)	Avg C (ppm)
Reach 1	5,000	5.61	0.0002	7,965
Reach 2	5,000	5.61	0.0002	7,965
Reach 3	5,000	5.61	0.0002	7,218
Total Reach	5,000	5.61	0.0002	7,716
1972				
Reach 1	5,000	3.96	0.0002	7,965
Reach 2	5,000	3.96	0.0002	7,965
Reach 3	5,000	3.96	0.0002	10,706
Total Reach	5,000	3.96	0.0002	8,879
1992				
Reach 1	5,000	3.96	0.0003	2,287
Reach 2	5,000	3.96	0.0003	2,287
Reach 3	5,000	3.96	0.0002	2,224
Total Reach	5,000	3.96	0.0003	2,266
2002				
Reach 1	5,000	3.96	0.0002	1,126
Reach 2	5,000	3.96	0.0002	1,126
Reach 3	5,000	3.96	0.0002	2,992
Total Reach	5,000	3.96	0.0002	1,748

The following hydraulic geometry equations were applied to estimate the equilibrium width of the Rio Puerco reach and subreaches for 1962, 1972 and 1992 using the data shown in Figure 5-2:

- Leopold & Maddock (1953) developed a set of empirical equations that relate the hydraulic geometry of alluvial channels to a power function of bankfull discharge:

$$W = aQ^b$$

$$D = cQ^e$$

$$V = kQ^m$$

where, ack = 1 and b+e+m = 1 and b=0.50, e=0.40 and m=0.10.

- Julien and Wargadalam's (1995) regime geometry equations are "semi-theoretical" equations based on four fundamental hydraulic relationships – continuity, resistance, sediment transport and secondary flow. The simplified equations that use discharge, bed material size and slope as the independent variables to calculate depth, width, velocity and Shield's parameter are:

$$D = 0.200 Q^{\frac{2}{6m+5}} d^{\frac{6m}{6m+5}} S^{\frac{-1}{6m+5}}$$

$$W = 1.330 Q^{\frac{4m+2}{6m+5}} d_s^{-\frac{4m}{6m+5}} S^{\frac{-(2m+1)}{6m+5}}$$

$$V = 3.758 Q^{\frac{2m+1}{6m+5}} d_s^{-2m(6m+5)} S^{\frac{2m+1}{6m+5}}$$

$$\tau_* = 0.121 Q^{\frac{2}{6m+5}} d_s^{\frac{-5}{6m+5}} S^{\frac{6m+4}{6m+5}}$$

$$m = \frac{1}{(\ln \frac{12.2D}{d_{50}})}$$

- Simons & Albertson [(1960), from Wargadalam (1993)] developed the equations from analysis of Indian and American canals.

  1) Sand bed and banks:

  $$P = 3.5 Q^{0.512} \text{ , (ft)}$$

  2) Coarse non-cohesive material:

  $$P = 1.75 Q^{0.512} \text{ , (ft)}$$

  where,

  P = wetted perimeter ≅ width (for width >> depth)

- Blench [(1939-1957), from Wargadalam (1993)] developed a relationship that accounts for the cohesiveness of the sides of the channel:

  $$W = \left(\frac{9.6(1 + 0.012c)}{F_s} \right)^{\frac{1}{2}} d^{\frac{1}{4}} Q^{\frac{1}{2}} \text{ , (ft)}$$

  where,

  c = sediment load concentration (ppm),

  d = d_{50} (mm), and

  F_s = 0.1, 0.2, 0.3 (scale of cohesiveness of banks from slight to high).

- Lacey [(1930-1958), from Wargadalam (1993)]

$$P = 2.667Q^{0.5} \text{ (ft)}$$

where,

P = wetted perimeter (feet)

Klaassen-Vermeer (1988) developed a relationship for braided rivers based on work on the Jamuna River:

$$W = 16.1Q^{0.53} \text{ (m)}$$

- Nouh (1988) developed equations for extremely arid channels in Saudi Arabia:

$$W = 28.3\left(\frac{Q_{50}}{Q}\right)^{0.83} + 0.018(1+d)^{0.93}c^{1.25}, \text{ (m)}$$

where,

Q_{50} = peak discharge for 50 yr. Return period (m^3/s)

Q = annual mean discharge (m^3/s)

d = d_{50} (mm)

c = mean suspended sediment concentration (Kg/m^3).

Additionally, empirical width-discharge relationships specific to the Rio Puerco reach were developed from the GIS active channel widths and the averaged peak flows from the 5-years prior to the survey date. The input data are presented in Table 5-3. The empirical equations were determined by a power-law fit to the width and peak discharge data. The resulting equations take the following form:

$$W = a\,Q^b$$

where:

W = Active channel width (feet); and

Q = Peak discharge (cfs).

Table 5-3 - Input data for empirical width-discharge relationships

		Active Channel Width (feet)			
Year	Discharge (cfs)	Subreach 1	Subreach 2	Subreach 3	Total Reach
1918	11,630	1,616	776	3,086	1,721
1935	6,608	1,887	826	2,394	1,745
1949	7,320	1,377	826	1,513	1,263
1962	5,158	569	556	1,122	695
1972	4,238	623	282	891	603
1985	5,656	731	181	973	653
1992	4,581	459	172	649	432
2002	3,456	501	167	582	432

Results

The equilibrium width predicted by the hydraulic geometry equations for 5,000 cfs are summarized in Table 5-4. The equations that do not include sediment concentration (Simons and Albertson, Lacey and Julien-Wargadalam) predict lower widths than those that do include sediment concentration (Nouh and Blench). The equations developed by Nouh and Blench do not appear to apply to Rio Puerco reach based on the conditions for which they were developed (extremely arid regions and cohesive banks).

Table 5-4 Predicted Equilibrium Widths from Hydraulic geometry equations for Q = 5,000 cfs

				Predicted Width (feet)						
Q = 5,000 cfs	Subreach #	GIS Active Channel Width (feet)	Reach-Averaged HEC-RAS Main Channel Width (feet)	Simons and Albertson	Klassen & Vermeer	Nouh	Blanch	Lacey	Julien-Wargadalam	Bernardo Empirical Equations
1962	**1**	569	686	274	729	5,068	1,891	189	284	-
	2	556	501	274	729	5,272	2,032	189	286	-
	3	1,122	840	274	729	4,662	1,936	189	278	-
	Bernardo	695	675	274	729	5,067	2,001	189	283	-
1972	**1**	623	727	274	729	5,270	2,032	189	276	-
	2	282	342	274	729	5,270	2,032	189	290	-
	3	891	970	274	729	7,624	2,353	189	284	-
	Bernardo	603	684	274	729	6,035	2,145	189	281	-
1992	**1**	459	499	274	729	1,198	1,221	189	286	695
	2	172	193	274	729	1,198	1,221	189	306	316
	3	649	406	274	729	1,157	1,204	189	251	989
	Bernardo	432	393	274	729	1,184	1,215	189	278	674
2002	**1**	459	492	274	729	477	825	189	289	716
	2	172	215	274	729	477	825	189	297	314
	3	649	476	274	729	1,578	1,287	189	258	998
	Bernardo	432	413	274	729	817	1,008	189	281	682

Figure 5-2 is a plot of the measured non-vegetated active channel width versus the predicted width from the hydraulic geometry equations. Subreach 2 most closely matches the equilibrium width predicted by Lacy, Julien-Wargadalam, and Simons and Albertson in 1972, 1992 and 2002. Also, the width of subreach 1 in 1972 is approximated by Klaassen and Vermeer's equation.

Hydraulic geometry equations are intended to compute the width of a stable or equilibrium channel. The fact that the equation results do not match the measured channel width does not imply that the equations are erroneous. Most likely, it suggests that the channel historically was not in an equilibrium state, which is validated by the evidence of both aggradation/degradation and narrowing of the channel during the time period analyzed. The width calculated from the hydraulic geometry equations may suggest the single-thread equilibrium width toward which the channel is moving.

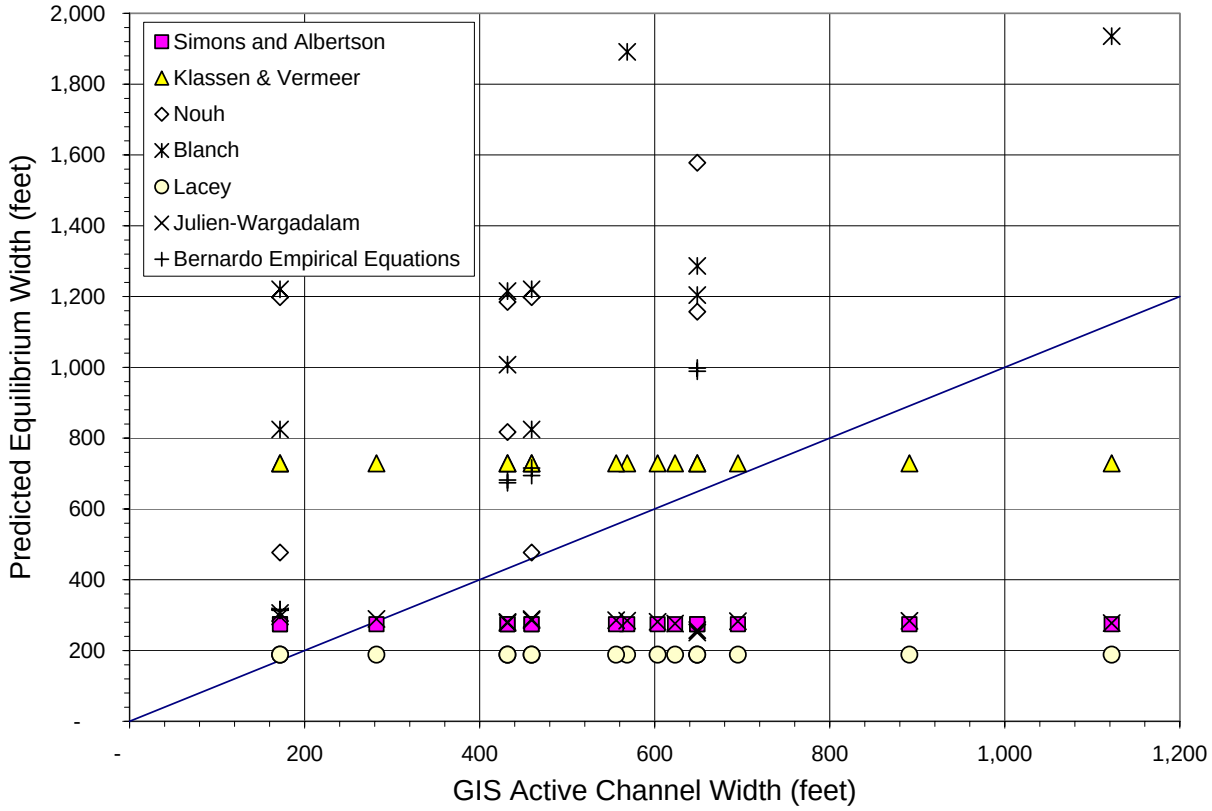

Figure 5-2 - Hydraulic Geometry equation results - observed non-vegetated active channel width vs. predicted equilibrium width.

Empirical width-discharge relationships ($W = a\,Q^b$) were developed for the Rio Puerco reach and the subreaches based on the active channel width measured from the GIS coverages of the non-vegetated active channel. The results are shown in Figure 5-3. The widths predicted for each of the reaches for 5,000 cfs are given in the last column of Table 5-4. These widths do not necessarily represent the equilibrium width of the subreaches. The empirical equations are based on historic data, when the channel may not have been in an equilibrium state. However, these equations are useful in comparing channel characteristics between the subreaches.

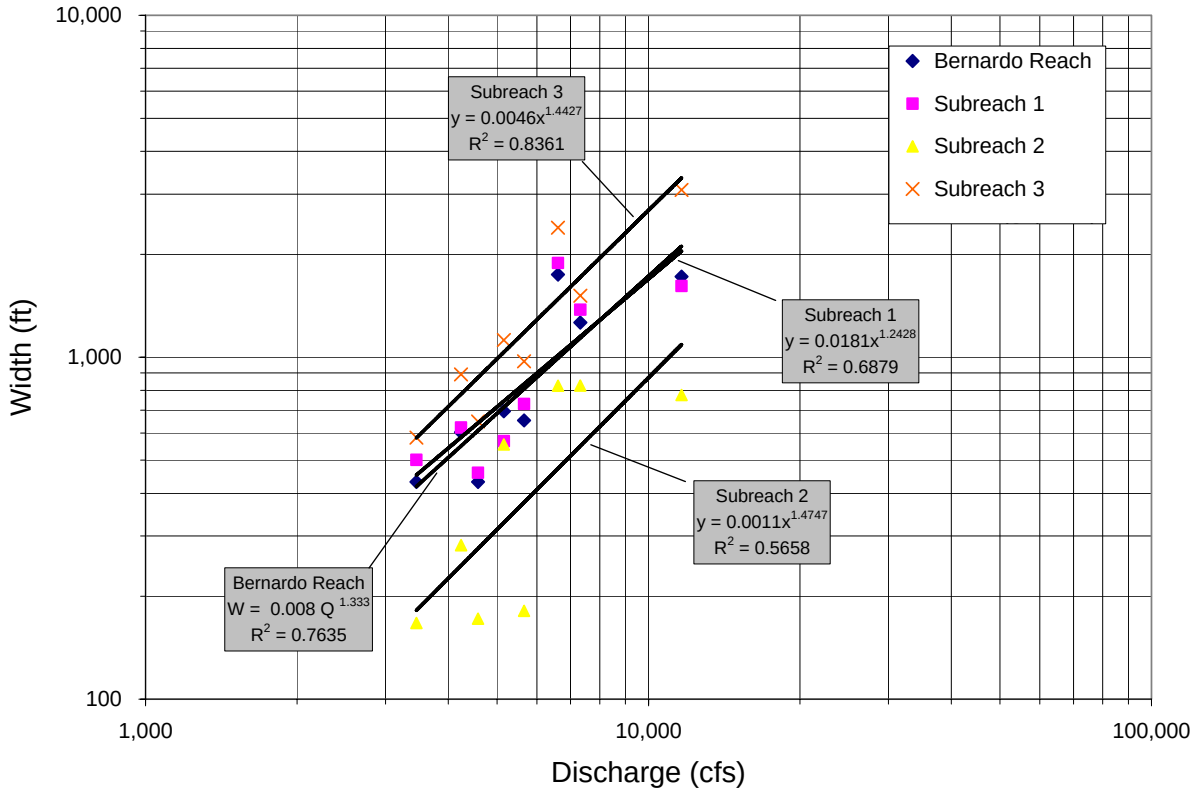

Figure 5-3 Empirical width-discharge relationships for the Rio Puerco reach

5.3 ADJUSTED HYDRAULIC GEOMETRY EQUATIONS

Nouh's Equation

Nouh (1988) developed regime equations from ephemeral channels located in the south and southwest regions of Saudi Arabia. The equations provide information of channel dimensions

under varying flash flood and sediment flow conditions in an extremely arid zone. The ephemeral channels carry water and large amounts of fine suspended sediment only during flash floods. Soils vary from sand to sandy clay.

A total of 37 ephemeral, stable channel cross sections were identified. Measurements of bed slope, channel width, depth as well as flow discharge and suspended sediment concentration were performed in each cross section during several flood events. Nouh (1988) found that the ratio of annual peak flood flow for a return period of 50 years (Q_{p50} in m^3/s) to annual mean flood flow (Q in m^3/s) yielded the best correlation with the width, depth and slope of the ephemeral channel in the study area.

The following regression equation was obtained for the channel width:

$$B = 28.30\left(\frac{Q_{p50}}{Q}\right)^{0.83} + 0.018(1+d)^{0.93} C^{1.25}$$

where: B is the channel width (in meters), d is the median size diameter of suspended sediment (in millimeters), C is the mean concentration of suspended sediment in (Kg/m^3).

Nouh's equation was applied in the Rio Puerco reach as described in Chapter 5.2. The predicted width values exceeded more than 100% the GIS active channel widths and reach-averaged HEC-RAS main channel widths. However, this equation yielded changes in width with time due to its dependency to variables other than the flow discharge. In order to better predict the changes in the channel width, the coefficients of the equations were adjusted until the predicted width values were close to the observed values. The resulting equations corresponded to the equations that yielded the minimum sum of square errors (SSE) between the predicted and measured values. The 1962 and 1972 data were used to adjust the equations. The 1992 and 2002 data were used for verification of the equations. An equation for each subreach was obtained.

Adjusted coefficients and input data used in the width computations are summarized in Table 5-5. Predicted and measured widths are also included for comparison. The shaded area in Table 5-5 contains the predicted 1992 and 2002 widths using the adjusted equations generated from the 1962 and 1972 data. Modified equations for each subreach are summarized in Table 5-6.

Table 5-5 Nouh's width equation adjusted coefficients and input data

				Coefficients		Exponents				
	Avg from San Acacia Gage d50 (mm)	Avg C (Kg/m^3)	Q50/Q	ε_1	ε_2	α	β	γ	GIS Active Channel Width (feet)	Nouh's Width using adjusted coefficients
Year :1962										
Subreach 1	0.20	7,965	5.6	0.01	0.007	0.83	0.93	1.25	569	594
Subreach 2	0.20	7,965	5.6	2,176	0.003	0.83	0.93	1.25	556	466
Subreach 3	0.20	7,218	5.6	1,102	0.008	0.83	0.93	1.25	1,122	759
Year: 1972										
Subreach 1	0.20	7,965	4.0	0.01	0.007	0.83	0.93	1.25	623	594
Subreach 2	0.20	7,965	4.0	2,176	0.003	0.83	0.93	1.25	282	417
Subreach 3	0.20	10,706	4.0	1,102	0.008	0.83	0.93	1.25	891	1,153
Year: 1992										
Subreach 1	0.31	2,287	4.0	0.01	0.007	0.83	0.93	1.25	459	136
Subreach 2	0.32	2,287	4.0	2,176	0.003	0.83	0.93	1.25	172	211
Subreach 3	0.20	2,224	4.0	1,102	0.008	0.83	0.93	1.25	649	227
Year: 2002										
Subreach 1	0.24	1,126	4.0	0.01	0.007	0.83	0.93	1.25	501	53
Subreach 2	0.24	1,126	4.0	2,176	0.003	0.83	0.93	1.25	167	173
Subreach 3	0.22	2,992	4.0	1,102	0.008	0.83	0.93	1.25	582	298

Nouh's Equation: $B = \varepsilon_1\left(\frac{Q_{p50}}{Q}\right)^{\alpha} + \varepsilon_2(1+d)^{\beta}C^{\gamma}$

Table 5-6 Adjusted Nouh's Equation by subreach

Subreach #	Adjusted Nouh's Equation
1	$B = 0.01\left(\frac{Q_{p50}}{Q}\right)^{0.83} + 0.007(1+d)^{0.93}C^{1.25}$
2	$B = 2{,}176\left(\frac{Q_{p50}}{Q}\right)^{0.83} + 0.003(1+d)^{0.93}C^{1.25}$
3	$B = 1102\left(\frac{Q_{p50}}{Q}\right)^{0.83} + 0.008(1+d)^{0.93}C^{1.25}$

Blench's Equation

Blench (1957) developed regime equations from flume data. The equations account for the differences in bed and bank material by means of a bed and a side factor (Fs) (Thorne et al. 1997). The range of application of Blench's equation is (Thorne et al. 1997):

Discharge (Q): 0.03-2800 m^3/s

Sediment discharge (c): 30-100 ppm

Bed material size (d): 0.1-0.6 mm

Bank material type: cohesive

Bedforms: ripples – dunes

Planform: straight

Profile: uniform

The regime equation for channel width (*W*) is (from Wargadalam (1993)):

$$W = \left(\frac{\varepsilon_1 (1 + \varepsilon_2 c)}{Fs} \right)^{\alpha} d^{\beta} Q^{\gamma}, (ft)$$

where: *Fs* = 0.1, 0.2, 0.3 (scale of cohesiveness of banks from slight to high);

α = 0.5;

β = 0.25;

γ = 0.5;

$\varepsilon_1 = 9.6$; and

$\varepsilon_2 = 0.012$

Blench's equation was applied in the Rio Puerco reach as described in Chapter 5.2. The resulting width predictions overestimated the GIS active channel widths and the reach-average HEC-RAS main channel widths. In order to predict values closer to the observed values, the coefficients of the equation ($\varepsilon_1, \varepsilon_2$) were adjusted. The final equations were selected following the same procedures used in the selection of Nouh's equation. An equation for each subreach was obtained.

Adjusted coefficients and input data used in the width computations are summarized in Table 5-7. Predicted and measured widths are also included for comparison. The shaded area in Table 5-7 contains the 1992 and 2002 predicted widths using the adjusted equations developed from the 1962 and 1972 data. Modified equations for each subreach are summarized in Table 5-8.

Table 5-7 Blench's width equation adjusted coefficients and input data

	Avg from San Acacia Gage d50 (mm)	Avg C (Kg/m^3)	Q50/Q	ε_1	ε_2	α	β	γ	GIS Active Channel Width (feet)	Nouh's Width using adjusted coefficients
Year :1962										
Subreach 1	0.20	7,965	5.6	0.01	0.007	0.83	0.93	1.25	569	594
Subreach 2	0.20	7,965	5.6	2,176	0.003	0.83	0.93	1.25	556	466
Subreach 3	0.20	7,218	5.6	1,102	0.008	0.83	0.93	1.25	1,122	759
Year: 1972										
Subreach 1	0.20	7,965	4.0	0.01	0.007	0.83	0.93	1.25	623	594
Subreach 2	0.20	7,965	4.0	2,176	0.003	0.83	0.93	1.25	282	417
Subreach 3	0.20	10,706	4.0	1,102	0.008	0.83	0.93	1.25	891	1,153
Year: 1992										
Subreach 1	0.31	2,287	4.0	0.01	0.007	0.83	0.93	1.25	459	136
Subreach 2	0.32	2,287	4.0	2,176	0.003	0.83	0.93	1.25	172	211
Subreach 3	0.20	2,224	4.0	1,102	0.008	0.83	0.93	1.25	649	227
Year: 2002										
Subreach 1	0.24	1,126	4.0	0.01	0.007	0.83	0.93	1.25	501	53
Subreach 2	0.24	1,126	4.0	2,176	0.003	0.83	0.93	1.25	167	173
Subreach 3	0.22	2,992	4.0	1,102	0.008	0.83	0.93	1.25	582	298

Blench's equation $W = \left(\frac{\varepsilon_1(1+\varepsilon_2 c)}{Fs} \right)^{\alpha} d^{\beta} Q^{\gamma}, (ft)$

Table 5-8 Adjusted Blench's equation by subreach

Subreach #	Adjusted Blench's Equation
1	$W = \left(\frac{1.0(1+0.01c)}{Fs} \right)^{0.50} d^{0.25} Q^{0.50}, (ft)$
2	$W = \left(\frac{0.1(1+0.07c)}{Fs} \right)^{0.50} d^{0.25} Q^{0.50}, (ft)$
3	$W = \left(\frac{2.4(1+0.01c)}{Fs} \right)^{0.50} d^{0.25} Q^{0.50}, (ft)$

5.4 SAM

Methods

The SAM Hydraulic Design Package for Flood Control Channels, within HEC-RAS (v. 3.1.3, May 2005), was applied to estimate the equilibrium channel width and slope given specified water and sediment discharges and bed material composition. The US Army Corps of Engineers developed SAM for preliminary design of stable flood control channels. The method determines

the dependent design variables of width, depth and slope from the independent variables of discharge, sediment inflow (concentration in mg/l), and bed material composition. Using Copeland's flow resistance and sediment transport equations, the program produces multiple solutions for the width, depth and slope given the input values. The minimum point in the resulting width versus slope curve represents the point of minimum stream power for the given input conditions. The method assumes a trapezoidal cross-section and steady uniform flow conditions.

SAM's stable channel dimensions analysis was applied to the 2002 conditions of the Rio Puerco reach. A series of curves with varying incoming sediment concentrations were plotted. The discharge, slope, and bed material conditions used in the development of Copeland's equations are appropriate for application to the Rio Grande. The input data to SAM included a discharge of 5,000 cfs, valley slope of 0.000752 ft/ft, bank slope of 2H/1V and bank roughness of n = 0.055.

Results

The width-slope curves resulting from the application of SAM are presented in Figure 5-4. The stable channel or minimum stream power width corresponds to the value at the minimum slope on each curve. The equilibrium width for the BORAMEP estimated sand-sized sediment concentration of 800mg/l is 178 feet. For all of the sediment concentrations modeled, the minimum stream power width is narrower than the reach averaged width of subreaches 1 and 3 of the Rio Puerco reach. The 2002 HEC-RAS results of mean channel slope and main channel width for Q = 5,000 cfs are also plotted as points in Figure 5-4 for comparison.

The SAM program estimates the equilibrium or stable channel width for a single-thread channel given a water discharge, sediment concentration, bank slope and bank roughness. The minimum slope corresponds to the minimum stream power for a given discharge. In 2002, the Rio Puerco reach may not have been in equilibrium, hence, it is not surprising that the 2002 measured widths and slopes do not match the minimum stream power configuration for the estimated bed material sand-load and channel-forming discharge.

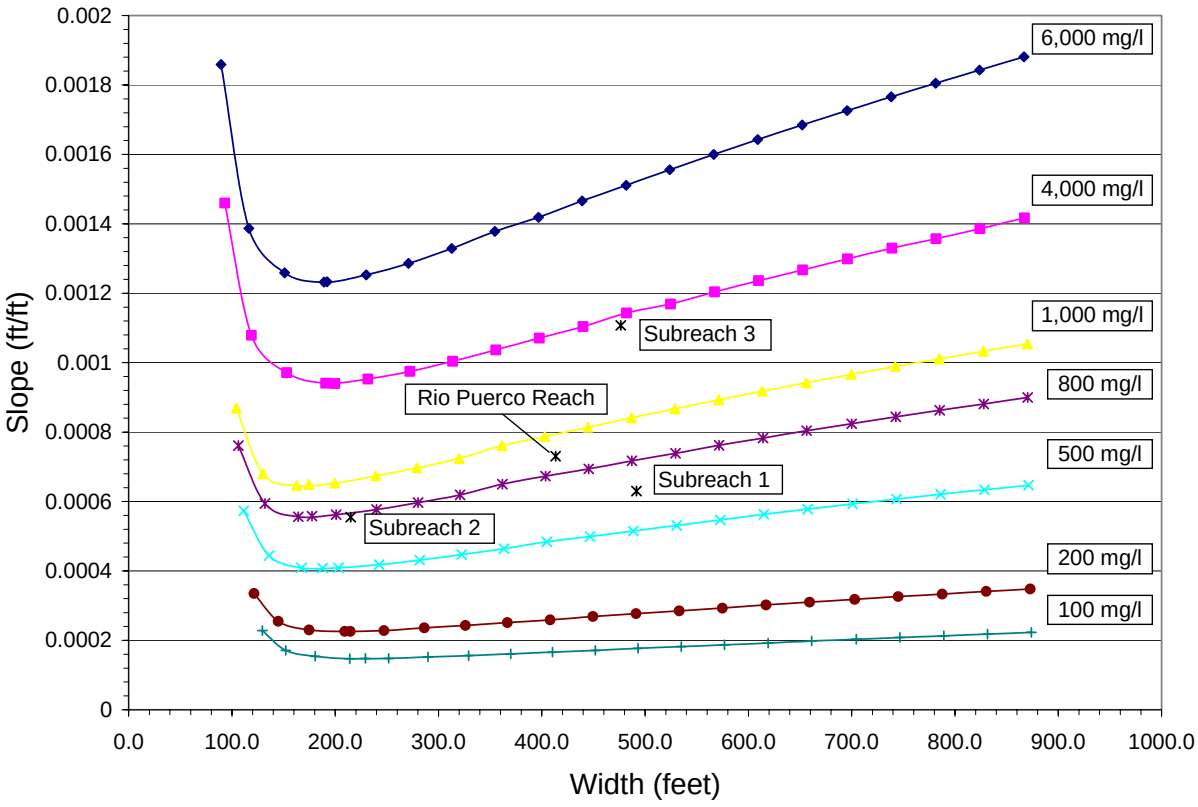

Figure 5-4 - Results from stable channel analysis (SAM) for 2002 conditions and Q = 5,000 cfs.

5.5 HYPERBOLIC MODEL

Method

Williams and Wolman (1984) studied the downstream effects of dams on alluvial rivers. The changes in channel width with time were described by a simple hyperbolic equation of the form:

$$(1/Y) = C1 + C2\,(1/t)$$

where: Y is the relative change in channel width, $C1$ and $C2$ are empirical coefficients, and t is time in years after the onset of the particular channel change. The relative change in channel width is equal to the ratio of the initial width (Wi) to the width at time t (Wt). Coefficients $C1$ and $C2$ might be a function, at least, of flow discharges and boundary materials.

Hyperbolic equations were fit to the Rio Puerco reach data. One equation for each subreach was generated. The time $t = 0$ was taken as the year at which narrowing began. This initial time is different for each subreach and for the entire reach. To adjust the data to an origin of 0, 1.0 was subtracted from each Wt/W1 before performing the regression. The data to which the hyperbolic regressions were applied is shown in Table 5-9.

Table 5-9 - Hyperbolic regression input data

Subreach 1					
Year	t (year)	1/t	Wi (ft)	Wt (ft)	1/(Wt/Wi -1)
1935	0		2160	2160	
1949	14	0.07143		1494	-3.242
1962	27	0.03704		563	-1.352
1972	37	0.02703		691	-1.470
1985	50	0.02000		778	-1.563
1992	57	0.01754		479	-1.285
2002	67	0.01493		501	-1.302

Subreach 2					
Year	t (year)	1/t	Wi (ft)	Wt (ft)	1/(Wt/Wi -1)
1949	0		889	889	0
1962	13	0.0769		576	-2.8413
1972	23	0.0435		287	-1.4774
1985	36	0.0278		181	-1.2564
1992	43	0.0233		173	-1.2415
2002	53	0.0189		167	-1.2312

Subreach 3					
Year	t (year)	1/t	Wi (ft)	Wt (ft)	1/(Wt/Wi -1)
1918	0		2945	2945	0
1935	17	0.0588		2465	-6.14120
1949	31	0.0323		1561	-2.12835
1962	44	0.0227		1231	-1.71837
1972	54	0.0185		954	-1.47939
1985	67	0.0149		1004	-1.51747
1992	74	0.0135		657	-1.28728
2002	84	0.0119		582	-1.24632

Results

Two hyperbolic equations were developed in order to describe the changes in channel width with time. Figure 5-5 and Figure 5-6 show the best fit curves and

Table 5-10 contains the regression equations and coefficients for subreaches 1 and 3. The regression curve for subreach 2 yielded unrealistic predictions, therefore, it was not included in the results.

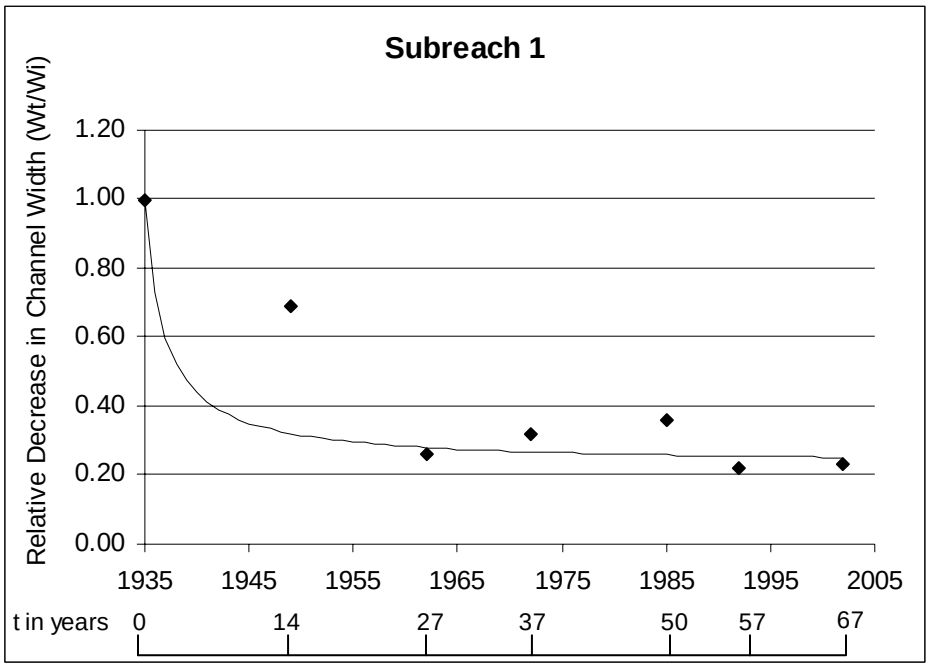

Figure 5-5 - Relative Decrease in Channel Width in Subreach 1

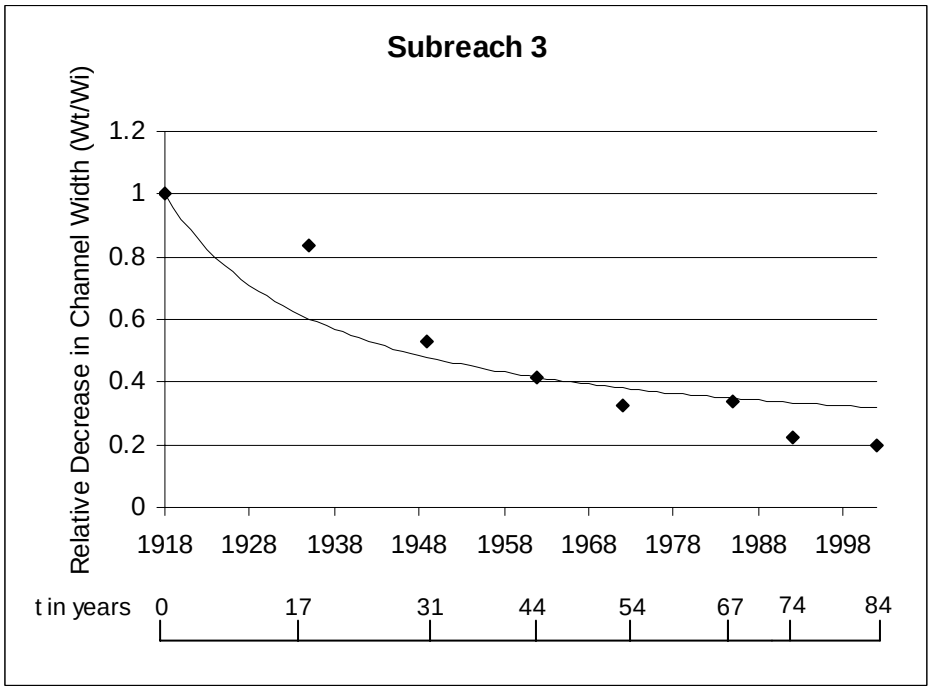

Figure 5-6 - Relative Decrease in Channel Width in Subreach 3

Table 5-10 - Hyperbolic equations describing width change of the Rio Puerco reach.

Subreach	R^2	Regression Equation	Estimated Width (ft)
1	0.9063	$\frac{W_t}{W_i} = \frac{t}{-1.3t - 2.4} + 1$	538
3	0.9387	$\frac{W_t}{W_i} = \frac{t}{-1.2t - 22.4} + 1$	564

6 DISCUSSION

6.1 HISTORIC TREND ANALYSIS AND CURRENT CONDITIONS

Entire Rio Puerco reach

Discharge - Total annual water discharge at the Bernardo and San Acacia gages increased by a factor of two from 1978 to 1999, but has since decreased and now resembles the flow associated with the period of record before 1978 (Figure 4-1). Many factors may influence this including management of Cochiti Dam, irrigation, municipal and industrial water diversions, climatic changes, and efficiency of the riverside drains in retaining subsurface seepage.

Suspended Sediment - The total annual suspended sediment discharge has continued to decrease since 1973 at the San Acacia gage (Figure 4-2). This decrease corresponds to the construction of Cochiti Dam. However, for this time period this change is not evident at the Bernardo gage, which exhibited a constant annual sediment discharge rate from 1967 to 1991. At Bernardo, the discharge rate increased in 1991 to a rate greater than that at San Acacia. However, since 1991, the discharge rate has been decreasing significantly. Sediment concentration at both the Bernardo and San Acacia gages declined from the late 1960's to 2003 (Figures 4-3 and 4-4) as a result of increasing water discharge and decreasing sediment discharge.

Bed Material - The median grain size of the bed material in the Rio Puerco reach falls into the sand classification for the entire period of record analyzed. The largest median grain size was in the medium sand class and very little gravel is seen in the samples before 1983. Changes in the bed material in the Rio Puerco reach included fining with distance downstream from mouth of the Rio Puerco and fining with time since the 1990's.

Channel Pattern - Qualitative observation of the GIS coverages of the active channel show that the trend between 1918 and 2002 has been toward a narrower and straighter channel. The 1962 and 1972 aerial photos of the channel reveal a wide channel bed indicative of a braided planform, in which multiple channels exist at discharges below bankfull. It is likely, based on results of running HEC-RAS at 5,000 cfs that the mid-channel bars were inundated at bankfull or higher flows and therefore gives the appearance of a single thread channel. It is also evident that subreach 2 exhibits a single-thread pattern at all flows in 1962, 1972, 1992 and 2002.

Based on analysis using different channel classification methods, the aforementioned observed spatial and temporal trends in the channel pattern are illustrated best by Parker's method, noting that his meandering classification represents a single thread channel and not necessarily high sinuosity. Lane and Leopold and Wolman both demonstrate the low sinuosity (<1.5) of the channel throughout the time period analyzed.

Vertical Movement - Analysis of the mean bed elevation shows that the channel aggraded from 1962 to 1972, degraded from 1972 to 1992, and aggraded from 1992 to 2002 (Table 3.3). Even though the reach physically aggradation overall from 1962 to 1972, the sediment continuity analysis shows that the sediment leaving the reach decreased from 1967 to 1972, thus suggesting degradation. The data set is not complete thus causing some inconclusive results. However based on Figure 3-4 the channel is both aggrading and degrading at different cross sections with an overall reach aggradation of 0.5 feet. This suggests that the reach is very dynamic. This analysis uses only suspended sediment data and does not include sediment inputs from the Rio Salado, which contributes sand-sized sediment. This additional unmeasured contribution by the Rio Salado could shift this trend from degradation to more stable or even aggradation.

The reach-averaged mean bed degradation from 1972 to 1992 was 4 feet (Table 3-3) and is supported by evidence of degradation in the sediment continuity analysis from 1972 to 1987 (Figure 4-5). From 1987 to 1993, the sediment continuity analysis shows a relatively constant value for the difference between the sediment inflow and outflow. The thalweg elevations from the CO-line surveys in the 1990's also show relatively constant bed elevations (Figure 3-3).

From 1992 to 2002, the reach-averaged mean bed aggradation was approximately 1.5 feet (Table 3-3) and is supported by the sediment continuity analysis from 1992 to 2002 (Figure 4-5). The continuity analysis displayed a rapid increase in sediment storage within the reach.

Channel Geometry - General trends in channel geometry based on HEC-RAS runs of 5,000 cfs using the agg/deg line surveys from 1962 to 1992 were decreasing width, width-depth ratio, and cross-section area, while the depth and velocity increased and energy-grade line slope remained relatively constant, characterized by slight increases and decreases. However, from 1992 to 2002 the HEC-RAS run of 5,000 cfs shows an increased width, width-depth ratio, and cross-section area, while the depth, velocity and energy-grade line decreased. The changes in active channel width measured from the GIS coverage also demonstrate decreasing width since 1935.

Overbank flow/channel capacity - The amount of flow that the main channel can convey also changed with time. Based on HEC-RAS runs of channel-forming discharges the overbank flow area is greater for the 1962 and 1972 data than for 1992 and 2002. The 1992 channel had the fewest cross sections in which the channel-forming discharges flowed out of the main channel into the overbank area. This illustrates the degradational or incising trend as evidenced by the decreased bed elevation and increased velocity and depth discussed above. The majority of the 2002 cross sections were capable of containing the channel-forming discharges within the main channel, particularly at flow rates at or less than 5,000 cfs.

Subreach Trends

Subreaches 1 and 3 exhibit similar temporal trends in channel pattern, geometry and vertical movement, while subreach 2 exhibits different behavior. As a result, discussions of the changes in subreaches 1 and 3 are combined.

Subreaches 1 and 3

Channel Pattern - The general trend with time is toward narrower straighter channel as discussed above for the entire Rio Puerco reach. Based on Parker's channel classification method, in 1962 and 1972, subreaches 1 and 3 tended toward a transition to meandering from single thread. Also, in 1992, subreach 3 exhibits a very steep slope, resulting in a braided classification according to Henderson and Lane's methods. In 2002, the slope of subreach 3 was less steep in than in 1992 and therefore the classification of Lane changed to intermediate.

Vertical Movement - Overall, both subreaches 1 and 3 aggraded between 1962 and 1972 and between 1992 and 2002 and degraded between 1972 and 1992. Between 1962 and 1972, subreach 1 exhibited degradation of up to two feet between agg/deg 1131 and 1151. However, the reach-averaged change in mean bed elevation was 0.2 feet of aggradation (Figure 3-4 and Table 3-3). The reach-averaged aggradation in subreach 3 was one foot between 1962 and 1972. Between 1972 and 1992 both subreaches degraded more than 4 feet (Figure 3-5 and Table 3-3). Between 1992 and 2002, subreach 1 aggraded up to 2 feet and subreach 3 aggraded up to 4.5 feet. The reach-averaged aggradation in subreach 1 and subreach 3 was 0.92 and 2.69 feet, respectively (Figure 3-6 and Table 3-3).

Channel Geometry - Subreaches 1 and 3 exhibit similar trends between 1962 and 2002 for width, velocity, width-depth ratio, depth, wetted perimeter, and cross-section area. However, for energy grade line slope, subreach 3 increases while subreach 1 decreases. This is a result of significant degradation (> 7.5 feet) at the end of subreach 3 just upstream of San Acacia diversion dam between the 1972 and 1992 agg/deg line surveys resulting in a slope of 0.0016 in 1992. In 2002, the trends of subreaches 1 and 3 responded in the opposite manner than they did in 1992. The energy grade line slope decreased in both subreaches, but the width, velocity, width-depth ratio, depth, wetted perimeter, and cross-sectional area did not exhibit the same trends in both subreaches. This is likely a result of the significant aggradation in subreach 3 just upstream of the dam.

Based on both the GIS coverages and the HEC-RAS analysis, the width of both subreaches 1 and 3 decreased from > 1,500 feet to 400 to 700 feet. Subreach 1 is slightly wider than subreach 3 and the difference between the widths of the subreaches decreases from 1962 to 2002. In 2002, the HEC-RAS widths of subreaches 1 and 3 differ by only 15 feet. Based on the

GIS coverages, subreach 3 was wider in 1918. Therefore, the total decrease in width of subreach 3 from 1918 to 2002 is much greater than for subreach 1.

General trends in channel geometry based on HEC-RAS runs of 5,000 cfs using the agg/deg line surveys from 1962 to 2002 were decreasing width, width-depth ratio, and cross-section area, while the depth and velocity increased. Both subreaches approach width-depth ratios of about 200 and depths of close to 3 feet in 2002. The velocity from 1972 to 1992 increased; however, from 1992 to 2002 the velocity slightly decreased. This change in velocity is primarily the result in the change in the bed slope. From 1972 to 1992 these reaches had a tendency to degrade causing the bed slope and velocity to increase. However, from 1992 to 2002 the reaches began to aggrade causing the bed slope and velocity to increase. In addition, the velocity of subreach 3 is slightly higher than that of subreach 1 in 2002. The higher velocity is a direct result of the bed slope within these two reached. Subreach 3 has a steeper slope then subreach 1. The wetted perimeter (approximately 500 feet) and cross section areas (1,300 to 1,400 sq. ft.) are comparable between the two subreaches in 2002.

Subreach 2

Channel Pattern - Subreach 2 is a narrow, confined section of the river that follows a mesa. Based on the aerial photos and GIS coverages subreach 2 appears to be single thread since 1918, however the active channel width has decreased with time. The greatest changes in the planform of subreach 2 occurred between 1949 and 1972. Also, the channel pattern of this subreach appears to be different from subreaches 1 and 3 in all of the GIS coverages. The width of subreach 2 is more consistent temporally and spatially than those of subreaches 1 and 3, which vary more both spatially and temporally.

Vertical Movement - The bed of subreach 2 also aggrades from 1962 to 1972 and 1992 and 2002 degrades from 1972 to 1992. Some degradation occurs in the upstream portion (agg/deg lines 1152 to 1157) of subreach 2 between 1962 and 1972 (Figure 3-4), but overall, aggradation dominates during this time period. The degradation between 1972 and 1992 is about 50% less for subreach 2 than for subreach 1 and 3 (Table 3-3). The aggradation between 1992 and 2002 is approximately 55% greater than subreach 1 and 38% less than subreach 3.

Channel Geometry - The width of subreach 2 did not change from 1918 to 1949. From 1949 to 1972, it decreased from > 900 feet to about 300 feet. The rate of decline has decreased from 1972 to 1992 resulting in a width of about 200 feet in 1992 and 2002. Through the entire period of analysis, subreach 2 has been the narrowest of the three subreaches.

General trends in channel geometry based on HEC-RAS runs of 5,000 cfs using the agg/deg line surveys from 1962 to 2002 were decreasing width, width-depth ratio, energy-grade line slope and cross-section area, while the depth and velocity increased. Due to the narrower width of this subreach, the width-depth ratio is at least 50% less than for subreaches 1 and 3, and the average channel depth is higher than subreaches 1 and 3. In 2002, the width-depth ratio was approximately 40, the depth was the highest of the subreaches (5.0 feet) and the velocity was comparable to subreach 3 at 5 ft/sec.

6.2 SCHUMM'S (1969) RIVER METAMORPHOSIS MODEL

The changes in the characteristics of the Rio Puerco reach can be compared with Schumm's (1969) qualitative model of channel metamorphoses in response to changes in mean annual flood and bed-material load. The hypothesis of this model is that significant changes in discharge and sediment load result in changes in channel geometry (width, depth and width-depth ratio), longitudinal profile (channel slope) and planform (sinuosity and meander wavelength). This model is particularly appropriate for application to rivers in semi-arid regions because they are typically more adjustable than rivers in humid regions due their less cohesive and less vegetated banks. Schumm's results can be summarized with the following equations in which a plus exponent indicates an increase in the value of a parameter and a minus indicates a decrease:

- Decrease in bed material load:

$$Q_s^- \sim W^- D^+ P^+ L^- S^-$$

- Increase in bed material load:

$$Q_s^+ \sim W^+ D^- P^- L^+ S^+$$

- Increase in water discharge:

$$Q^+ \sim W^+ D^+ L^+ S^-$$

- Decrease in water discharge:

$$Q^{-} \sim W^{-}D^{-}L^{-}S^{+}$$

- Increase in water discharge and bed material load:

$$Q^{+}Q_t^{+} \sim W^{+}D^{\pm}F^{+}L^{+}S^{\pm}P^{-}$$

- Decrease in water discharge and decrease in bed material load:

$$Q^{-}Q_t^{-} \sim W^{-}D^{\pm}F^{-}L^{-}S^{\pm}P^{+}$$

where:

Q = water discharge;

Q_s = bed material load;

Q_t = percentage of total sediment load that is sand or bed-material load;

W = channel width;

D = flow depth;

F = width/depth;

L = meander wavelength;

P = sinuosity; and

S = channel slope.

These equations are summarized in Table 6-1. Tables 6-2, 6-3 and 6-4 summarize the trends in channel changes in the Rio Puerco reach from 1962 to 1972, 1972 to 1992 and 1992 to 2002, respectively, in a similar manner to Schumm's equations for comparison.

Table 6-1 Summary of Schumm's (1969) channel metamorphosis model.

	W	D	S	W/D =F	P	L
Qs^-	-	+	-		+	-
Q^+	+	+	-			+
Qs^+	+	-	+		-	+
Q^-	-	-	+			-
Q^-Qs^-	-	+ -	+ -	-	+	-
Q^+Qs^+	+	+ -	+ -	+	-	+

Table 6-2 Summary of channel changes between 1962 and 1972 based on reach-averaged main channel parameters from HEC-RAS modeling runs at Q = 5,000 cfs.

	Width	Depth	Area	Velocity	EG Slope	W/D = F	P
1	+	+	+	-	-	+	-
2	-	+	-	+	+	-	-
3	+	-	+	-	-	+	+
Total	=	+	+	+	-	=	-

Table 6-3 Summary of channel changes between 1972 and 1992 based on reach-averaged main channel parameters from HEC-RAS modeling runs at Q = 5,000 cfs.

	Width	Depth	Area	Velocity	EG Slope	W/D = F	P
1	-	+	-	+	+	-	-
2	-	+	-	+	-	-	-
3	-	+	-	+	+	-	-
Total	-	+	-	+	+	-	-

Table 6-4 Summary of channel changes between 1992 and 2002 based on reach-averaged main channel parameters from HEC-RAS modeling runs at Q = 5,000 cfs.

	Width	Depth	Area	Velocity	EG Slope	W/D = F	P
1	- / =	+	-	+	- / =	- / =	- / =
2	+	-	+	- / =	- / =	+ / =	+
3	+	=	+	-	-	+	+
Total	+	- / =	+	-	-	+ / =	+

Comparing the changes in channel geometry, slope and planform of the Rio Puerco reach (particularly subreaches 1 and 3) from 1962 to 1972 with Schumm's model suggests that the channel was responding to an increase in mean annual flood (Q^+) and an increase in bed-material load (Q_t^+). Subreach 2 exhibits different trends than the rest of the reach. The modeled changes in subreaches 1 and 3 are supported by the increase in suspended sediment concentration (Figures 4-3 and 4-4) observed at the Bernardo and San Acacia gages prior to and during this time period, assuming that the bed-material load also increased. However, it appears that the peak water discharge at Bernardo and San Acacia was lower between 1962 and 1972 than during previous years (Figure 2-7), though a statistical analysis of the discharge record was not performed. Schumm (1969) suggests using mean-annual flood for this analysis.

It is possible that the peak discharges shown in Figure 2-7 during the 1962-1972 time period are not indicative of the channel-forming discharge regime. It is also possible that changes in the discharge regime were not as significant as the changes in the sediment load and that the channel was responding primarily to changes in the sediment load. Schumm (1969) also points out that changes in channel geometry may occur on a shorter time scale than changes in planform and that long periods of channel instability may be present following changes in hydrologic regime.

The 1972 to 1992 and 1992 to 2002 channel changes (subreaches 1 and 3) appear to correspond most closely to Schumm's relationships described by a decrease in the percentage of sand load (Q_t^-) possibly combined with a decrease in discharge (Q). However, the decrease in sinuosity exhibited by the reach from 1972 to 1992 does not match the increase predicted by Schumm's (1969) model. This may be a result of channelization or channel maintenance activities, which would have steepened and straightened the channel. Once again, changes in river planform occur on a longer time scale than changes in channel geometry and bed elevation (Schumm 1969).

The model predictions are supported by the observed decrease in suspended sediment supply (Figures 4-1, 4-2 and 4-4) with time since 1946. A decrease in annual flood or total annual discharge is not apparent during this time period (Figure 2-7 and Figure 4-1). Continued decrease in the sand-sized sediment supply as the channel upstream becomes armored due to downstream impacts of Cochiti Dam and other tributary dams and the decreased sand-sized sediment supply from the Rio Puerco suggest that a continued narrowing and deepening trend is possible in the future. However, recent trends have indicated that the reach may be closer to a dynamic equilibrium condition than was previously thought. It is difficult to know if the observed channel changes are an initial short-term response to changes in the hydrologic and sediment regimes or if this is a long-term trend. Continued monitoring and study of the reach would be helpful in identifying long-term trends.

6.3 POTENTIAL FUTURE EQUILIBRIUM CONDITIONS

Five different methods were applied to predict the equilibrium configuration of the channel. The results of the different methods varied and the differences and similarities are discussed below.

Equilibrium Slope

The sediment transport analyses for prediction of equilibrium slope for subreaches 1 and 2 yielded varying results. Some of the equations, applied to subreach 1, produced an equilibrium slope greater than the 2002 slope, and some predicted a milder equilibrium slope. The historic geomorphic analysis presented in Chapters 3 and 4 revealed an aggradational trend of the channel bed between 1992 and 2002. Channel bed aggradation suggests that the incoming sediment load exceeds the sediment transport capacity of the channel. Reversal of the previous degradational trend has occurred, and while attainment of sediment transport equilibrium has not yet been reached, the recent trend of aggradation has shifted the channel toward equilibrium.

The sediment transport results agree with the historic and current trends of subreach 3. The sediment transport analysis shows that the equilibrium slope for subreach 3 should be less steep than the 2002 slope, indicating that the existing transport capacity exceeds the sediment input to this reach. The degradational trend observed from 1972 to 1992 illustrated that the capacity exceeded the input, but the recent trend of aggradation has reversed the previous degradational trend, however, the bed elevation of the reach is still far below the elevation that was present before the degradation.

Based on this analysis, the equilibrium slope for subreach 3 is less than the channel slope calculated from the 2002 analysis. Whereas, subreaches 1 and 2 are relatively close to the equilibrium slope, based on Yang's sediment transport equation and the 2002 agg/deg line survey. Further iterations between HEC-RAS modeling and use of the sediment transport capacity equations could help determine a combination of altered width, depth and slope that would convey the incoming sediment and water, without degrading/aggrading the channel.

Cross-section plots of the 1990's CO-lines in reaches 1 and 2 (CO-1104, CO-1164 and CO-1179) show stable river banks and bed. CO-1179 in the lower part of subreach 2 shows about

4 feet of aggradation between July 1995 and September 1998. The 1998 survey was performed after the spring runoff, when sediment deposition in the river occurs. CO-1194 in subreach 3 shows erosion at the right bank between 1992 and 1998. It seems that subreach 3 is not as stable as subreaches 1 and 2. Existing slopes of subreaches 1 and 2 seem to be closer to an equilibrium condition.

Hydraulic Geometry

The hydraulic geometry equations developed for single thread channels (Simons and Albertson, Lacey and Julien-Wargadalam) predict narrow channels that are comparable to the widths measured in subreach 2 for 1972, 1992 and 2002. It should be noted that in the Julien and Wargadalam (1995) equations, the width-depth ratio cannot vary from a value of 20-40. As a result, it is impossible to find a wide and shallow (high width-depth ratio) equilibrium channel. Decreasing the input slope to Julien and Wargadalam's equations produces increased widths and depths in order to transport the same amount with a reduced velocity and slope. Klaassen and Vermeer was developed for a braided channel and produces a higher width, which is closer to the measured channel width of subreaches 1 and 3 in 1962 and 1972.

Adjusted Hydraulic Geometry Equations

The modified Blench and Nouh's equations yield almost the same results for the 1962 and 1972 data and for subreach 2 in 1992. The modified Blench's equation predicted better results for the 1992 subreaches 1 and 3 data than the modified Nouh's equation. In general, width predictions at subreaches 1 and 2 are closer to the measured values than at subreach 3. The adjusted equations should be used with caution and should be validated with more data. It is not recommended to make predictions with these equations without validating the results with other methodology.

Hyperbolic Model

Hyperbolic equations fit the historical data very well as indicated by the regression coefficients. Therefore, they could be used to describe the past trends of channel width.

However, the existing channel is approximately the same width as the predicted decrease, which is highly unlikely and the prediction is inappropriate for future prediction. The rates of decrease in channel width predicted by the hyperbolic functions from data provided from 1935 to 2002 result in the rate the channel width is decreasing are listed in Table 6-5. The rate of channel narrowing of subreach 2 is smaller than the rate of subreach 1. However, the two values seem reasonably high, indicating that the channel is far from attaining a mean width value representative of an equilibrium state, especially in subreach 1.

Table 6-5 Rate of decrease in channel width by 2002

Subreach #	2002 rate of decrease in channel width (ft/yr)
1	-482
2	-143

SAM

The results from the SAM stable channel for a bed-material sediment concentration of 800 mg/L (corresponding to Q = 5,000 cfs and Q_s = 9,800 tons/day) show that the channel slope should not be less than 0.00056 (minimum point in the curve). 2002 channel slope-width combinations for subreach 1 plot just slightly below the 800 mg/l SAM curve, which indicates that the incoming bed material load exceeds the capacity of the channel to transport the bed material load. These results are in agreement with the aggradational trend observed from 1992 to 2002. Subreach 2 conditions plot very close to the predicted stable configuration of the channel, indicating that this subreach is attaining equilibrium. Subreach 3 conditions plot above the predicted 800 mg/l SAM curve, which indicates degradation of the reach, however, the reach has aggraded since 1992. This discrepancy is likely attributable to the significant degradation of the reach between 1972 and 1992, which presently has not fully recovered (aggraded) to the pre-degradational period's bed elevation. Additionally, the operation of the San Acacia Diversion Dam has likely also affected the flow regime and depositional trends within the reach, particularly near the dam.

7 SUMMARY

- The general trend of the entire Rio Puerco reach between 1972 and 1992 was toward a narrower and deeper channel with a greater slope and average velocity and decreased sinuosity and width-depth ratio. Between 1992 and 2002 changes in the width, velocity and depth were relatively minimal. Overall, the slope deceased throughout the reach and aggradation was prevalent (Table 6-4).
- Mean bed elevation changes between 1992 and 2002 (Figure 3-6) corroborated the results of the sediment continuity analysis (Figure 4-5), which indicated that the sediment input exceeded the sediment output, indicating aggradation.
- The suspended sediment continuity analysis showed that the difference between the annual inflow and outflow of sediment has been small since 1987. The small difference may be due to reduction in coarse sediment load contributed by the Rio Puerco. The suspended sediment concentration of the main channel decreased slightly as the mean yearly discharge decreased (Figure 4-4). The fining of the bed material led to an increased bed material load, which resulted in aggradation of the channel bed. It is not possible to corroborate this with cross-section survey data because no new surveys have been completed since the last version of this report.
- From 1992 to 1998 based on limited CO-line survey data, the bed elevation of the reach did not change significantly (Figure 3-3 and Appendix B).
- As a result of natural confinement, subreach 2 is a single-thread channel with a narrower width than either subreach 1 or 3. At bankfull discharge, all of the reaches are single thread (Baird, pers. comm., 2000).

- According to HEC-RAS models of the reach, the 1992 and 2002 channels had greater capacity to convey the modeled discharges than the channel in 1962 or 1972. As a result, there was less overbank flow in 1992 and 2002 than in 1962 and 1972.
- Also, according to HEC-RAS models using 1992 and 2002 data, some sections in subreaches 1 and 3 had overbank flow occurring at lower discharges, therefore possibly more conducive for restoration efforts for the silvery minnow and the SWWF. Subreach 2 was the most incised, narrow, and single-thread, therefore less overbank inundation occurred.
- The sediment transport, hydraulic geometry and SAM analyses showed that subreach 2 is closest to an equilibrium configuration. Based on the sediment transport capacity equations, the channel slope should continue to be decreased to reverse the degradational trend of 1992. According to Yang's equation, the channel slope should be increased 6% and decreased 4% and 43% from the measured 2002 slopes for subreaches 1, 2 and 3, respectively.
- Three of the hydraulic geometry equations predict an equilibrium width that is narrower than the 2002 measured width of the channel for subreaches 1 and 3.
- Evidence of a slight narrowing trend in the entire reach (Figures 3-8 and 3-9) is supported by the trend toward an equilibrium width as predicted by the Julien-Wargadalam, Lacey and Simons-Albertson hydraulic geometry equations. The narrowing trend is consistent with a decreased sediment supply as suggested by Schumm's (1969) river metamorphosis model.
- This geomorphic study only accounts for channel changes from 1962 to 2002.
- Overall, the 2002 analysis has shown that the reach has not yet reached a dynamic equilibrium condition. However, recent aggradational and stable width, depth, and velocity trends indicate that the reach is moving toward equilibrium.

8 REFERENCES

Baird, D. 2000. Personal Communication. U.S. Bureau of Reclamation, Albuquerque, NM.

Bauer, T.R. 1999. Morphology of the Middle Rio Grande from Bernalillo Bridge to the San Acacia Diversion Dam, New Mexico, M.S. Thesis, Colorado State University, Fort Collins, CO, 308 pp.

Bauer, T., Leon, C., Richard, G., and Julien, P. 1999. Middle Rio Grande, Bernalillo Bridge to San Acacia - Hydraulic Geometry, Discharge and Sediment Data Base and Report, Colorado State University, Fort Collins, CO, pp. 6 Volumes and CD-ROM.

Blench,T. 1957. Regime Behaviour of Canals and Rivers. London, Butterworths Scientific publications. pp.138.

Bullard, K. L. and Lane, W. L. 1993. Middle Rio Grande Peak Flow Frequency Study. U.S. Department of Interior, Bureau of Reclamation, Albuquerque, NM.

Chang, H.H. 1979. Minimum stream power and river channel patterns. *Journal of Hydrology*, 41, 303-327.

Ferguson, R. 1987. Hydraulic and sedimentary controls of channel pattern. in *River Channels*, K. Richards (ed.), 129-158.

Gellis, A.C. 1992. Decreasing trends of suspended-sediment loads in selected streamflow stations in New Mexico: New Mexico Water Resources Research Institute Report No. 265, Proceedings of the 36th Annual New Mexico Water Conference, Las Cruces, New Mexico, 77-93.

Gomez, B. and Church, M. 1989. An assessment of bed load sediment transport formulae for gravel bed rivers, *Water Resources Research*, 25(6), 1161-86.

Graf, W. L. 1994. *Plutonium and the Rio Grande - Environmental Change and Contamination in the Nuclear Age*, Oxford University Press, New York, NY.

Henderson, F.M. 1966. *Open channel flow.* Macmilllan Publishing Co., Inc. New York, NY, 522 pp.

Julien, P.Y. 1995. *Erosion and Sedimentation,* Cambridge University Press, NY, NY, 280 pp.

Julien, P. Y. and Wargadalam, J. 1995. Alluvial Channel Geometry: Theory and Applications. *Journal of Hydraulic Engineering*, 121(4), 312-25.

Klaassen, G. J. and Vermeer, K. 1988. Channel Characteristics of the Braiding Jamuna River, Bangladesh. In *International Conference on River Regime, 18-20 May, 1988*, W.R. White (ed.), Hydraulics Research Limited, Wallingford, UK, 173-89.

Knighton, A.D. 1998. *Fluvial Forms and Processes,* John Wiley & Sons, Inc, New York, NY, 383 pp.

Knighton, A.D. and Nanson, G.C. 1993. Anastomosis and the continuum of channel pattern. *Earth Surface Processes and Landforms*, 18, 613-625.

Leon, C. 1998. Morphology of the Middle Rio Grande from Cochiti Dam to Bernalillo Bridge, New Mexico. M.S. Thesis, Colorado State University, Fort Collins, CO.

Leopold, L. B. and Maddock, T. Jr. 1953. The Hydraulic Geometry of Stream Channels and Some Physiographic Implications: USGS Professional Paper 252, 57 pp.

Leopold, L.B. and Wolman, M.G. 1957. River Channel Patterns: Braided, Meandering and Straight, USGS Professional Paper 282-B, 85 pp.

Nanson, G.C. and Croke, J.C. 1992. A genetic classification of floodplains. *Geomorphology*, 4, 459-486.

Nouh, M. 1988. Regime channels of an extremely arid zone. *International Conference on River Regime, 18-20 May, 1988*, W.R. White (ed.), Hydraulics Research Limited, Wallingford, UK, 55-66.

Parker, G. 1976. On the cause and characteristic scales of meandering and braiding in rivers. *Journal of Fluid Mechanics*, vl.76, part 3, pp. 457-480.

Richard, G.A. 2001. Quantification and prediction of lateral channel adjustments downstream from Cochiti Dam, Rio Grande, NM. Ph.D. Dissertation, Colorado State University, Fort Collins, CO, 276 pp.

Rosgen, D., 1996. *Applied River Morphology*, Pagosa Springs, CO, Wildland Hydrology.

Schumm, S.A. and Khan, H.R. 1972. Experimental study of channel patterns. *Geological Society of America Bulletin,* 83, 1755-1770.

Scurlock, D. 1998. *From the Rio to the Sierra: An Environmental History of the Middle Rio Grande Basin,* Fort Collins, CO, U.S. Department of Agriculture Forest Service, 440 pp.

Stevens, H.H. and Yang, C.T. 1989. Summary and use of selected fluvial sediment-discharge formulas, USGS Water Resources Investigations Report 80-4026, 62 pp.

Thorne,C.R., Hey, R.D., Newson, M.D.1997. Applied Fluvial Gomorphology for River Engineering and Management. John Wiley and Sons, 376 pp.

Tofaletti, F.B. 1969. Definitive computations of Sand Discharge in Rivers. *Journal of the Hydraulics Division*, 95, HY1, 225-246

U.S. Bureau of Reclamation, 2003. Geomorphic Assessment of the San Acacia Reach, Middle Rio Grande, Albuquerque, NM.

US Fish and Wildlife Service. 1999. Final Designation of Critical Habitat for the Rio Grande Silvery Minnow, 50 CFR Part 17, Federal Register: July 6, 1999 (V. 64, No. 128).

US Fish and Wildlife Service. 2000. http://pacific.fws.gov/vfwo/SpeciesAccount/birds/SWWF.htm

Van den Berg, J.H. 1995. Prediction of alluvial channel pattern of perennial rivers. *Geomorphology*. 12, 259-279.

Wargadalam, J. 1993. Hydraulic Geometry Equations of Alluvial Channels, Ph.D. Dissertation. Fort Collins, CO, Colorado State University, 203 pp.

Williams G. and Woman G. 1984. Downstream Effects of Dams on Alluvial Rivers. US Geological Survey Professional Paper 1286. 83 pp.

Woodson, R. C. and Martin, J. T. 1962. The Rio Grande comprehensive plan in New Mexico and its effects on the river regime through the middle valley, Control of Alluvial Rivers by Steel Jetties, *American Society of Civil Engineers Proceedings, Waterways and Harbors Division Journal 88,* E.J. Carlson and E.A. Dodge (eds.), NY, NY, American Society of Civil Engineers, pp. 53-81.

APPENDIX A – DATA LISTS

AERIAL PHOTOS

Aerial Photos digitized in the Rio Grande Geomorphology Study, v. 1 by the USBR, Remote Sensing and Geographic Information Group, Denver, CO:

1) 1918 – Scale: 1:12,000, Hand drafted linens (39 sheets), USBR Albuquerque Area Office. Surveyed in 1918, published in 1922.

2) 1935 – Scale: 1:8,000. Black and white photography, USBR Albuquerque Area Office. Flown in 1935, published 1936.

3) 1949 – Scale 1:5,000. Photo-mosaic. J. Ammann Photogrammetric Engineers, San Antonio, TX. USBR Albuquerque Area Office.

4) March 15, 1962 – Scale: 1:4,800. Photo-mosaic. Abram Aerial Survey Corp. Lansing, MI. USBR Albuquerque Area Office.

5) April 1972 – Scale: 1:4,800. Photo-mosaic. Limbaugh Engineers, Inc., Albuquerque, NM. USBR Albuquerque Area Office.

6) March 31, 1985 – Scale: 1:4,800. Orthophoto. M&I Consulting Engineers, Fort Collins, CO. Aero-Metric Engineering, Sheboygan, MN. USBR Albuquerque Area Office.

7) February 24, 1992 – Scale: 1:4,800. Ratio-rectified photo-mosaic. Koogle and Poules Engineering, Albuquerque, NM. USBR Albuquerque Area Office.

8) March 2002 – Scale: 1:4,800. Digital ortho-imagery. Pacific Western Technologies, Ltd. Albuquerque, NM. USBR Albuquerque Area Office.

Aerial Photo Dates	Discharge at San Acacia (cfs)	Discharge at Bernardo (cfs)
March 2002	Mean = 311 Max = 628 Min =154	Mean = 165 Max = 414 Min = 23
February 24, 1992	753	627
March 31, 1985	2,860	3,000
April 1972	4	0
March 15, 1962	5	1
1949 (unknown date)	Extreme low flow (from Jan's meta-data)	
1935 (unknown date)	Annual data from Otowi: Mean = 1,520 Max = 7,490 Min = 350	
1918 (unknown date)	No data	No data

APPENDIX B – CROSS-SECTION GRAPHS

CROSS SECTION DATA

This Appendix includes the following plots:

- Cross-section plots for agg/deg and CO-lines
- Time series of mean bed and thalweg elevations
- Time series of cross-section area.

Aggradation-degradation line taken from aerial photos is presented for the following dates:

1) March 15, 1962
2) April 1972
3) February 24, 1992
4) March 2002

CO-line field surveyed data is presented for the following dates:

1) August 1992
2) July 1995
3) September 1998

AggDeg-1104 / CO2-1104
Rio Grande, NM

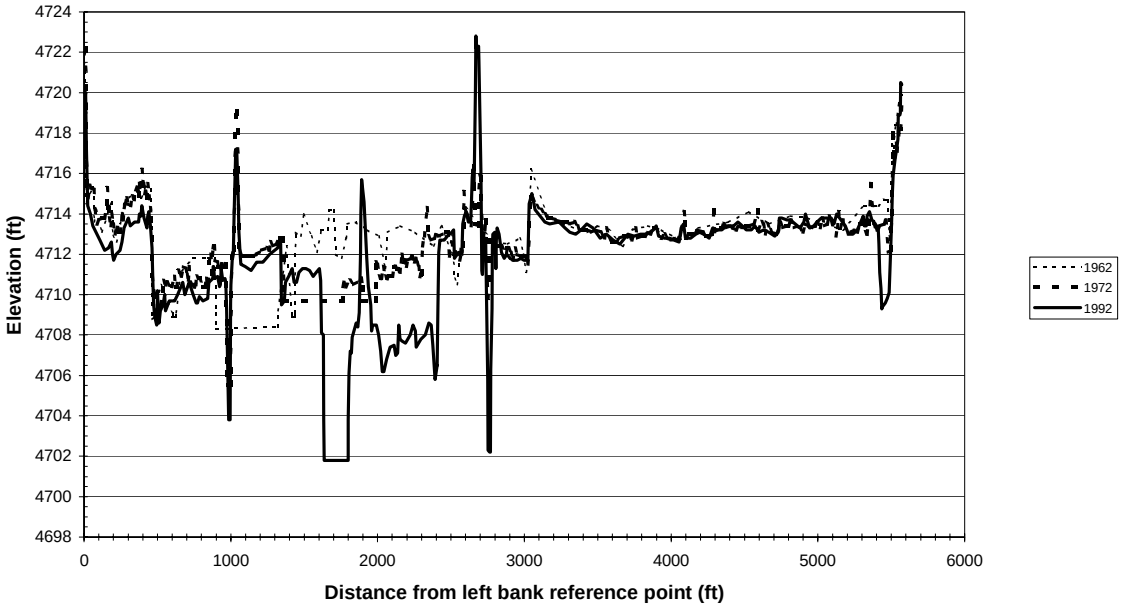

CO2-1104
Rio Grande, NM

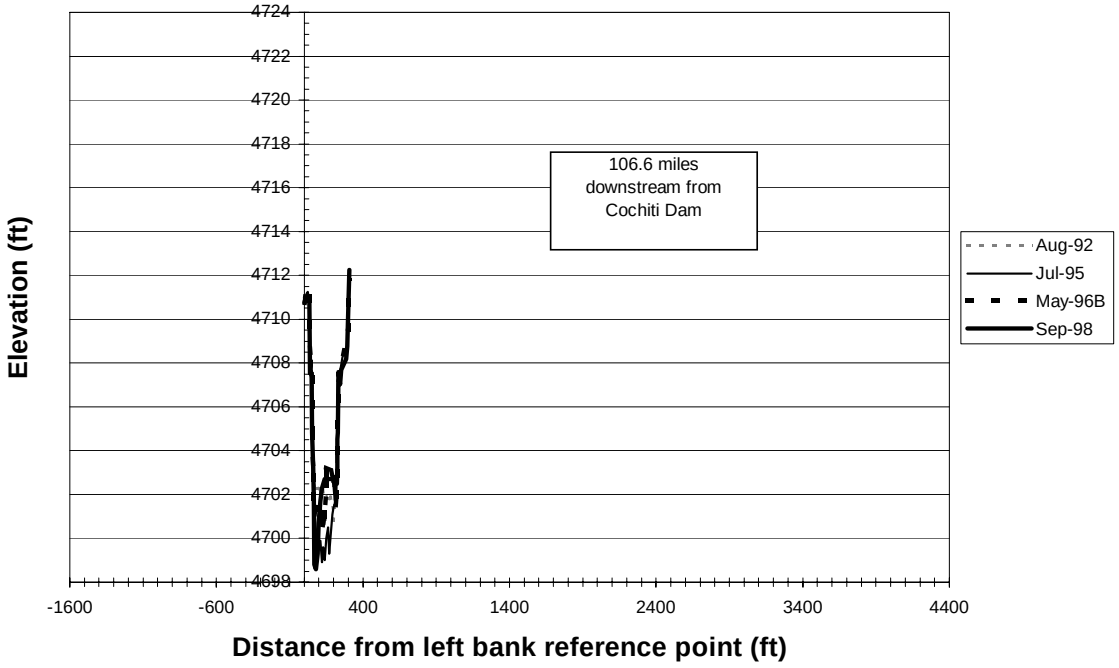

AggDeg-1164 / CO2-1164
Rio Grande, NM

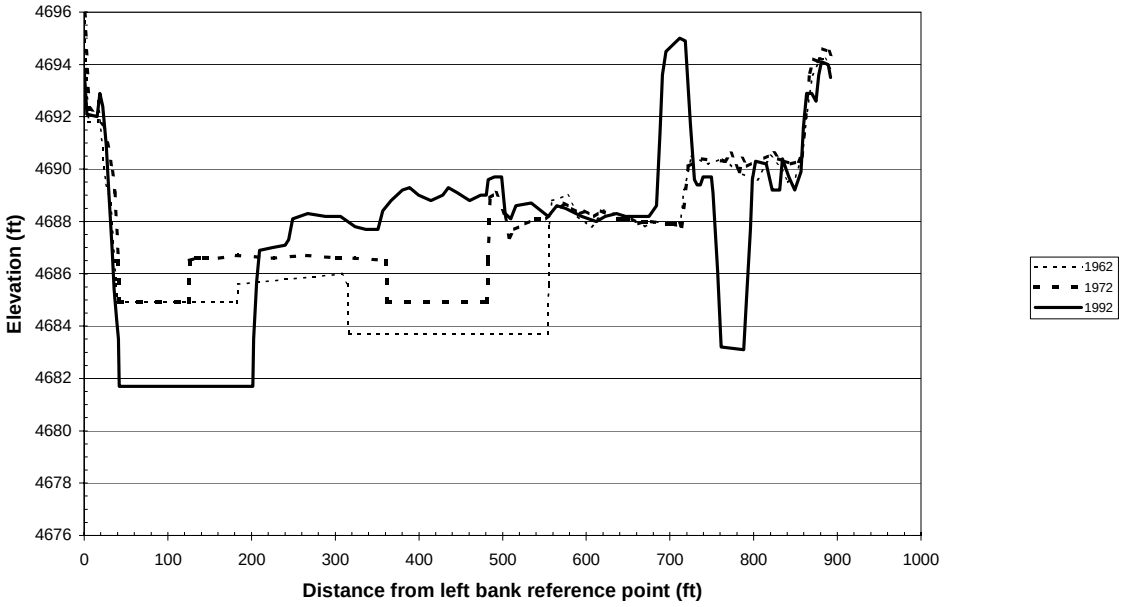

CO2-1164
Rio Grande, NM

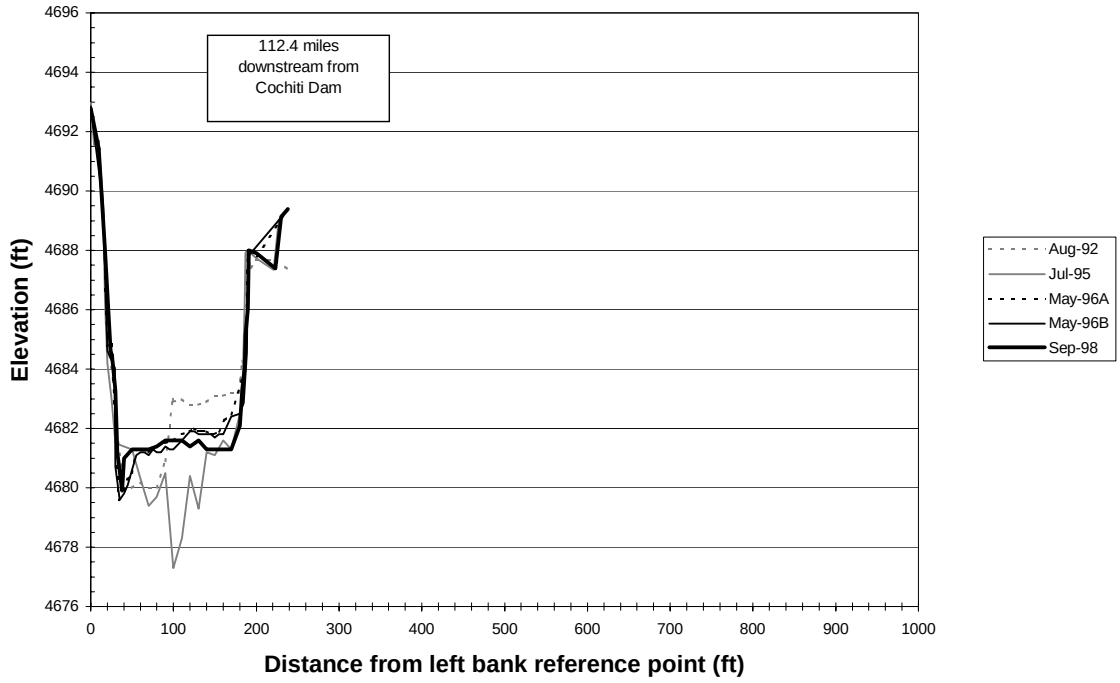

AggDeg-1179 CO2-1179
Rio Grande, NM

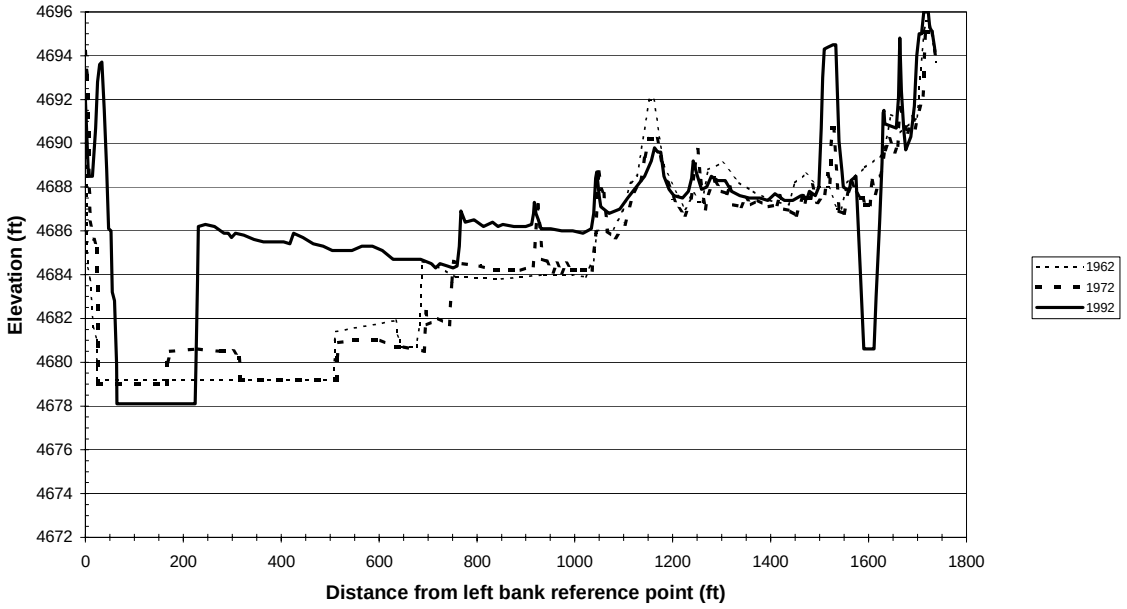

CO2-1179
Rio Grande, NM

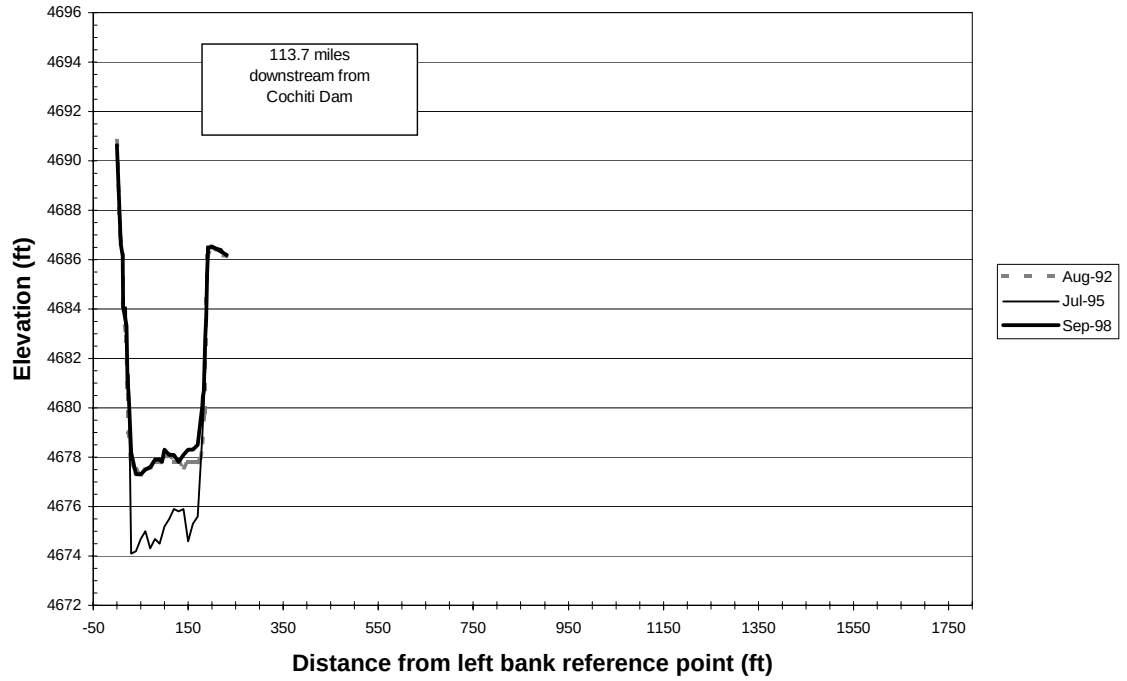

AggDeg-1194 / CO2-1194
Rio Grande, NM

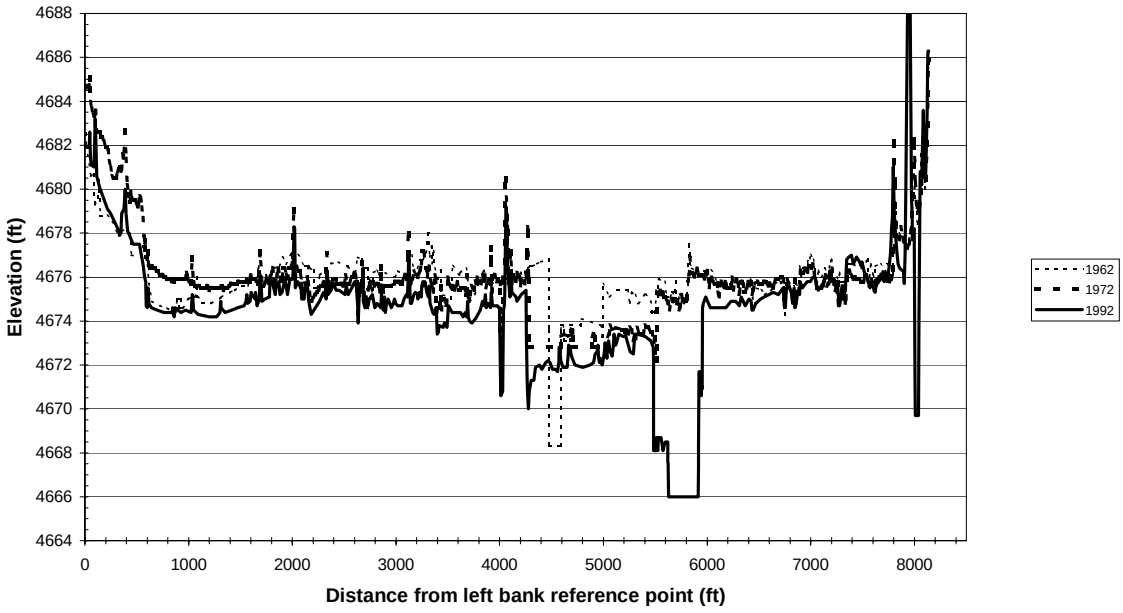

CO2-1194
Rio Grande, NM

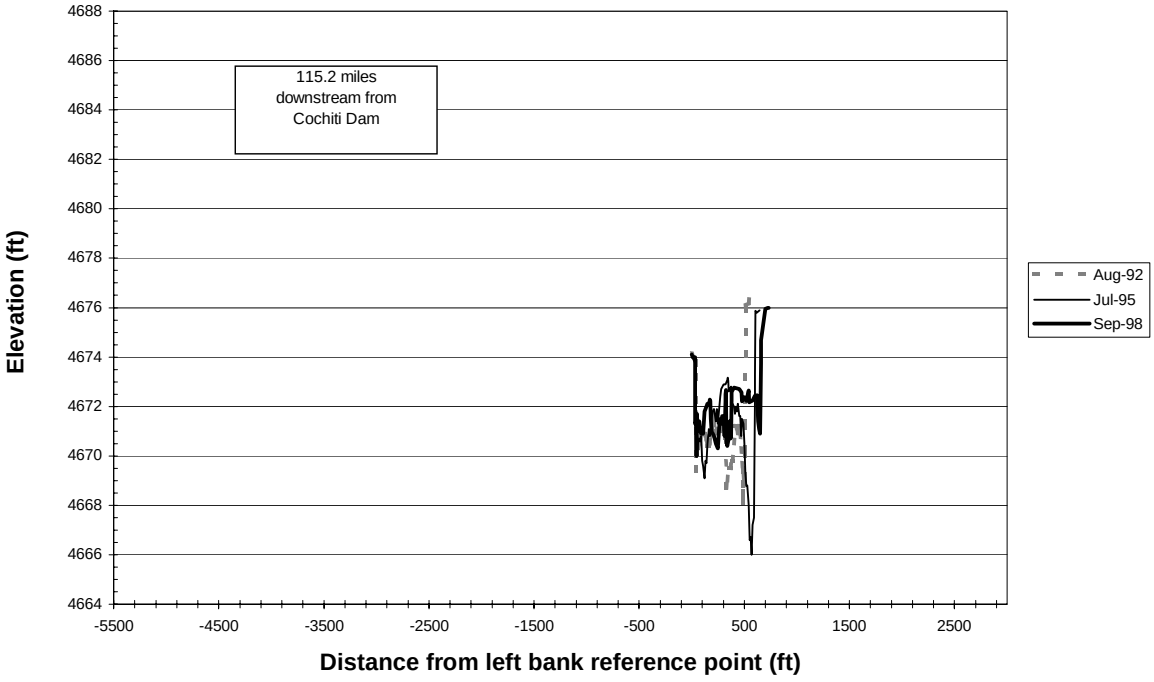

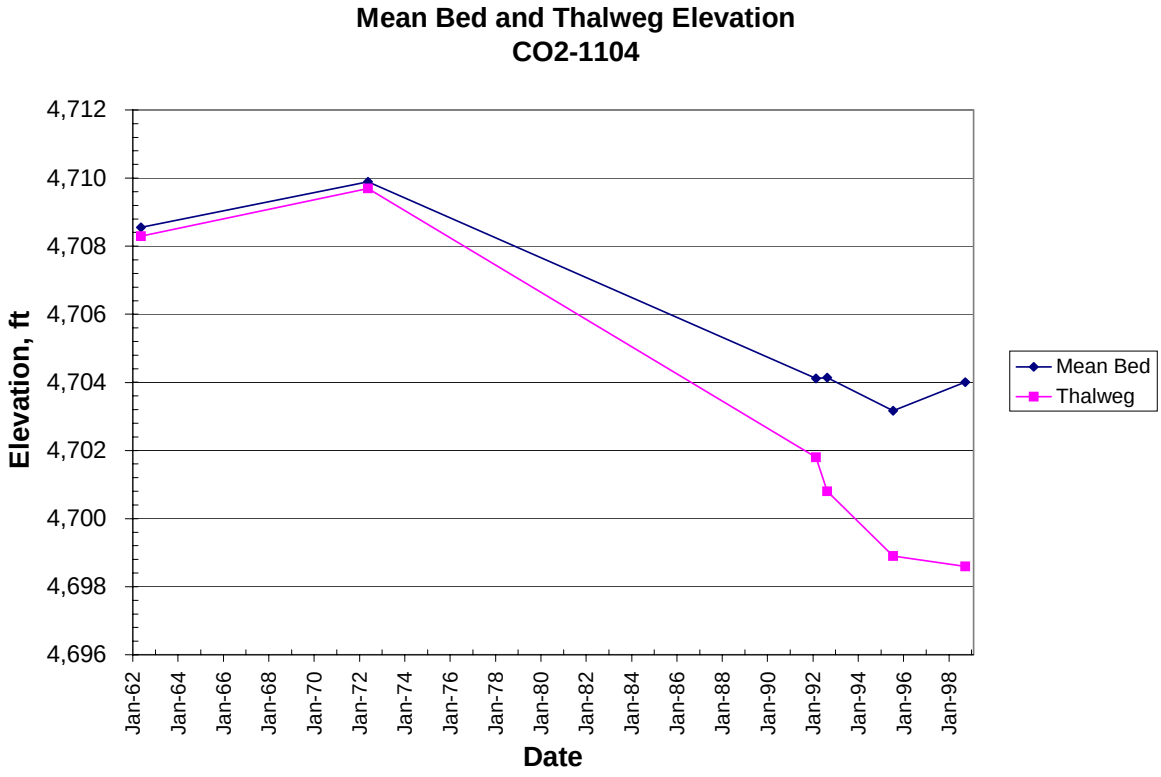
Mean Bed and Thalweg Elevation
CO2-1104
Elevation, ft
4,712
4,710
4,708
4,706
4,704
4,702
4,700
4,698
4,696
Jan-62
Jan-64
Jan-66
Jan-68
Jan-70
Jan-72
Jan-74
Jan-76
Jan-78
Jan-80
Jan-82
Jan-84
Jan-86
Jan-88
Jan-90
Jan-92
Jan-94
Jan-96
Jan-98
Date
Mean Bed
Thalweg

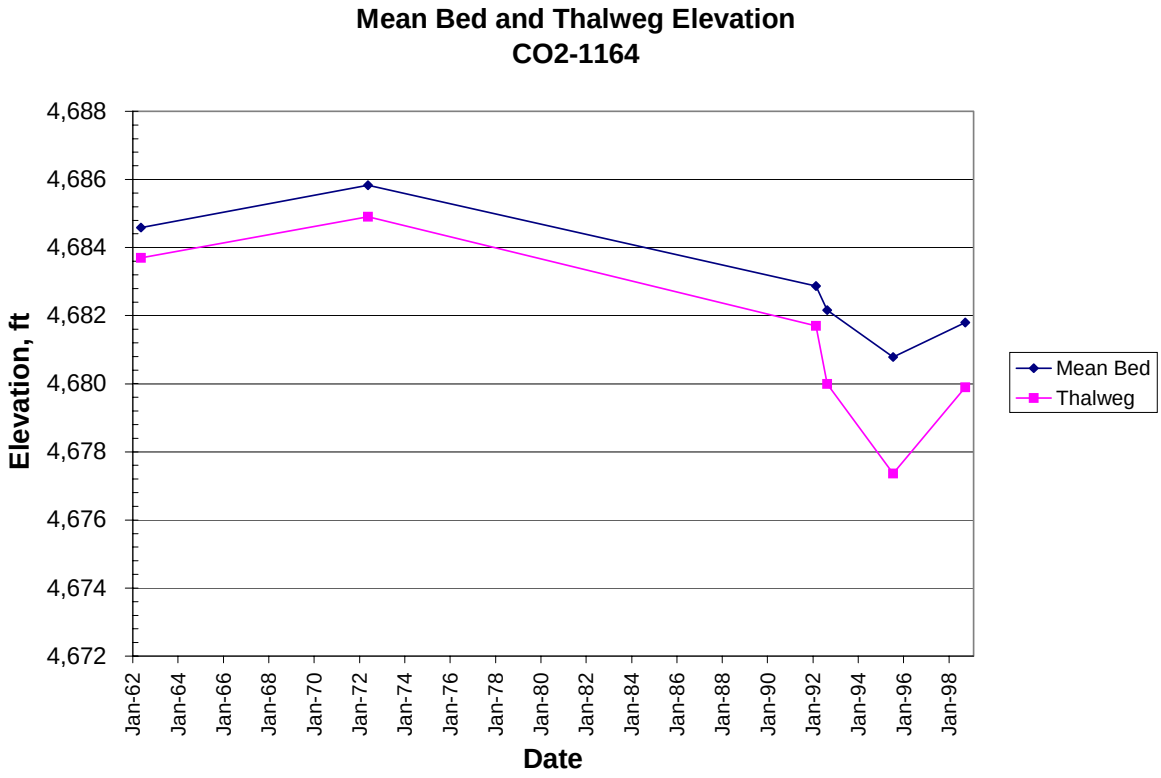
Mean Bed and Thalweg Elevation
CO2-1164
Elevation, ft
4,688
4,686
4,684
4,682
4,680
4,678
4,676
4,674
4,672
Jan-62
Jan-64
Jan-66
Jan-68
Jan-70
Jan-72
Jan-74
Jan-76
Jan-78
Jan-80
Jan-82
Jan-84
Jan-86
Jan-88
Jan-90
Jan-92
Jan-94
Jan-96
Jan-98
Date
Mean Bed
Thalweg

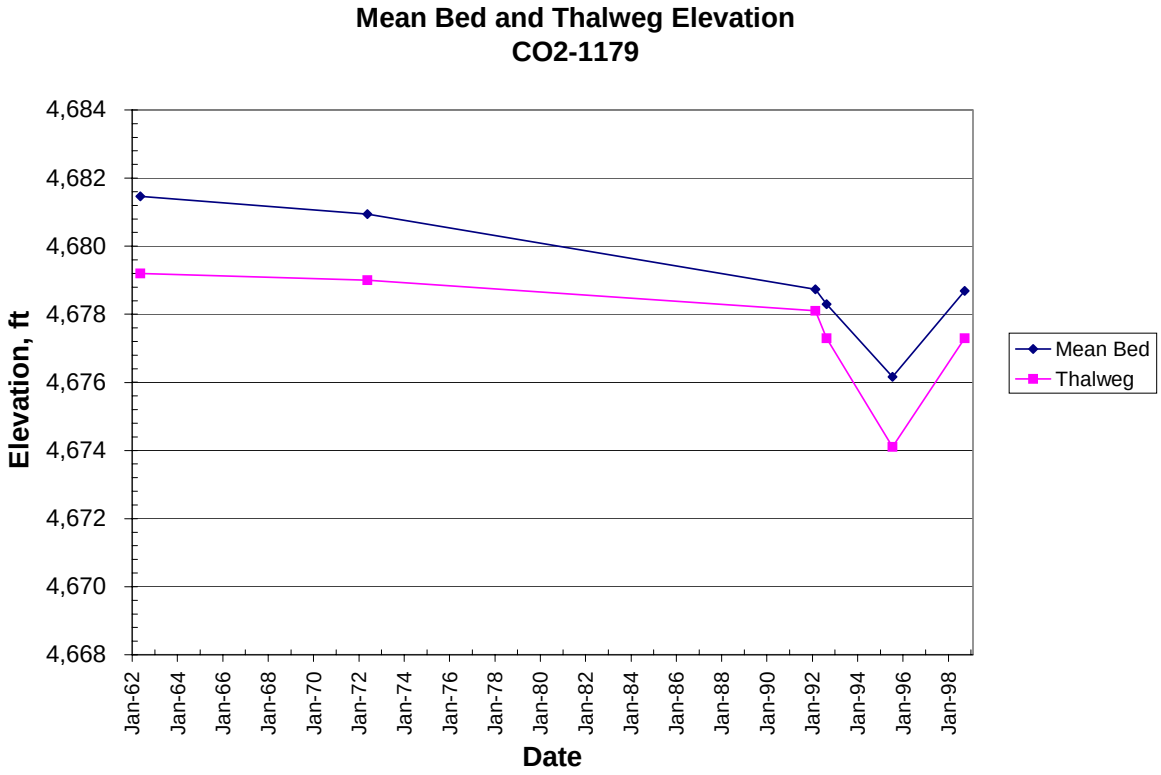
Mean Bed and Thalweg Elevation
CO2-1179
Elevation, ft
4,684
4,682
4,680
4,678
4,676
4,674
4,672
4,670
4,668
Jan-62
Jan-64
Jan-66
Jan-68
Jan-70
Jan-72
Jan-74
Jan-76
Jan-78
Jan-80
Jan-82
Jan-84
Jan-86
Jan-88
Jan-90
Jan-92
Jan-94
Jan-96
Jan-98
Date
Mean Bed
Thalweg

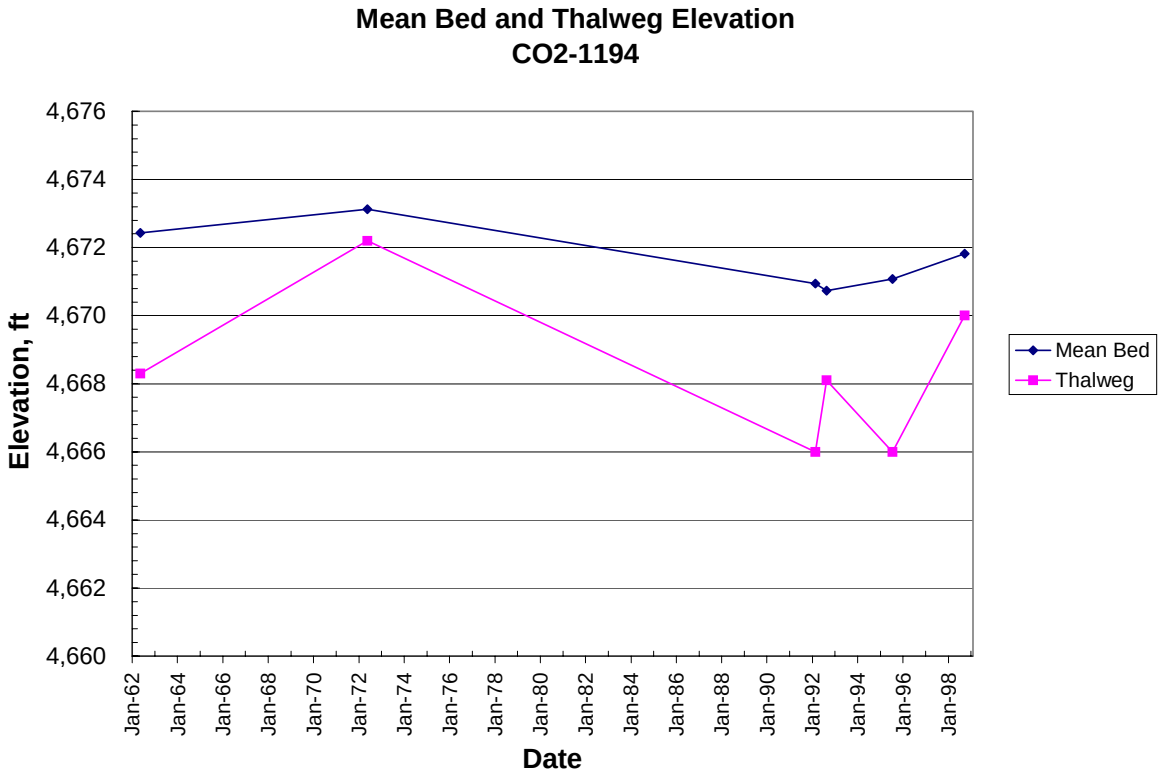
Mean Bed and Thalweg Elevation
CO2-1194
Elevation, ft
4,676
4,674
4,672
4,670
4,668
4,666
4,664
4,662
4,660
Jan-62
Jan-64
Jan-66
Jan-68
Jan-70
Jan-72
Jan-74
Jan-76
Jan-78
Jan-80
Jan-82
Jan-84
Jan-86
Jan-88
Jan-90
Jan-92
Jan-94
Jan-96
Jan-98
Date
Mean Bed
Thalweg

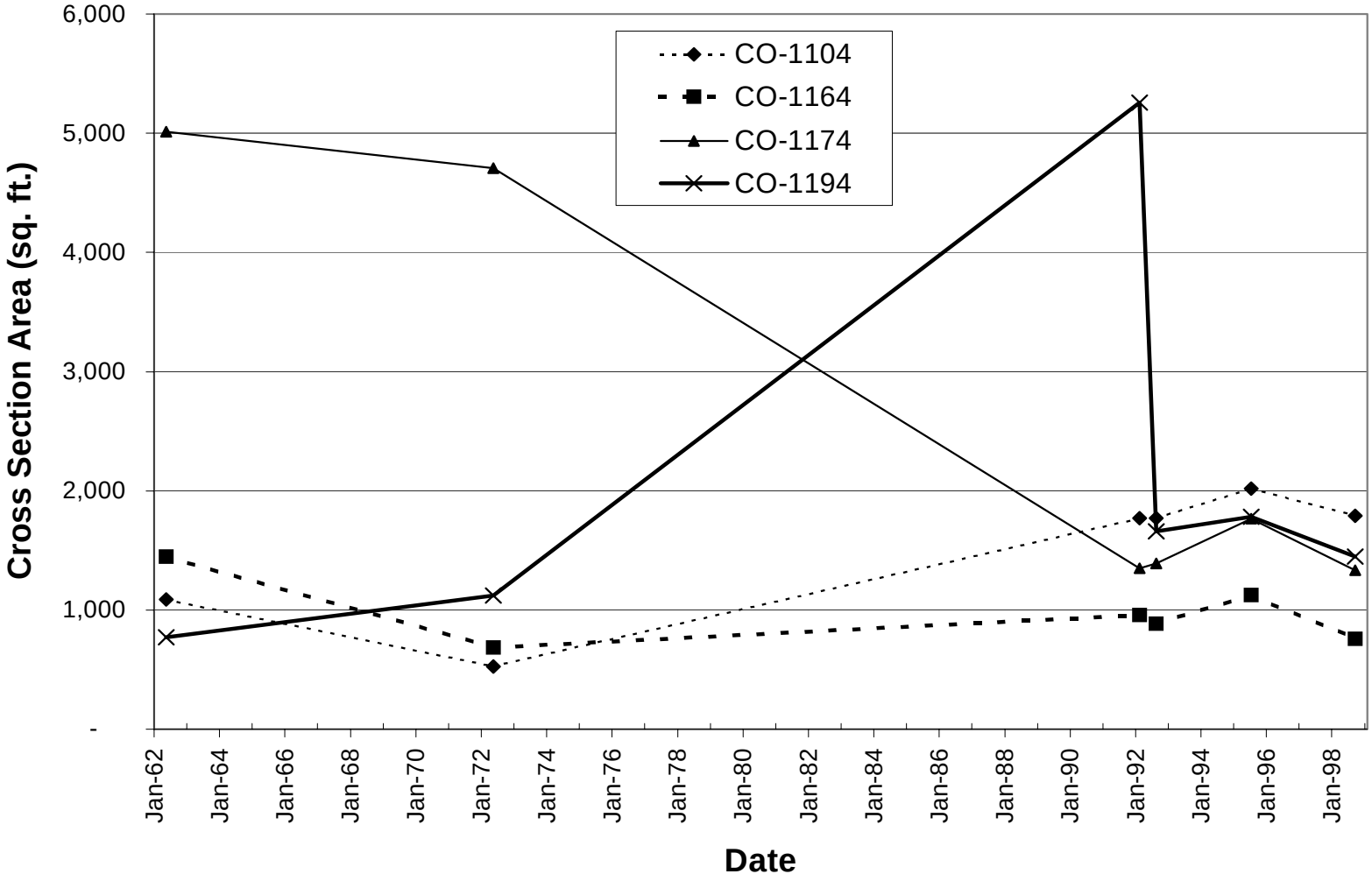
6,000
5,000
4,000
3,000
2,000
1,000
-
Cross Section Area (sq. ft.)
CO-1104
CO-1164
CO-1174
CO-1194
Jan-62
Jan-64
Jan-66
Jan-68
Jan-70
Jan-72
Jan-74
Jan-76
Jan-78
Jan-80
Jan-82
Jan-84
Jan-86
Jan-88
Jan-90
Jan-92
Jan-94
Jan-96
Jan-98
Date

APPENDIX C- INPUT AND RESULTS FROM CHAPTER 5

Table C1 - BORAMEP input data for Bernardo Gage

Sample Date	Discharge (cfs)	Conc (PPM)	Suspended Sample (tons/day)	Total Load (tons/day)	Total Sand Load (>0.625mm)(tons/day)	d65 (mm)	d35 (mm)	Temp F
4/9/1991	1,140	172	529	1,715	965	0.235	0.151	55.4
5/10/1991	2,310	354	2,208	4,894	2,596	0.177	0.092	60.8
6/17/1992	2,670	1,890	13,625	16,999	16,034	0.398	0.265	75.2
7/20/1992	202	137	75	111	84	0.425	0.318	84.2
6/17/1993	3,730	568	5,720	8,415	7,020	0.447	0.325	69.8
4/18/1994	2,710	1,640	12,000	20,297	17,888	0.282	0.213	62.1
5/27/1994	6,090	1,400	23,020	31,798	20,875	0.457	0.299	65.1
6/21/1994	4,450	445	5,347	10,169	8,344	0.413	0.233	72.5
7/18/1994	166	48	22	36	21	0.486	0.362	83.8
4/18/1995	2,840	629	4,823	7,348	4,451	0.393	0.265	54.1
5/18/1995	4,830	1,050	13,693	21,949	16,347	0.249	0.208	58.8
7/21/1995	4,480	1,240	14,999	19,805	9,450	0.384	0.242	77.0
7/10/1996	448	5,680	6,871	7,595	2,474	0.411	0.261	71.6
5/20/1997	4,520	2,090	25,506	33,769	27,468	0.476	0.314	66.2
6/24/1997	2,060	429	2,386	3,114	2,192	0.421	0.292	74.5
4/21/1998	974	313	823	1,796	1,529	0.425	0.297	60.0
5/18/1998	3,040	676	5,549	7,555	5,363	0.376	0.243	63.5
6/23/1998	301	71	58	123	99	0.446	0.329	60.0
4/22/1999	53	88	13	18	11	0.355	0.234	60.0
6/15/1999	2,130	1,490	8,569	24,520	23,122	0.426	0.314	60.0
4/10/2000	460	111	138	256	159	0.415	0.290	71.6
5/30/2001	1,510	287	1,170	1,966	1,323	0.405	0.247	78.8

Table C1 (cont) - BORAMEP input data - Bernardo Gage

Sample Date	Computed total load by size fraction (tons/day)							
	0.001 - 0.002	0.002 - 0.004	0.004 - 0.016	0.016 - 0.0625	0.0625 - 0.125	0.125 - 0.25	0.25 - 0.5	0.5 - 1
4/9/1991	0.0	0.0	0.0	749.9	174.9	385.0	353.6	51.7
5/10/1991	0.0	0.0	0.0	2,298.4	786.3	1,511.6	297.9	0.0
6/17/1992	0.0	0.0	0.0	964.6	283.5	10,109.6	5,368.5	268.7
7/20/1992	0.0	0.0	0.0	26.7	1.0	12.3	59.9	10.7
6/17/1993	0.0	0.0	0.0	1,394.6	923.1	3,379.2	2,185.0	502.2
4/18/1994	0.0	0.0	0.0	2,409.5	924.5	11,829.3	4,589.7	544.4
5/27/1994	0.0	0.0	0.0	10,922.9	3,325.6	6,996.3	7,169.2	3,019.6
6/21/1994	0.0	0.0	0.0	1,824.6	1,041.3	3,622.1	1,919.3	1,586.6
7/18/1994	0.0	0.0	0.0	14.5	0.3	7.0	10.4	3.8
4/18/1995	0.0	0.0	0.0	2,896.8	934.1	1,858.0	1,519.1	139.4
5/18/1995	0.0	0.0	0.0	5,602.2	4,199.0	7,929.8	4,088.5	129.4
7/21/1995	5,131.8	1,209.0	1,670.4	2,343.6	877.9	4,954.7	2,797.6	794.1
7/10/1996	3,388.9	345.8	968.7	417.7	0.0	1,124.6	1,199.9	149.2
5/20/1997	1,542.9	257.8	1,298.1	3,202.4	3,710.4	6,013.3	12,027.9	5,299.0
6/24/1997	0.0	0.0	0.0	921.3	357.2	1,131.4	633.6	67.6
4/21/1998	0.0	0.0	0.0	266.7	115.2	450.6	772.0	185.8
5/18/1998	0.0	0.0	0.0	2,191.9	1,330.7	2,210.3	1,681.1	137.6
6/23/1998	0.0	0.0	0.0	24.2	4.7	47.5	37.6	9.0
4/22/1999	0.0	0.0	0.0	7.9	1.5	4.5	4.6	0.0
6/15/1999	0.0	0.0	0.0	1,397.8	221.9	6,152.2	13,815.1	2,649.7
4/10/2000	0.0	0.0	0.0	97.2	11.8	63.6	51.3	31.8
5/30/2001	0.0	0.0	0.0	643.6	129.7	627.7	437.2	126.9

Table C1 (cont) - BORAMEP input data - Bernardo Gage

Sample Date	Computed total load by size fraction (tons/day)							
	37,988.0	38,021.0	38,085.0	38,215.0	16 - 32	32 - 64	64 - 128	128 - 256
4/9/1991	0.0	0.0	0.0	0.0	0.0	0.0	0.0	0.0
5/10/1991	0.0	0.0	0.0	0.0	0.0	0.0	0.0	0.0
6/17/1992	3.9	0.0	0.0	0.0	0.0	0.0	0.0	0.0
7/20/1992	0.0	0.0	0.0	0.0	0.0	0.0	0.0	0.0
6/17/1993	28.0	2.4	0.0	0.0	0.0	0.0	0.0	0.0
4/18/1994	0.0	0.0	0.0	0.0	0.0	0.0	0.0	0.0
5/27/1994	347.4	16.4	0.7	0.0	0.0	0.0	0.0	0.0
6/21/1994	170.5	4.1	0.0	0.0	0.0	0.0	0.0	0.0
7/18/1994	0.0	0.0	0.0	0.0	0.0	0.0	0.0	0.0
4/18/1995	0.0	0.0	0.0	0.0	0.0	0.0	0.0	0.0
5/18/1995	0.0	0.0	0.0	0.0	0.0	0.0	0.0	0.0
7/21/1995	21.8	3.8	0.0	0.0	0.0	0.0	0.0	0.0
7/10/1996	0.3	0.0	0.0	0.0	0.0	0.0	0.0	0.0
5/20/1997	391.0	26.4	0.0	0.0	0.0	0.0	0.0	0.0
6/24/1997	2.6	0.0	0.0	0.0	0.0	0.0	0.0	0.0
4/21/1998	5.9	0.0	0.0	0.0	0.0	0.0	0.0	0.0
5/18/1998	3.7	0.0	0.0	0.0	0.0	0.0	0.0	0.0
6/23/1998	0.2	0.0	0.0	0.0	0.0	0.0	0.0	0.0
4/22/1999	0.0	0.0	0.0	0.0	0.0	0.0	0.0	0.0
6/15/1999	283.1	0.0	0.0	0.0	0.0	0.0	0.0	0.0
4/10/2000	0.1	0.0	0.0	0.0	0.0	0.0	0.0	0.0
5/30/2001	1.0	0.0	0.0	0.0	0.0	0.0	0.0	0.0

Table C2 - BORAMEP results - Bernardo Gage data

Sample Date	Discharge (cfs)	Total Load (tons/day)	Total Sand Load (>0.625mm)(tons/day)
4/9/1991	1,140	1,715	965
5/10/1991	2,310	4,894	2,596
6/17/1992	2,670	16,999	16,034
7/20/1992	202	111	84
6/17/1993	3,730	8,415	7,020
4/18/1994	2,710	20,297	17,888
5/27/1994	6,090	31,798	20,875
6/21/1994	4,450	10,169	8,344
7/18/1994	166	36	21
4/18/1995	2,840	7,348	4,451
5/18/1995	4,830	21,949	16,347
7/21/1995	4,480	19,805	9,450
7/10/1996	448	7,595	2,474
5/20/1997	4,520	33,769	27,468
6/24/1997	2,060	3,114	2,192
4/21/1998	974	1,796	1,529
5/18/1998	3,040	7,555	5,363
6/23/1998	301	123	99
4/22/1999	53	18	11
6/15/1999	2,130	24,520	23,122
4/10/2000	460	256	159
5/30/2001	1,510	1,966	1,323

Table C3 - SSE computation results

	S = 0.00063	S = 0.00055	S = 0.00111
	Reach 1	***Reach 2***	***Reach 3***
Discharge (cfs)	**5,000**	**5,000**	**5,000**
Sediment Transport Equations	**Bed Material Load (tons/day)**		
Laursen	11,542	13,044	26,670
Engelund & Hansen	16,367	20,955	40,006
Colby	14,556	16,496	17,417
Ackers and White (d50)	14,907	18,235	26,739
Ackers and White (d35)	28,103	38,487	58,472
Yang Sand (d50)	8,982	10,283	20,683
Yang Sand (size fraction)	11,823	13,449	28,867
Yang Mixture (size fraction)	11,765	13,373	28,758
Einstein	7,371	18,570	20,487
Toffaleti	27,429	45,018	56,913

Estimated bed material load = 55% total sand load (tons/day)	9,790	9,790	9,790
Laursen (obs - expected)^2	3,069,434	10,589,557	284,942,840
E and H (obs - expected)^2	43,262,980	124,663,477	912,981,275
Colby (obs - expected)^2	22,713,707	44,967,888	58,165,638
A and W d50 (obs-expected)^2	26,181,847	71,310,425	287,261,482
A and W d35 (obs-expected)^2	335,380,986	823,490,834	2,369,983,859
Yang Sand d50 (obs - expected)^2	653,317	243,138	118,647,210
Yang Sand sf (obs - expected)^2	4,131,707	13,389,598	363,946,428
Yang Mixture sf (obs - expected)^2	3,902,561	12,840,827	359,794,508
Einstein (obs - expected)^2	5,853,545	77,092,614	114,426,879
Toffaleti (obs - expected)^2	311,145,963	1,241,045,803	2,220,575,244

Sediment Transport Equations	**SSE for Reach 1, 2 and 3**	**Ranking**
Laursen	298,601,831	4
Engelund & Hansen	1,080,907,732	8
Colby	125,847,233	2
Ackers and White (d50)	384,753,754	7
Ackers and White (d35)	3,528,855,679	9
Yang Sand (d50)	119,543,664	1
Yang Sand (size fraction)	381,467,733	6
Yang Mixture (size fraction)	376,537,896	5
Einstein	197,373,038	3
Toffaleti	3,772,767,010	10

Table C4 - Discrepancy ratio results

	S = 0.00063	S = 0.00055	S = 0.00111
	Reach 1	*Reach 2*	*Reach 3*
Discharge (cfs)	**5,000**	**5,000**	**5,000**
Sediment Transport Equations	**Bed Material Load (tons/day)**		
Laursen	3,270	3,389	27,340
Engelund & Hansen	11,121	12,574	60,577
Colby	8,251	12,490	23,343
Ackers and White (d50)	7,497	9,799	51,126
Ackers and White (d35)	9,457	11,203	82,849
Yang Sand (d50)	6,151	6,748	31,975
Yang Sand (size fraction)	7,215	7,452	36,926
Yang Mixture (size fraction)	7,210	7,445	36,899
Einstein	4,643	6,662	32,387
Toffaleti	5,179	11,597	71,775

BORAMEP Power regresion $Q_s = i_{b(BORAMEP)} = 55\% (0.0105\ Q^{1.6843})$	**9790 tons/day**	**9791 tons/day**	**9792 tons/day**
	Discrepancy ratio	**Discrepancy ratio**	**Discrepancy ratio**
Sediment Transport Equations	$i_{b(BORAMEP)} / i_{b\ (eq)}$	$i_{b(BORAMEP)} / i_{b\ (eq)}$	$i_{b(BORAMEP)} / i_{b\ (eq)}$
Laursen	2.99	2.89	0.36
Engelund & Hansen	0.88	0.78	0.16
Colby	1.19	0.78	0.42
Ackers and White (d50)	1.31	1.00	0.19
Ackers and White (d35)	1.04	0.87	0.12
Yang Sand (d50)	1.59	1.45	0.31
Yang Sand (size fraction)	1.36	1.31	0.27
Yang Mixture (size fraction)	1.36	1.31	0.27
Einstein	2.11	1.47	0.30
Toffaleti	1.89	0.84	0.14